Oxidation of volatile organic compound vapours by potassium permanganate in a horizontal permeable reactive barrier under unsaturated conditions;

Experiments and modeling

Mojtaba Ghareh Mahmoodlu

Environmental Hydrogeology Group

Utrecht University

Utrecht Studies in Earth Sciences 65

Oxidation of volatile organic compound vapours by potassium permanganate in a horizontal permeable reactive barrier under unsaturated conditions;

Experiments and modeling

Mojtaba Ghareh Mahmoodlu

Utrecht University 2014

ISBN: 978-90-6266-374-3

Title: Oxidation of volatile organic compound vapours by potassium permanganate in a horizontal permeable reactive barrier under unsaturated conditions; Experiments and modeling

Keywords: VOC vapours; Horizontal permeable reactive barrier; Unsaturated zone; water saturation; In-situ chemical oxidation; Solid potassium permanganate; pH

NUR-code: 934

NUR-description: Hydrogeology

Number of pages: 190

Cover illustration: Mahmoodlu, M.G.

Cover lay-out: Margot Stoete, Faculty of Geosciences, Utrecht University

Printed by: Uitgeverij BOXPress || Proefschriftmaken.nl

This research was supported financially by the Ministry of Science, Research and Technology of Iran.

Oxidation of volatile organic compound vapours by potassium permanganate in a horizontal permeable reactive barrier under unsaturated conditions;

Experiments and modeling

Oxidatie van de dampen van vluchtige organische stoffen door kaliumpermanganaat in een horizontale permeabele reactieve barrière onder onverzadigde condities;

Experimenten en modellering

(met een samenvatting in het Nederlands)

Proefschrift
ter verkrijging van de graad van doctor aan de Universiteit Utrecht
op gezag van de rector magnificus, prof. dr. G.J. van der Zwaan,
ingevolge het besluit van het college voor promoties
in het openbaar te verdedigen
op dinsdag 25 november 2014 des avonds te 6.00 uur

door

Mojtaba Ghareh Mahmoodlu
geboren op 21 maart 1979 te Minudasht, Iran

Promoter: Prof.dr.ir. S.M. Hassanizadeh

Copromoter: Dr. N. Hartog

The Reading and Examination Committees

Prof. dr.ir. T.J. Heimovaara	Delft University of Technology
Prof. dr.ir. H.H.M. Rijnaarts	Wageningen University
Prof. dr.ir. M.Th. van Genuchten	Federal University of Rio de Janeiro
Prof. dr. J. Griffioen	Deltares and TNO Geological Survey
Dr. T. Behrends	Utrecht University

Acknowledgements

"Knowledge is in the end based on acknowledgement"
Ludwig Wittgenstein

I take this opportunity to extend my sincere gratitude and appreciation to all those who truly helped and supported me, and made this thesis possible over the last four years.

Special thanks go to my promoter, Majid Hassanizadeh, who was the reason that brought me to The Netherlands. Majid, I always enjoyed our thoughtful discussions and learned extensively from you. I gratefully acknowledge your careful review and constructive comments and suggestions for my research. Thank you so much for allowing me the opportunity to work independently. I would also like to thank my co-promoter, Niels Hartog, for his supervision and valuable comments on my research. Niels, thanks for sharing your remediation knowledge with me.

I am very grateful to Amir Raoof for his valuable input, continuous help on simulation results, advice and also his encouragements. My special gratitude to Rien van Genuchten, for his discussion and comments on experimental setups and results, for his careful review and constructive comments on my manuscripts, and his encouragements in general. I am grateful to Kótai László (Hungarian Academy of Sciences, Hungary) for his valuable advice and comments on permanganate reactions, in particularly the comments on barium permanganate. I deeply appreciate the time you devoted to my questions. I would also like to thank Emilio Rosales Villanueva (University of Vigo, Spain) for his critical review and comments on my manuscripts and his time to answer my questions. I would like to express my thankfulness to Hamid M. Nick for his advice and comments on experimental setups and simulation results. I further acknowledge Jack Schijven, Tom Bosma, Toon Lijnse, Mart Oostrom (Pacific Northwest National Laboratory, USA), and Thilo Behrends for their advice and their willingness to share their

extensive knowledge with me, which was very fruitful for shaping my ideas and research. I gratefully acknowledge the technical support of Jan Kubiak (Wageningen University), Pieter Kleigeld, Michiel Kienhuis, Dineke van de Meent-Olieman, Habiba, Randolph Van Kasteren, and Bernadette Marchand.

I would like to thank my colleagues and friends of the Environmental Hydrogeology Group at Utrecht University. First of all, thanks to Ruud Schotting for his support and lovely dinners at his place, in particularly the BBQ that we made together. Special thanks to Margreet for her kind help in administrative tasks, translating and filling out Dutch forms, and inviting us to the zoo. A big thank goes to my friend and colleague, Shuai (帅), for being always helpful during the most difficult time of my research. Shuai, I always enjoyed our short talks during lunch time and tea break. I also would like to express my appreciation to my friends and colleagues: Reza, Imran, Qiu, Vahid, Nikos, Chaozhong, Wouter, Luwen, Elaheh, Thomas, Xiaoguang, Ehsan, Willem-Bart, John, and Jan. I am grateful to Thomas and Willem-Bart for their help to translate the summary into Dutch.

My special regards to Forooz for her support, advice and her delicious dinners. I will never forget her kindness and grace. I wish to thank Betty May for being always so helpful to us, her encouragement, travel and food recommend-ations, lovely dinner invitations, and buying a new bike for Rien so that I could use his old bike.

I am grateful to Maryam's supervisors (my academic mothers-in-law!), Brigitte Unger and Stephanie Rosenkranz for their support and understanding of our situation and their patience.

I owe much to my uncle and aunt, Ardalan and Sara for their support, and also a lovely couple, Hossein and Shahnaz. Thank you for your kindness and generosity.

From September 2010 when I came to The Netherlands I was very fortunate to meet many great Iranian friends. I would like to mention a few in particular: Reza and Fatemeh, Ali and Fariba, Hamed and Mina, Jahan and Tala, Rahim and Sara, Jafar and Nahid, Ali and Maryam, Siyavash and Mahshid, Mahdi

and Samineh, Ali and Reyhaneh, Ali and Mehrnoush, Yaser and Neda, Hadi and Parvin, Soheil and Nafise, Fatemeh, Efaf, Fafa, Ali, Farshad, Mazda, Frough, Jabiz, Toraj, Ramin, Sara, Bahar, Romina, Pasha, Ardavan, Sina, El, Sol, Peyman, Arash, Amir, and Nasrin.

Many thanks go to my lovely friends in Iran, Hadi, Javad, Ehya, Hossein, Shahram, Amir, Roya, Elham, Ali, Ebi, and Kamal for their encouragement, support and care.

From the time I came to The Netherlands I was so lucky to meet many great people who contributed indirectly to this study. I would like to mention a few in particular: David, Lidwein, Anne, Andre, Jasperien, Sara, Johan, Andrea, Tom, Karoliina, Agis, Niels, Arjen, Matthias, Rick, Chiara, Gosia, Inan, Pieter, Wouter, Olav, Sander, Arjan, Jiawang, Jinfeng, George, and Luca. I really enjoyed being a member of Tommy's Tigers futsal team. I would like to express my appreciation to my friends and teammates: Tom, Jon, Douwe, René (Z), Stan, Joe, Pétur, Bjarni, Thomas, René (K), Ali, Agis, Gareth, Davide, Andrea, and Massimiliano. I would also like to thank my friends and teammates of the Sciencemedia.nl futsal team.

I would like to express my hearty gratitude to my parents for their unlimited love, support, care, and devotion. I would also like to express my gratitude to all my family members, in particular my elder brother, Reza, for his endless support, encouragement, and the time he devoted to me.

Last but not the least, my deepest gratitude to my beloved wife, Maryam, for her understanding of my goals and aspirations. Her infallible love and support has always given me much strength. Her patience and sacrifice will remain an inspiration throughout my life. To her I dedicate this thesis.

Mojtaba G. Mahmoodlu

Utrecht

November 2014

Contents

List of Figures

List of Tables

Notation

The following table shows the symbols used in this study.

Symbol	Definition	Dimension
A_{KMnO_4}	Surface area of potassium permanganate	$[L^2]$
a_i	Specific air-water interfacial area	$[L^{-1}]$
a_{i0}	Initial specific air-water interfacial area	$[L^{-1}]$
C	Concentration of reactants	$[N\ L^{-3}]$
C_A	Concentration of VOC (target compound)	$[N\ L^{-3}]$
C_{A0}	Initial concentration of VOC	$[N\ L^{-3}]$
C_B	Concentration of potassium permanganate	$[N\ L^{-3}]$
C_{B0}	Initial concentration of potassium permanganate	$[N\ L^{-3}]$
C_B^f	Final concentration of potassium permanganate	$[N\ L^{-3}]$
C_0^g	Initial vapour concentration of compound	$[NL^{-3}]$
C^g	Vapour concentration of VOC	$[N\ L^{-3}]$
C_A^g	Concentration of VOC in gas phase	$[NL^{-3}]$
C_A^w	Concentration of VOC in the water phase	$[NL^{-3}]$
C_B^w	Concentration of dissolved permanganate in water	$[NL^{-3}]$
$C_{B,max}^w$	Maximum concentration of dissolved permanganate in water	$[NL^{-3}]$
ΔC	Consumed concentration of reactants	$[NL^{-3}]$
D_A^g	Molecular diffusion coefficient of VOC in free air	$[L^2T^{-1}]$
$D_{e,A}^g$	Effective gas diffusion coefficient	$[L^2T^{-1}]$

$D^{w}_{e,A}$	Effective diffusion coefficient in water	$[L^2T^{-1}]$
D^{w}_{A}	Molecular diffusion coefficient of VOC in water	$[L^2T^{-1}]$
$D^{w}_{e,A}$	Effective diffusion coefficient in water	$[L^2T^{-1}]$
H^+	Molar concentration of proton ion	$[NL^{-3}]$
$H_{C,A}$	Henry's constant of VOC	[-]
k	Reaction rate coefficient in water phase	$[N^{-1} s^{-1}]$
k^g	Reaction rate constant in gas phase	$[L\ s^{-1}]$
k^{diss}_{A}	Dissolution rate constant	$[LT^{-1}]$
K(h)	Unsaturated hydraulic conductivity	$[L\ T^{-1}]$
K_s	Saturated hydraulic conductivity	$[L\ T^{-1}]$
M_{KMnO_4}	Mass of solid potassium permanganate	[M]
m	Shape parameters relating to the pore size distribution	[-]
m^{oxid}_{A}	Oxidized mass of VOCs per unit volume of permeable reactive layer	$[NL^{-3}]$
N	Number of moles of potassium permanganate consistent with the stoichiometric reaction	[-]
n	van Genuchten soil hydraulic shape factor	[-]
n_A	Initial number of VOC moles	[N]
OH^-	Molar concentration of hydroxide ion	$[NL^{-3}]$
P	Ratio of initial concentration of potassium permanganate to initial concentration of VOC	[-]
r^{diss}_{A}	Rate of dissolution in water	$[LT^{-1}]$
r^{oxid}_{A}	Oxidation rate of VOC in the water phase	$[NL^{-3}\ T^{-1}]$
S_0	Initial relative surface area	$[L^{-1}]$
S	Relative surface area	$[L^{-1}]$

S^w	Water saturation	[-]
S_e^w	Effective water saturation	[-]
t	Time	[T]
V^g	Volume of gas phase	$[L^{-3}]$
X_A	Consumed fraction of VOC	[-]
X_B	Consumed fraction of potassium permanganate	[-]
X_B^f	Final consumed fraction of potassium permanganate	[-]
x	Spatial coordinate	[-]

Greek symbols

α	van Genuchten soil hydraulic parameter	$[L^{-1}]$
β_A	Fitting parameter in Equation 4.13 as part of the simulation results	[-]
γ	Coating factor (number of moles of produced MnO_2 per area of potassium permanganate grains)	$[NL^{-2}]$
θ^g	Air content	[-]
θ_r^w	Residual water content	[-]
θ_s^w	Saturated water content	[-]
θ^w	Water content	[-]
κ_{TCE}	Reaction rate constant in water	$[N^{-1}T^{-1}]$
ζ_A	Number of produced proton or hydroxide ion consistent with the stoichiometric reaction	[-]
σ	Fitting parameter in Equation 4.7	[-]
ϕ	Porosity of the porous medium	[-]

φ	Number of moles of MnO_2 produced per mole of target compound	[-]
ω_A	Fitting parameter in Equation 4.11 as part of the simulation results	[-]
η	Fitting parameter in Equation 4.16	[-]

Subscripts

0	Initial
A	VOC; TCE, ethanol, and toluene
B	Oxidant; potassium permanganate
C	Constant
e	Effective
i	Interfacial
$KMnO_4$	Potassium permanganate
MnO_4^-	Permanganate
r	Residual
s	Saturated

Superscript

diss	Dissolution
f	Final
g	Gas
oxid	Oxidation
w	Water

Chapter 1

General introduction

1.1. Overview of volatile organic compounds (VOCs)

Soil and groundwater contamination by volatile organic compounds (VOCs) is a major environmental problem at sites currently or formerly occupied by large-scale chemical industries or small-scale users such as dry cleaners or fuel stations (Rivett et al., 2011; Schubert et al., 2011). VOCs are defined as organic compounds with boiling points (at 1 atm) below 260 ºC (De Nevers, 2000). VOCs have high vapour pressures under normal conditions, thus allowing them to easily vapourize into the atmosphere or form vapour plumes in soils (Kim et al., 2007). VOCs are groundwater contaminants of widespread concern because of (1) very large volumes that are often released into the environment and (2) their toxicity. Releases of VOCs into the environment have occurred through surface spills, leaking underground storage tanks, and inadequate disposal practices (Fig. 1.1). Small quantities of VOCs may contaminate large volumes of water. When released as a free product, VOCs may migrate downward to significant depths through the soil. In addition, VOC vapours can migrate upward to the soil surface through diffusion (Berscheid et al., 2010). Extended exposure to some VOCs may affect central nervous system and internal organs, and also cause symptoms such as headache, respiratory tract irritation, dizziness, and nausea, known as the Sick Building Syndrome (Yu and Lee, 2007).

Petroleum hydrocarbons (PHCs) and chlorinated hydrocarbons or solvents comprise two classes of VOCs that together account for a large number of soil and groundwater contamination sites (EPA, 2012). PHCs are mainly used in gasoline, diesel, and jet fuel, whereas chlorinated solvents are the main constituents of dry cleaners and degreasing solvents (EPA, 2012). Among the various PHCs, benzene, toluene, ethylbenzene, and meta- (m), para- (p), and ortho- (o) xylene (collectively known as BTEX) are the most common soil and groundwater contaminants (Picone, 2012). Currently, a significant portion of petroleum products contains BTEX compounds (Serrano and Gallego, 2004). The presence of BTEX compounds (approximately 20-40% of the total concentration of VOCs) in urban areas

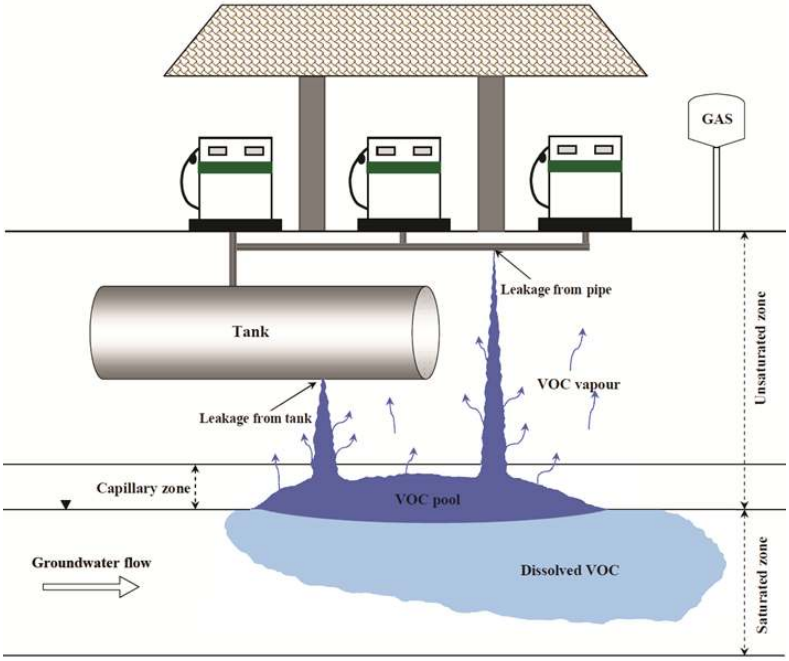

Fig. 1.1: Schematic view of possible VOC release from a gas station into the subsurface.

commonly was reported by a variety of the European Union countries (Costa et al., 2012). Furthermore, ecosystems can also be influenced by BTEX compounds. For example, the presence of BTEX in soil has an adverse effect on the survival of earthworms (Picone, 2012). High water solubility of BTEX compounds relative to other petroleum components makes them also more mobile (Farhadian et al., 2008). This may increase the extent of contaminated areas in the subsurface.

Chlorinated hydrocarbons are another class of man-made VOCs. These compounds are hydrocarbon molecules in which hydrogen atoms are displaced by chlorine. Examples are tetrachloroethylene (PCE), trichloroethylene (TCE), dichloroethlyene (DCE) and vinyl chloride (VC). Chlorinated hydrocarbons are soil and groundwater contaminants widely found at sites occupied by large-scale chemical industries or small-scale users such as dry cleaners (Badawi et al., 2000; Cho et al., 2002; EPA, 2012). These chemicals are mainly used as an intermediate constituent in plastic production, degreasers in metal industry and solvents in dry

cleaning facilities (Picone, 2012). Exposure to chlorinated hydrocarbons has adverse effects on human health and ecosystems. For instance, extended exposure to chlorinated hydrocarbons may cause various human cancers (Badawi et al., 2000; EPA, 2012; Picone, 2012). Furthermore, exposure of marine fauna and aquatic invertebrates to dissolved chlorinated hydrocarbons can have a significant effect on their growth, reproduction, and mortality (NAS, 1971; Picone, 2012).

Among the various VOCs, we selected three for our studies: TCE, ethanol, and toluene. These three constituents are considered to be model VOCs (target compounds) for chlorinated hydrocarbons, biofuel, and mineral oil, respectively, for reasons explained below. Relevant physical and chemical properties of the target compounds are given in Table 1.1.

TCE is one of the most common man-made chlorinated hydrocarbons found in soil and groundwater (Albergaria et al., 2012). TCE has been widely used as a dry cleaning solvent, chemical intermediate, degreasing agent, and chemical extraction agent (Sadeghi et al., 2014). The market requirement for TCE in Europe was about 25,000 tons, in 2006. However, its use decreased dramatically due to the carcinogenicity of TCE (EuroChlor, 2008; Picone, 2012). Prolonged exposure to TCE may cause negative health effects to internal organs (e.g., kidney, liver, cervix) and the lymphatic system (Yu and Lee, 2007; Rastkari et al., 2011; Picone, 2012; Sadeghi et al., 2014). Since TCE is carcinogenic, its movement from contaminated groundwater and soil into indoor air of overlying buildings is of serious concern (EPA, 2011).

Ethanol is being used increasingly in (renewable) fuel alternatives and as a replacement for methyl tertiary-butyl ether (MTBE) (Bassam, 2010). The increased use of ethanol as a gasoline additive has raised concerns over its potential to contaminate groundwater (Johnson et al., 2000; Capiro et al., 2007; Freitas et al., 2010). In North America, 10% ethanol is commonly being added to gasoline (termed E10). Ethanol is usually denatured with gasoline compounds before being transported; for this reason E95 (95% ethanol) mixtures are also common. Therefore, spills with compositions ranging from E10 to E95 can be anticipated

Table 1.1: Physical properties of selected VOCs used in this study (Picone, 2012).

VOC	**TCE**	**Toluene**	**Ethanol**
Formula	C_2HCl_3	C_7H_8	C_2H_6O
Molecular Weight (g mol^{-1})	131.39	92.14	46.07
Density (g cm^{-3})	1.46	8.7×10^{-1}	7.9×10^{-1}
Solubility (g cm^{-3})	1.47×10^{-3}	4.7×10^{-4}	Fully miscible
Sorption coefficient (g cm^{-3})	166	182	16
Vapour pressure (Pa)	2527	3990	5866
Henry's Law constant (20 ºC)	4.3×10^{-1}	2.8×10^{-1}	2.4×10^{-4}
Diffusion coefficient in air (cm^2 s^{-1})	7.6×10^{-2}	7.9×10^{-2}	1.1×10^{-1}
Diffusion coefficient in water (cm^2 s^{-1})	9.4×10^{-6}	9.1×10^{-6}	1.2×10^{-5}

(Freitas et al., 2010). Ethanol is thought to increase the mobility of NAPLs, create higher hydrocarbon concentrations in groundwater due to cosolvency, and decrease the rate of gasoline hydrocarbon biodegradation, with consequently a possible increase in the length of dissolved contaminant plumes (Freitas et al., 2010).

As a petroleum hydrocarbon, toluene is a primary constituent of oil, gasoline, diesel, and a variety of solvents and penetrating oils. Toluene is used mainly as an additive to improve the octane number of gasoline (Yu and Lee, 2007). This compound is listed as one of six major classes of indoor VOCs (aromatic, aldehyde, alkane, ketone, alcohol, and chlorocarbon) (Yu and Lee, 2007). Although toluene has a relatively low toxicity, it still may have adverse health effects (Picone, 2012). Exposure to toluene may cause irritation of the eye, nasal and mucous membranes, and the respiratory tract (Yu and Lee, 2007). Moreover, overexposure to toluene can damage the central nervous system and the brain (ATSDR, 1994).

1.2. Vapour intrusion

VOC partitioning into the air phase can lead to relatively rapid transport in unsaturated media. Vapours of VOCs may migrate upward from subsurface sources (e.g., buried waste, contaminated soil or groundwater) and enter overlying buildings (USEPA, 2002; KDHE, 2007; Picone, 2012; Yao et al., 2013). Vapour intrusion is a potential concern since it is a pathway for exposure to VOC vapours. However, the improper maintenance of household solvents, gasoline, and cleaners in the buildings may increase also the concentration of VOCs in indoor spaces (Picone, 2012). Although VOC concentrations in air are commonly low and, depending upon site-specific conditions, may be below detection limits, long-term accumulation of VOC vapours may cause human health risk (EPA, 2012) or explosion hazards (Freitas, 2009; EPA, 2012).

Rates of VOC vapour intrusion are very much influenced by natural barriers such as low-permeability geological layers and high soil water contents in the unsaturated zone (Kotvis, 2011; Frank, 2011; USEPA, 2012). Low-permeability layers (soil or rock) within the unsaturated zone can impose a considerable resistance to the upward migration of VOC vapours (Kotvis, 2011; Frank, 2011; USEPA, 2012). Low-permeable layers that are laterally extensive compared to the size of a building or contaminated area, in particular, may provide very effective barriers against the migration of VOC vapours in the unsaturated zone (Frank, 2011). Low-permeability layers also prevent the downward percolation of water (Fairley et al., 2006; Frank, 2011; Briaud, 2013), possibly leading to perched water that would further increase the residence time of VOCs migrating upward from contaminated soil or groundwater. Percolation of water through soil due to rainfall or artificial recharge (e.g., irrigation or the presence of retention ponds) may similarly create a lens of water in the unsaturated zone above VOC-contaminated soil or groundwater before reaching the water table (Frank, 2011). This may likewise create an effective natural barrier against the upward migration of VOCs in the unsaturated zone.

1.3. Fate and transport processes of VOCs in the unsaturated zone

VOC transport processes in the unsaturated zone have been studied extensively (e.g., Frank, 2011; Rivett et al., 2011; Picone, 2012; Costanza-Robinson, 2013; You and Zhan, 2013). Water saturation in the unsaturated varies from unity at the upper part of the capillary fringe to as low as residual saturation in the upper part of vadose zone close to the soil surface (Weiner, 2000; Sara, 2003; Picone, 2012). VOC transport processes from contaminated groundwater to indoor spaces typically starts from the upper part of the capillary fringe. In this portion of soil, volatilization and partitioning processes first transfer VOC into the gas phase at the interface between water-filled pores and the first water-air-filled pores. Diffusion and advection processes then further cause VOC transport VOC upward to the surface or indoor spaces (Picone, 2012; Costanza-Robinson, 2013; You and Zhan, 2013).

The transport of VOC vapours from contaminated soil and groundwater into indoor spaces is dominated in most field situations by diffusion (USEPA, 1993; Berscheid et al., 2010; Picone, 2012; You and Zhan, 2013; Shen et al., 2014). The overall effective diffusion coefficient of a VOC is equal to the weighted sum of the diffusion coefficients of the air and water phases. Since the effective diffusion coefficients in the gas phase are up to 3 to 4 orders of magnitude greater than those in the aqueous phase (Wiedemeier et al., 1999; Pasteris et al., 2002; Tillman and Weaver, 2005), the diffusive flux in the aqueous phase can generally be disregarded as long as the air phase is continuous. Effective diffusion in relatively dry soils can be very high. By contrast, an increase in water saturation reduces effective diffusion in the unsaturated zone. Effective diffusion in the capillary fringe near the water table for this reason is relatively low. Effective diffusion is also expected to be low for VOCs having relatively low Henry's Law constants, such as ethanol (Frank, 2011). High water saturation and low Henry's Law Constant are hence the two main factors limiting VOC vapour transport from contaminated surface into indoor spaces.

Advection of air due to pressure gradients in the air phase (EAP, 2012) is one of mechanisms causing the transport VOC vapours into indoor spaces. The main physical factors resulting in vapour phase advection are temperature, wind, air conditioning operations, and water table fluctuations. The pressure inside buildings can change as a result of heating and cooling systems. When the pressure inside a building is lower than the pressure in the subsurface (e.g., due to a higher temperature), VOC vapours can be advected upward into the building. Changes in barometric pressure or wind may also cause the advection of VOC vapours (Massmann and Farrier, 1992; Frank, 2011; Picone, 2012). The wind pressure on a building may create pressure changes inside the building and subsequent VOC movement into the subsurface or buildings (Lundegard et al., 2008; Frank, 2011; Picone, 2012). Additionally, water table fluctuations can influence gas pressures in the unsaturated zone, leading to the upward migration of VOC vapours from contaminated groundwater into indoor spaces (Li and Jiao, 2005; You and Zhan 2012; You and Zhan, 2013).

Sorption is another process affecting VOC concentration during their migration in the subsurface. Sorption of VOC vapours onto soil and sediments can retard VOC vapour transport within the unsaturated zone (Breus and Mishchenko, 2006; Bell and LeBoeuf, 2013). Sorption is strongly impacted by the physical and chemical composition of a soil. In general, VOC vapour sorption is affected by two mechanisms: (1) adsorption on mineral surfaces (e.g., iron oxides) when soils are very dry (e.g., water content $< 2\%$), and (2) partitioning into water present the unsaturated zone. Several studies have shown that adsorption is very much affected by water content, with vapour adsorption decreasing rapidly with increasing moisture content (Smith et al., 1990; Ong and Lion, 1991; Breus and Mishchenko, 2006). Additionally, VOC partitioning onto soil organic matter commonly occurs in wetter soil (water content $> 4\%$) (Farrell and Reinhard, 1994; Batterman et al., 1995; Picone, 2012). This mechanism can indirectly affect VOC concentrations.

Biodegradation is another important natural attenuation process that can reduce the concentration of VOC vapours during their migration in the unsaturated zone (EPA, 2012). Fan and Krishnamurthy (1995) reported that some 200 different

species of microorganisms (e.g., bacteria, yeast, and fungi) are able to degrade VOCs in soil. Both aerobic and anaerobic biodegradation of VOC vapours may occur in the unsaturated zone. Aerobic biodegradation requires sufficient levels of oxygen, nutrients, moisture, hydrocarbon, and microbial populations. Among these, oxygen is the main limiting factor for aerobic processes at most sites (DeVaull et al., 1997). In the presence of sufficient oxygen, indigenous microbes produce enzymes that are able to degrade certain VOCs. The literature shows that aerobic biodegradation of VOC vapours can effectively decrease the concentration and subsurface migration of VOCs (particularly PHCs) in the unsaturated zone (Lahvis et al. 1999; DeVaull et al., 1997; Hers et al. 2000; EPA, 2012).

Anaerobic biodegradation rate of VOCs is much slower than aerobic degradation, particularly for chlorinated solvents (Simon et al., 1994; Kristensen et al., 1995; Wise et al., 2000; EPA, 2012). Anaerobic or anoxic biodegradation is strongly affected by the types of electron acceptors present, pH ambient conditions, and potential oxidation or reduction conditions (Frank, 2011). The estimation of both aerobic and anaerobic degradation rates may not be easy. The degradation rate can differ significantly from site to site because of many site-specific factors, including the various processes discussed above.

1.4. Remediation techniques for VOCs in the unsaturated zone

Unsaturated zone treatment for VOCs may rely on various in-situ techniques, including biological (e.g., bioventing, phytoremediation), chemical (e.g., chemical oxidation, soil flushing), and physical (e.g., soil vapor extraction, thermal treatment) methods. The principal characteristic of many in-situ treatment technologies is the method of delivery and recovery of fluids or other reactants to the unsaturated zone (USEPA, 2006). Depending upon the unsaturated zone specification and contaminant present (e.g., dissolved, adsorbed, separate phase or vapour phase) and properties, each in-situ technology has benefits and limitations in term of its ability to effectively deliver, control, and recover administered fluids and/or reactants and contaminants (USEPA, 2006). For instance the permeability of

subsurface formations is an important factor in the delivery of an oxidant for chemical oxidation or a gas (e.g., oxygen) for bioventing. In contrast, permeability is not an important factor for heat transfer. Consequently, permeability is generally more critical for chemical oxidation or bioventing than for conductive heating (USEPA, 2006). Three common in-situ techniques are described briefly below.

In-situ bioremediation is a possible treatment technology for VOC contaminants in the unsaturated zone (Romantschuk et al., 2000: Zargar et al., 2014). However, biodegradation processes are relatively slow and have their limitations. For instance, some contaminants are not easily biodegradable under aerobic condition (e.g., certain chlorinated compounds and radionuclides). Also, the biodegradation of chlorinated solvents may produce toxic degradation by-products (EPA, 2012; Langevoort, 2009). Furthermore, bioremediation of high concentrations of VOCs may be very difficult or impossible (Langevoort, 2009). Bioventing is an in-situ bioremediation technology for a VOC-contaminated unsaturated zone by providing air or oxygen to soil microorganisms. As explained earlier, performance of this method can be affected by soil permeability as well as water content. Bioventing may lead to a decrease in the soil moisture content. This can affect indigenous microorganisms and consequently limit biodegradation of VOCs in the unsaturated zone.

One of the most common techniques for the physical treatment of VOCs in the unsaturated zone is soil vapour extraction (SVE). As illustrated in Fig. 1.2, SVE is a remediation technology in which a vacuum is applied to induce controlled subsurface air flow to VOCs within the unsaturated zone. The configuration of the system usually involves attaching blowers to extraction wells, which then bring contaminated air to the surface (USEPA, 2006). This technique does not convert the contaminants to less toxic compounds (Cho et al., 2002), and hence may require an additional process to treat the contaminated air (USEPA, 2006). Furthermore, SVE requires long-term operation, with efficiencies declining substantially in low-permeability zones where mass transfer is generally diffusion-limited (Cho et al., 2002).

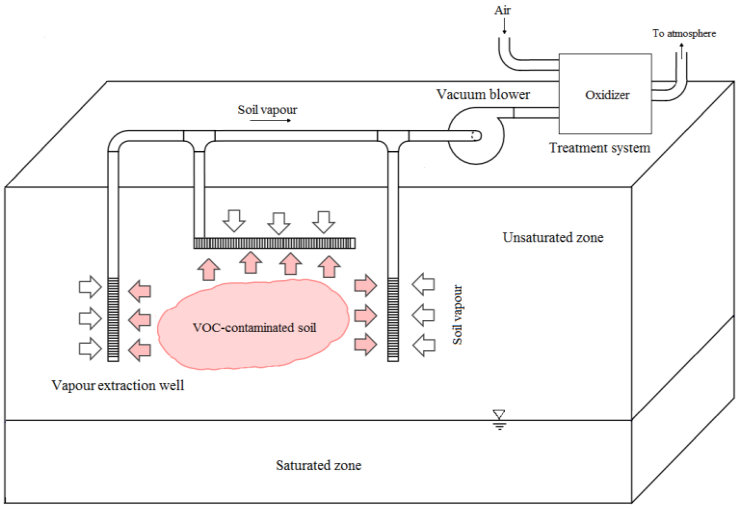

Fig. 1.2: Schematic view of soil vapour extraction in the unsaturated zone.

In-situ chemical oxidation (ISCO) has been shown to be a promising treatment technology of soils and groundwater. ISCO of VOCs has been well developed as a remediation technology for dissolved VOCs in groundwater (Heiderscheidt et al., 2008; Tsitonaki et al., 2010; Yuan et al., 2013). However, only a few studies have applied ISCO to the unsaturated zone using permanganate (Hesemann and Hildebrandt, 2009) or other oxidants (Cronk et al., 2010). In these studies, the oxidant was mostly introduced into the unsaturated zone as an aqueous solution. This method hence targets dissolved VOCs and cannot be employed for degrading a long-term supply of VOCs via the gas phase. The ISCO methodology is discussed in more detail in the next section.

1.5. Chemical oxidation of VOCs

Among various remediation technologies, chemical oxidation has been widely used for treatment of an extensive range of contaminants, such as petroleum hydrocarbons and chlorinated solvents, as well as numerous other contaminants in soil (Komárek et al., 2013; Wang et al., 2013; Siegrist et al., 2014), surface water or

wastewater (Wenk, et al., 2013; Oturan and Aaron, 2014) and groundwater (Baciocchi et al., 2014; Siegrist et al., 2014). The general principle of chemical oxidation is to use chemicals (called oxidants) to transform or degrade contaminants. During the oxidation of contaminants, the oxidant is reduced by accepting electrons, which are released through oxidation of VOCs (Wang et al., 2005). Chemical oxidation is able to convert VOCs or other contaminants to non-toxic or less toxic by-products (Cook, 2009). Various processes may occur during chemical oxidation, such as oxygen addition, hydrogen removal, and withdrawal of electrons with or without losing protons (Huling and Pivetz, 2006). The oxidation process may be affected by a variety of environmental factors (e.g., pH, soil organic matter, minerals, temperature, soil type, and heterogeneity). These factors may change the oxidation rates and pathways. For example, partial oxidation of TCE could produce intermediate by-products that include dichloroacetaldehyde and dichloroacetic acid; compounds with lower toxicity (Dobaradaran et al., 2014). However, full oxidation of TCE produces CO_2 and H^+ (Liang et al., 2014). Reaction products of chemical oxidation of VOCs are known to be used often by soil microorganisms. This may result in an increase in natural attenuation (Huling and Pivetz, 2006; Mora et al., 2014). Hence, chemical oxidation can be applied together with bioremediation for the pretreatment of toxic and resistant contaminants (Yen, et al., 2011).

1.5.1. In-situ chemical oxidation (ISCO)

In-situ chemical oxidation is one of more effective subsurface remediation technologies that has been developing rapidly over past few decades (Sercu et al., 2013). In ISCO, a chemical oxidant is introduced into the subsurface to transform soil or groundwater contaminants into less harmful chemical species or even environmental friendly compounds (Huling and Pivetz, 2006). Several chemical oxidants have been used for ISCO purposes including permanganate (MnO_4^-),

hydrogen peroxide (H_2O_2) and iron (Fe) (Fenton-driven or H_2O_2-derived oxidation), persulfate ($S_2O_8^{2-}$), and ozone (O_3) (MacKinnon and Thomson, 2002; TITRC, 2005; Huling and Pivetz, 2006; Wang et al., 2013; Liang et al., 2014). The properties of these oxidants for ISCO are given in Table 1.2. Of the various properties, oxidant persistence in the subsurface is an important issue for ISCO purposes. This property may affect the contact time between oxidant and contaminants and also the delivery of the oxidant into contaminated zone. For example, permanganate has proven to persist for relatively long periods of time in the subsurface depending upon the soil matrix and groundwater composition (Siegrist et al., 2001; Huling and Pivetz, 2006; Cave et al., 2007; Liang et al., 2014). A longer lifetime allows the oxidant to diffuse into low-permeability materials (Siegrist, 2011; Struse, 2002). By contrast, hydrogen peroxide has been reported to remain in soil and aquifer material for only minutes to hours, leading to very limited diffusive and advective transport distances (Watts et al., 1999; Huling and Pivetz, 2006; Xu and Thomson, 2010). Similarly, persulfate and ozone, although able to react quickly with various VOCs, persist for only very short periods of time (TITRC, 2005; Huling and Pivetz, 2006). Full oxidation of soil and groundwater contaminants using ISCO is affected by many factors such as geological conditions, which may decrease physical contact of oxidant and contaminant, and background reactions, which may decrease the oxidant concentration (Sercu et al., 2013). In general, ISCO has several advantages and disadvantages in comparison with other remedial technologies. The main advantages of ISCO are as follows (Lens et al., 2005; Huling and Pivetz, 2006; Sogaard, 2014):

(1) A wide range of contaminants can be transformed to non-toxic or environmental friendly compounds.
(2) ISCO is a relatively fast treatment technology.

Table 1.2: Properties of commonly used oxidants for ISCO (Huling and Pivetz, 2006)

Oxidant	Reactive Species	Form	[1]Persistence
Permanganate	MnO_4^-	Powder/liquid	>3 months
Fenton's	$^{\cdot}OH, {}^{\cdot}O_2^-, {}^{\cdot}H_2O, HO_2^-$	Liquid	Hours
Ozone	$^{\cdot}OH, {}^{\cdot}O_3$	Gas	Hours
Persulfate	$[S_2O_8]^{-2}$	Powder/liquid	Hours to weeks

[1]Persistence of the oxidant varies depending on site specificifications.

(3) ISCO may reduce costs compared to other technologies such as pump and treat.
(4) ISCO is effective for different forms of the contaminants (e.g., dissolved, sorbed, and residual VOCs).
(5) The produced heat during the reaction of some oxidants (e.g., H_2O_2) may increase mass transfer (enhanced dissolution of contaminants), reaction rates, and microbial activity.
(6) ISCO leads to increased microbial activity and hence natural attenuation due to the production of several by-products.

The main disadvantages of the ISCO technology are (Huling and Pivetz, 2006; Sogaard, 2014):
(1) Possible problems in delivering the oxidants due to reactive transport, background reactions (natural oxidant demand due to natural organic matter), and heterogeneity of porous medium.
(2) The longevity of some oxidants is relatively short in the subsurface due to their fast reaction rates.
(3) Possible health and safety issues regarding the handling of strong oxidants.
(4) ISCO may lead to the remobilization of some contaminants (e.g., heavy metals).
(5) Possible decrease in permeability of the soil medium due to precipitation of produced manganese dioxide (MnO_2).

(6) The contaminated plume with its mixture of contaminants may require a treatment train in that several measures in sequence may be needed for the treatment to become effective.

1.5.2. In-situ chemical oxidation using permanganate

Permanganate is one of the more common chemical oxidants used for treating wastewater, surface water, soil and groundwater, as well as for many other industrial applications (EPA, 2004; Siegrist et al., 2011). Permanganate is very much preferred for ISCO applications because of its relatively simple chemistry (EPA, 2004; Siegrist et al., 2011).

In general, two common forms of permanganate salts can be used for ISCO applications: potassium permanganate ($KMnO_4$) and sodium permanganate ($NaMnO_4$) (EPA, 2004; Siegrist et al., 2011). Although they have very similar oxidation chemistry, they also have significant differences in their physical properties (Table 1.3) which are important for the design of a permanganate ISCO system (Siegrist et al., 2011).

Of the two common forms of permanganate, potassium permanganate has received much attention for treating VOC-contaminated liquids, slurry soils, and sludges (Kao et al, 2008). Early laboratory studies have indicated that dissolved potassium permanganate can remediate a variety of organic compounds, chlorinated alkanes (Waldemer, and Tratnyek, 2006), chlorinated ethylenes (Hood et al., 2000; Huang et al., 1999; Kao et al., 2008; Urynowicz, 2008; Waldemer and Tratnyek, 2006; Yan and Schwartz, 2000), oxygenates (Damm et al., 2002; Jaky et al., 2000; Waldemer, and Tratnyek, 2006), BTEX (Gardner,1996; Rudakov and Lobachev, 2000; Waldemer, and Tratnyek, 2006), substituted phenols (Jin et al., 2003; Waldemer, and Tratnyek, 2006) and PAHs (Forsey, 2004) in the aqueous phase. Although ISPR has been employed for the treatment of a wide range of contaminants, the method is more effective for some chlorinated solvents in the subsurface (MacKinnon and Thomson, 2002; Liang et al., 2014), but less effective

Table 1.3: Physical and chemical properties of sodium and potassium permanganate (Siegrist et al., 2011).

Property	**Sodium permanganate ($NaMnO_4$)**	**Potassium permanganate ($KMnO_4$)**
Molecular weight (g/mole)	141.93	158.03
Most common physical form	Liquid	Crystalline solid
Solubility limit in distilled water (g/l)	Miscible in water (~900 g/l)	65.0 g/l (20 ºC) and 27.8 g/l (0 ºC)
Chemical incompatibility	Strong acids, organic peroxides, concentrated hydrogen peroxide,	

wt.%: weight percentage

for 1,1,1-trichloroethane, 1,1-dichloroethane, carbon tetrachloride, chloroform, methylene chloride, chlorobenzene, benzene, some pesticides, polychlorinated biphenyls, and others (Damm et al., 2002; Huling and Pivetz, 2006). This may limit the applicability of the ISCO process for rapid cleanup (Damm et al., 2002).

Also, the reaction rate of permanganate with contaminants is relatively slow in the saturated zone, which may lead to a relatively high stability or half-life of permanganate in the subsurface. High stability is an important advantage of an oxidant for ISCO applications. For example, the high stability of permanganate in the subsurface increases the contact time between permanganate and contaminants. This may also affect the transport within a heterogeneous porous medium and hence the delivery of permanganate into the contaminated zone (Siegrist et al., 2011). Struse et al. (2002) and Parker (2002) reported that the long-term persistence of permanganate facilitates diffusive transport of the oxidant into low-permeability materials, such as silt, clay and fractured shale. However, delivery of permanganate in the subsurface can also be affected by the production of by-products such as manganese dioxide. In general, the half-life of permanganate in the aquifer can be up to several weeks or more depending upon the soil matrix, the permanganate

concentration, and degradation of permanganate due to background reactions and the type and concentration of contaminants involved (Bryant et al., 2001; Siegrist et al., 2001; Siegrist et al., 2011). Permanganate can also react with a wide range of natural organic compounds, after referred to as background oxidant demand or background reaction (Yan and Schwartz, 1999; Urynowicz, 2008; Siegrist et al., 2011). The background oxidant demand reduces the delivery efficiency and hence oxidation efficiency of oxidants in the subsurface. The background oxidant demand can be high during highly reduced conditions (e.g., organic-rich aquifer materials). Only a small fraction of applied oxidant may then reach and react with a VOC during ISCO application. This may increase the mass and cost of permanganate needed to achieve ISCO purposes (Siegrist et al., 2011). To eliminate the background oxidant demand, an encapsulated particle method using wax or polymers is currently being employed to deliver solid oxidants into the contaminated zone (Kang et al., 2004; Ross et al., 2005). These materials are commonly insoluble in water, but can be very soluble in most hydrophobic contaminants, particularly chlorinated solvents.

Some general advantages of ISCO using permanganate are its (1) effectiveness over a wide range of pH values (EPA, 2004; Siegrist et al., 2011), (2) low cost as compared with other oxidants (Huling and Pivetz, 2006; Siegrist et al., 2011; Liang et al., 2014), (3) predictable chemistry and nontoxic by-products (Siegrist et al., 2011), (4) oxidation potential (E_0), which varies from 0.6 to around 1.7 V under ambient pH conditions (EPA, 1999; Huling and Pivetz, 2006; Siegrist et al., 2011), and (5) significantly higher stability in the subsurface as compared to other chemical oxidants (Huang et al., 1999; Bryant et al., 2001; Parker, 2002; Siegrist et al., 2011; Liang et al., 2014). Moreover, ISCO using permanganate does not produce heat, steam, and vapours; which are often produced using peroxides (Huling and Pivetz, 2006).

As mentioned earlier, in-situ dissolved potassium permanganate oxidation using standard injection technologies has been well developed for treating subsurface contaminants during the past last decades (MacKinnon and Thomson, 2002; Liang et al., 2014). Some innovative methods (e.g., hydraulic or pneumatic

fracturing) now also exist for transferring slurry and solid phase potassium permanganate into low-permeable geological formations (Thiruvenkatachari et al., 2008; Siegrist et al., 2011). These applications show that permanganate is a very viable option for oxidizing VOCs in the saturated zone. However, the potential of solid potassium permanganate to oxidize VOC vapours in the unsaturated zone is currently still largely unknown.

1.5.3. Chemical reactions of permanganate

The oxidation ability of permanganate depends upon the direct transfer of electrons from one species to the reducing agent (oxidant) during a reaction. The number of transferred electrons is strongly affected by the pH of the ambient environment (EPA, 1999; Huling and Pivetz, 2006; Kao et al., 2008; Siegrist et al., 2011) as follows:

$$MnO_4^- + 2H_2O + 3e^- \rightarrow MnO_{2(s)} + 4OH^- \quad \text{when} \quad pH = 3.5\text{-}12 \qquad (1.1)$$

$$MnO_4^- + 8\,H^+ + 5e^- \rightarrow Mn^{+2} + 4H_2O \quad \text{when} \quad pH < 3.5 \qquad (1.2)$$

$$MnO_4^- + e^- \rightarrow MnO_4^{-2} \quad \text{when} \quad pH > 12 \qquad (1.3)$$

As a result, a reduction in pH increases the number of transferred electrons (Equations 1.1 to 1.3). Since the groundwater pH generally ranges between 4 to 8 during ISPO, Equation 1.1 is probably the dominant reaction in soil and groundwater systems, leading to precipitation of manganese dioxide in the porous medium (Yan and Schwartz, 1999; Kao et al., 2008; Siegrist et al., 2011). Several studies have shown that highly acidic conditions can be created during treatment of VOCs using permanganate, both in the laboratory and under field conditions (MacKinnon and Thomson, 2002; Petri, 2006). Equation 1.2 shows that under strongly acidic conditions (pH < 3.5), permanganate reduces to Mn^{+2} (manganese ion) (Yan and Schwartz, 1999; Kao et al., 2008; Siegrist et al., 2011). Moreover, manganese can also be present in other redox-dependent oxidative states (Mn^{+4},

Mn^{+7}) in highly acidic conditions (Siegrist et al., 2011). As shown by Equation 1.3, permanganate can transform into MnO_4^{2-} (manganate ion) in highly alkaline conditions (Yan and Schwartz, 1999; Kao et al., 2008; Siegrist et al., 2011). Several studies also show that manganese may be present as Mn^{+6} under high pH conditions (Siegrist et al., 2011). Since groundwater pH generally remains within the range of 4.0 to 8.0 during ISCO applications using permanganate, Equation 1.1 can be the dominate permanganate reaction, in which case manganese dioxide would be produced (Kao et al., 2008; Siegrist et al., 2011).

Under typical groundwater conditions, the oxidation of TCE, ethanol, and toluene by potassium permanganate occurs according to the following equations:

$$C_2HCl_{3(aq)} + 2KMnO_{4(aq)} \rightarrow 2K^+ + 3Cl^- + 2MnO_{2(s)} + H^+ + 2CO_{2(g)} \quad (1.4)$$

$$C_2H_5OH_{(aq)} + 4KMnO_{4(aq)} + 4H^+ \rightarrow 4K^+ + 4MnO_{2(s)} + 2CO_{2(g)} + 5H_2O \quad (1.5)$$

$$C_6H_5CH_{3(aq)} + 12KMnO_{4(aq)} + 12H^+ \rightarrow 12K^+ + 12MnO_{2(s)} + 10H_2O + 7CO_{2(g)} \quad (1.6)$$

As shown by Equations 1.4 to 1.6, the stoichiometric requirement for oxidizing one mole of TCE, ethanol, or toluene is 2.0, 4.0, or 12.0 moles of permanganate, respectively. These balanced redox reactions may indicate that the oxidant demand of the target compounds is correlated with not only their structure, and but also with chemical bonds.

The kinetics of oxidation reactions is an important ISCO remediation design aspect that affects the efficiency and oxidant persistence in the subsurface. Several studies have provided data on the oxidation of the target compounds by potassium permanganate, TCE (Huang et al., 2001; Kao et al., 2008; Siegrist et al., 2001; Waldemer and Tratnyek, 2006), toluene (Rudakov and Lobachev, 2000; Waldemer and Tratnyek, 2006), and ethanol (Barter and Littler, 1967). The second-order reaction rate constants for the oxidation of the target compounds by potassium permanganate and their corresponding experimental conditions are given in Table 1.4. The data clearly show that the second-order reaction rate constants of TCE are higher than those of ethanol and toluene.

1.6. Permeable reactive barrier (PRB)

A permeable reactive barrier (PRB) can be an effective technology for treating soil and groundwater contaminated by heavy metals (Blowes et al., 1997; Puls et al., 1995; Navarro et al., 2006; Moraci and Calabrò, 2010), halogenated organics (Gillham and O'Hannesin, 1992, 1994), gasoline derivatives (Bianchi-Mosquera et al., 1994; Yeh et. al, 2010), dissolved nutrients (Robertson and Cherry, 1995; Baker et al., 1996; Liu et al., 2013), and acid mine drainage (Benner et al., 1997; Waybrant et al., 1998; Benner et al., 1999; Cisse and Bezbaruah, 2012; Gibert et al., 2013). A PRB typically is the emplacement of a reactive medium in the subsurface for the purpose of treating a contaminated plume and transforming the contaminants into environmentally acceptable forms (Moraci and Calabrò, 2010; Yeh et al., 2010; Liu et al., 2013). As shown in Fig. 1.3, the plume is constrained to move through the reactive material (typically under a natural gradient) where the contaminants are transformed into less harmful (non-toxic) species, are immobilized, or are changed into readily biodegradable species (USAPA, 1998; Thiruvenkatachari et al., 2008; Liu et al., 2013).

A PRB is not a barrier to groundwater flow, but a barrier to contaminant transport (Liu et al., 2013). PRBs commonly are more permeable than the aquifer materials. Hence, the contaminants are able to pass through the PRB without significant changes in the groundwater flow regime (Thiruvenkatachari et al., 2008). Reactive materials within PRBs mainly react with contaminants to decrease their concentrations through physical, chemical or biological processes (Thiruvenkatachari et al., 2008; Yeh et al., 2010). The main processes in a PRB are:
(1) degradation or decomposition through chemical or biological reactions, leading to environmentally more acceptable constituents, (2) precipitation of contaminants through the formation of insoluble compounds within the PRB, and (3) sorption of contaminants within the reaction zone by adsorption or complexation. The chemical status of the contaminants in the latter two cases is not changed.

Table 1.4: Second-order rate constants and corresponding experimental conditions for the oxidation of TCE, toluene, and ethanol with potassium permanganate in the aqueous phase.

VOC	[VOC] (mM)	[$KMnO_4$] (mM)	pH	T (°C)	k ($M^{-1}s^{-1}$)	Reference
TCE	0.1	6.3	4.0 - 8.0	21.0	0.65-0.68	Yen and Schwartz (2000)
	0.14 ± 0.0 7	1.9 ± 0.07	7.0	20.0	0.8 ± 0.12	Huang et al. (2001)
	NA	NA	6.9	20.0	0.89	Siegrist et al. (2001)
	1.0 - 4.0	0.1	7.0	25.0	0.76 ± 0.03	Waldemer and Tratnyek (2006)
	0.038-0. 15	0.076-0.76	6.3	25.0	0.8	Kao et al. (2008)
	0.29	6.3	NA	20.0	0.95	Urynowicz (2008)
Toluene	4.0	0.1	7.0	25.0	83.2×10^{-5}	Waldemer and Tratnyek (2006)
	NA	NA	5.0 - 7.0	20.0	23.0×10^{-5}	Rudakov and Lobachev (2000)
	NA	NA	5.0 - 7.0	30.0	61.0×10^{-5}	Rudakov and Lobachev (2000)
Ethanol	171.5	9.2	4.6	20.0	16.7×10^{-4}	Barter and Littler (1967)
	171.5	9.2	4.6	30.0	40.3×10^{-4}	Barter and Littler (1967)

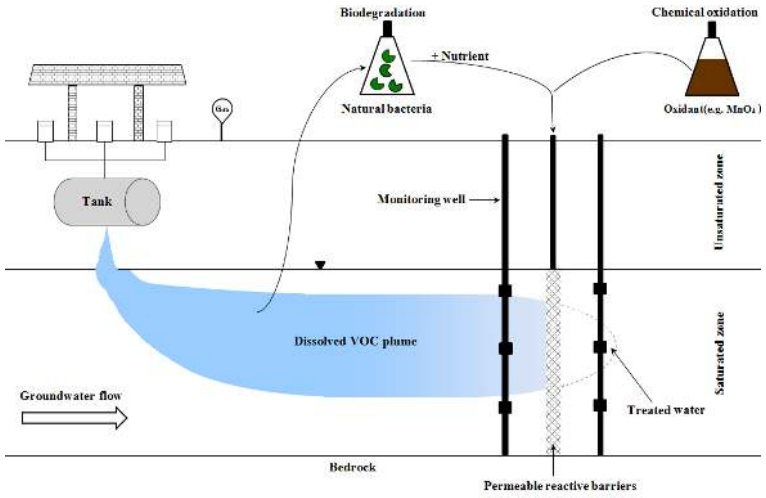

Fig. 1.3: Schematic view of a PRB.

1.6.1. PRB configurations

PRBs can be classified into two general categories: vertical and horizontal PRBs depending upon their direction relative to the soil surface. Vertical PRBs (VPRBs) are widely used for remediation of contaminants in the saturated zone (Fig. 1.3). They have been constructed using two different configurations: ordinary methods (e.g., continuous trench or wall and funnel and gate methods) and advanced methods (e.g., injection systems, hydraulic or pneumatic fracturing, and passive groundwater capture and treatment by reactor cells). The choice between these two configurations for constructing a VPRB depends upon many factors including the type of contaminants present and the reactive material, the concentration of the contaminants, the cost of the reactive material, the hydrogeological and geological characteristics of the site, and the depth of plume in the subsurface (Thiruvenkatachari et al., 2008; Comba et al., 2011).

Among the various PRB construction methods, injection methods and hydraulic or pneumatic fracturing approaches, further explained below, have proved to be more effective in delivering reactive materials to the subsurface. An injection system is an effective and common method for constructing PRBs and hence delivering reactive materials into the subsurface. Using this method, a series of boreholes or injection wells is first drilled into the contaminated zone boundaries (Truex et al., 2011). Reactive materials including oxidants (for chemical oxidation purposes) or nutrients and oxygen (for biodegradation purposes) are subsequently injected through the boreholes or wells to create a reaction zone (Hesemann and Hildebrandt, 2009; Cronk et al., 2010; Comba et al., 2011; Truex et al., 2011). The method does not require any excavation of soil in order to create a trench. Moreover, the method is applicable to deep contaminated zones. However, by-passing or fingering phenomena during its operation may affect the effectiveness of the injection method (Thiruvenkatachari et al., 2008).

Fracturing technology, either hydraulic or pneumatic using pumped water or air under high pressure, can be used to create fractures into rock and clay or any

low permeable formation. When the confining pressures are exceeded in the boreholes, relatively wide fractures may open and grow laterally or horizontally from the initiation point (Thiruvenkatachari et al., 2008; Stroo and Ward, 2010). Reactive materials, such as slurry or coated solid oxidants, are then introduced through these fractures into the contaminated zone (Thiruvenkatachari et al., 2008; Stroo and Ward, 2010; Comba et al., 2011). The main advantages of this technique are its ability to treat deep-contaminated zones, its relatively low-operation cost, and negligible disturbance of the near surface. However, the method has also several disadvantages such as difficulties in controlling fracture directions, which could lead to non-uniform distributions of the reactive materials, as well as its use being limited to low-permeable formations (Thiruvenkatachari et al., 2008; Stroo and Ward, 2010; Comba et al., 2011).

1.6.2. Horizontal permeable reactive barrier (HPRB)

At many contaminated sites (particularly contaminated unsaturated zones), vertical leaching or volatilization of contaminants and subsequent upward migration of VOCs can cause undue exposure and unacceptable human health or environmental risks. An alternative remediation method for treating these sites is to place reactive materials horizontally into the subsurface. Horizontal PRBs (HPRBs) have been employed recently in the unsaturated zone to limit or avoid any vertical leaching of VOCs. Below we describe four examples of possible HPRB uses.

Leaching and subsequent off-site migration of metals from treated unsaturated soil to groundwater is one of the most important limitations for increasing the use of phytoextraction in the unsaturated zone (Mackova et al., 2006). The use of a HPRB can efficiently prevent the leaching of heavy metals (e.g., As or Pb) during phytoextraction. This method can transform metal complexes into metal ions and as such increase adsorption of the metal onto soil grains. This approach enhances the biodegradation of heavy metal complexes and limits or prevents metal leaching (Mackova et al., 2006).

Some nutrients (such as phosphate and ammonium) and pharmaceutical or personal care products are not fully removed from water by conventional wastewater treatment methods. Since treated wastewater effluents are generally used in artificial recharge schemes, they are able to pollute groundwater with untreated contaminants. Hence, a HPRB in the unsaturated zone may be an effective method for removing remaining contaminants from treated wastewater effluents. Leal et al. (2013) evaluated the ability of zeolite in a HPRB to remove nutrients and personal care products from treated wastewater effluent in the unsaturated zone.

Horizontal wells are often used for injecting nutrients or oxygen into the saturated zone to enhance the biodegradation of liquid, dissolved, and adsorbed contaminants (Brockman et al., 1995; USDE, 1995; Hohener and Ponsin 2014). However, the literature has shown that horizontal wells can be used also for bioventing applications in the unsaturated zone (Mendoza et al., 1996). Hence, introducing nutrients or oxygen through horizontal wells into the unsaturated zone could be an option for creating a horizontal bio-reactive zone as a HPRB against the migration here of contaminants.

Soil fracturing techniques (by hydraulic or pneumatic fluids) have been used to evaluate the feasibility of creating HPRBs for emplacement of chemically reactive solids into the subsurface (Siegrist et al., 2001; Stroo and Ward, 2010).

Several studies focusing on soil mixing and hydraulic fracturing have been conducted also during the past decade to create a HPRB in the unsaturated zone (Siegrist et al., 2001; Stroo and Ward, 2010). Deep soil mixing, as a conventional method for constructing a HPRB, has been used with both hydrogen peroxide and permanganate. Development of direct push injection as a delivery method has been an important factor for ISCO applications in the unsaturated zone (Frazier et al., 2004). This technique allows for the rapid application of oxidants. Conventional injection methods using either vertical or horizontal wells can be employed to deliver reactive materials (e.g., solid oxidants, nutrients, and oxygen) into the unsaturated zone (Siegrist et al., 2001; Stroo and Ward, 2010). Moreover, hydraulic or pneumatic fracturing as an alternative method has been used to place solid permanganate or a permanganate-clay mixture horizontally in the unsaturated zone

(Siegrist et al., 2001; Stroo and Ward, 2010). Horizontal wells can also be employed for shallow or thin contaminant plumes, or for plumes beneath buildings or other constructions in urban areas (Stroo and Ward, 2010). However, while both conventional and advanced methods have been used for constructing HPRBs in the unsaturated zone, injection system and hydraulic or pneumatic fracturing approaches seem to be more effective.

Although a number of techniques (e.g., soil vapor extraction and bioventing) have been used successfully for treating VOC vapours in the unsaturated zone, they all suffer from shortcomings (e.g., requiring long-term operation and maintenance, and the high costs involved). Current literature lacks information about the feasibility of using HPRBs containing solid oxidant for oxidizing VOC vapours in the unsaturated zone and hence preventing their upward movement (Fig. 1.4). For this reason we investigated the possibility of using solid potassium permanganate in a partially saturated HPRB for oxidizing VOC vapours.

1.7. Research objectives

The goal of this study was to evaluate the potential of solid potassium permanganate to create a HPRB for oxidizing VOC vapours under partially saturated conditions. To achieve this goal, a series of batch and column experiments was performed. Specific objectives of the research were as follows:

(1) To study the ability of solid potassium permanganate to fully oxidize TCE, ethanol, and toluene vapours.

(2) To determine kinetic parameters of TCE, ethanol, and toluene vapour oxidation by solid potassium permanganate.

(3) To establish a suitable kinetic reaction rate model for oxidation of VOCs in the aqueous phase.

(4) To determine the oxidation kinetic parameters of dissolved TCE, toluene, and ethanol by aqueous permanganate.

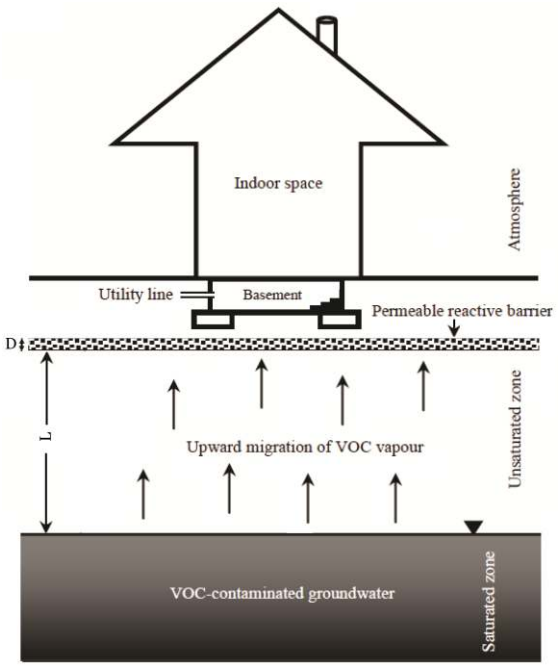

Fig. 1.4: A conceptual model for preventing vapour intrusion by a horizontal permeable reactive barrier.

(5) To evaluate the ability of solid potassium permanganate as a HPRB to oxidize the vapour of three VOCs under various degrees of water saturation.

(6) To investigate the impact of the accumulation of reaction products on the long-term reactivity of potassium permanganate in a HPRB.

(7) To study the effect of some minerals (e.g., calcium carbonate) and adding water on the reactivity of potassium permanganate in a HPRB.

(8) To investigate the effect of the HPRB thickness on the oxidation process.

(9) To evaluate the impact of a HPRB location relative to the water table on the long-term reactivity of the barrier.

(10) To numerically simulate the migration and oxidation process of VOCs in a HPRB.
(11) To obtain an approximate estimate of the reactivity of potassium permanganate within a HPRB.

1.8. Thesis outline

This thesis is organized in six chapters, with four core chapters (Chapters 2 to 5) written as stand-alone manuscripts.

Chapter 1 is devoted to a brief introduction of VOCs, vapour intrusion, fate and transport processes of VOCs in the unsaturated zone, remediation techniques for VOCs in the unsaturated zone, HPRBs, and delineation of the main objectives of this thesis.

Chapter 2 deals with the ability of solid potassium permanganate to oxidize VOC vapours. This chapter provides data on the reaction between potassium permanganate grains and vapour phase of TCE, ethanol, and toluene. It also shows that the oxidation process can be modelled using a kinetic model, linear in the gas concentration of VOC and the relative surface area of potassium permanganate grains (surface area of potassium permanganate divided by gas volume). Finally, the reaction rate constants for TCE, ethanol, and toluene vapours by potassium permanganate grains are estimated.

Chapter 3 presents the oxidation kinetics of aqueous TCE, ethanol, and toluene with aqueous potassium permanganate. Overall second-order rate constants are determined by direct fitting of a second-order model to the experimental data, instead of using a pseudo-first-order approach as is done typically in the literature. Evidence is provided that inappropriate use of the pseudo-first-order approach in several previous studies produced biased estimates of the second-order rate constants. In this chapter, the error is expressed as a function of the extent in which

the reactant concentrations deviate from the stoichiometric ratio of each oxidation reaction (P/N). The error associated with the inappropriate use of the pseudo-first-order approach was found to be negatively correlated with the P/N ratio and reached up to 25% of the estimated second-order rate constant in some previous studies of TCE oxidation.

Chapter 4 deals with the ability of solid potassium permanganate as a horizontal permeable reactive barrier (HPRB) for oxidizing the vapour of three VOCs under various degrees of water saturation. The impact of accumulated by-products on the long-term reactivity of the permeable reactive layer (PRL) is discussed also. Research documented in this chapter indicates that adding water and the use of carbonate minerals increases the reactivity of potassium permanganate during the oxidation of TCE vapour. Reactive transport of VOC vapours diffusing through the PRL was modelled, including the pH effect on the oxidation rates. A linear increase in total oxidized mass of VOCs with initial water saturation was found. The life time of the PBR based on 1D homogenous column experiments was estimated.

Chapter 5 is devoted to the transport and oxidation of VOC vapours under unsaturated conditions within a sand column of 30.0 cm length and 5.0 cm thickness. The effects of HPRB thickness, location of the HPRB above the water table, and water availability on removal oxidation are discussed. In this chapter, the migration of VOC vapours through the unsaturated soil and the HPRB was simulated numerically.

Chapter 6 presents a summary and conclusions of this research, as well as suggestions for future work.

1.9. References

[1] Albergaria, J.T., Alvim-Ferraz, M.dc.M, Delerue-Matos, C., 2012. Remediation of sandy soils contaminated with hydrocarbons and halogenated hydrocarbons by

soil vapour extraction. Environ. Manage. 104: 195-201.

[2] ATSDR (Agency for Toxic Substances and Disease Registry), 1994. Toxicological Profile for Toluene (Update). ATDSR, Atlanta, US.

[3] Baciocchi, R., D'Aprile, L., Innocenti, I., Massetti, F., and Verginelli, I., 2014. Development of technical guidelines for the application of in-situ chemical oxidation to groundwater remediation. J. Clean. Prod. 77: 47-55.

[4] Badawi, A.F., Cavalieri, E.L., and Rogan, E.G., 2000. Effect of chlorinated hydrocarbons on expression of cytochrome P450 1A1, 1A2 and 1B1 and 2-and 4-hydroxylation of 17β-estradiol in female Sprague-Dawley rats. Carcinogenesis. 21(8): 1593-1599.

[5] Baker, M.J., Blowes, D.W., and Ptacek, C.J., 1996. Development of a reactive mixture to remove phosphorous from on-site wastewater disposal systems. In Disposal Trenches, Pre-treatment and Re-use of Wastewater. Waterloo Centre for Groundwater Research Annual Septic System Conference, May 13. 51-60.

[6] Barter, R.M., and Littler, J.S., 1967. Hydride ion transfer in oxidations of alcohols and ethers. Chem. Soc. B. 205-10.

[7] Bassam, N.El., 2010. Handbook of Bioenergy Crops: A Complete Reference to Species, Development and Applications. Publisher: Taylor & Francis.

[8] Batterman, S., Kulshrestha, A., and Cheng, H.Y., 1995. Hydrocarbon vapor transport in low moisture soils. Environ. Sci. Technol. 29(1): 171-180.

[9] Bell, K.Y., and LeBoeuf, E.J., 2013. Influence of temperature and macromolecular mobility on sorption of TCE on humic acid coated mineral surfaces. Chemosphere 90: 176-181.

[10] Benner, S.G., Blowes, D.W., and Ptacek, C.J., 1997. Sulfate reduction in a permeable reactive wall for prevention of acid mine drainage. In Proc. 213th Am. Chem. Soc. Natl Mtg, Environ. Chem. Div., San Francisco, CA, April 13-17, 37(1): 140-141.

[11] Benner, S.G., Blowes, D.W., and Ptacek, C.J., 1999. A full-scale porous reactive wall for prevention of acid mine drainage. Groundwater Monit. R. 17(4): 99-107.

[12] Berscheid, M., Burger, K., Hutchison, N., Muniz-Ghazi, H., Renzi, B., Ruttan, P., and Sterling, S., 2010. Proven technologies and remedies guidance: remediation of chlorinated volatile organic compounds in vadose zone soil. California Department of Toxic Substances Control. http://www.dtsc.ca.gov/sitecleanup /upload/cVOC_040110.pdf.

[13] Blowes, D.W., Ptacek, C.J., and Jambor, J.L., 1997. In-Situ remediation of chromate contaminated groundwater using permeable reactive walls. Environ. Sci. Technol. 31: 3348-3357.

[14] Bianchi-Mosquera, G.C., Allen-King, R.M., and Mackay, D.M., 1994. Enhanced degradation of dissolved benzene and toluene using a solid oxygen-releasing compound. Ground Water Monit. Remediat. 120-128.

[15] Breus, I.P., and Mishchenko, A.A., 2006. Sorption of volatile organic contaminants by soils (a review). Eurasian Soil. Sci. 39: 1271-1283.

[16] Briaud, J.L., 2013. Geotechnical Engineering: Unsaturated and Saturated Soils. John Wiley & Sons, Inc.

[17] Brockman, F.J., Payne, W., Workman, D.J., Soong, A., Manley, S., and Hazen, T.C.,1995. Effect of gaseous nitrogen and phosphorus injection on in situ bioremediation of a trichloroethylene-contaminated site. J. Hazard. Mater. 41: 287-298.

[18] Bryant, D., Battey, T., Coleman, K., Mullen, D., and Oyelowo, L., 2001. Permanganate in-situ chemical oxidation of TCE in a fractured bedrock aquifer, Edwards Air Force Base, California. The First International Conference on Oxidation and Reduction Technologies for In-Situ Treatment of Soil and Groundwater, June 25-29, Niagara Falls, Ontario, Canada.

[19] Capiro, N.L., Stafford, B.P., Rixey, W.G., and Bedient, P.B., Alvarez, P.J.J., 2007. Fuel-grade ethanol transport and impacts to groundwater in a pilot-scale aquifer tank. Water Res. 41: 656-664.

[20] Cave, L., Hartog, N., Al, T., Parker, B., and Mayer, K.U., Cogswell, S., 2007. Electrical monitoring of in situ chemical oxidation by permanganate. Ground Water Monit. R. 27(2): 77-84.

[21] Cho, H.J., Jr., R.J.F., and Daly, M. H., 2002. Soil vapour extraction and chemical oxidation to remediate chlorinated solvents in fractured crystalline bedrock: pilot study results and lessons learned, Remediation J. 12(2): 35-50.

[22] Cisse, S., and Bezbaruah, A., 2012. Permeable reactive barriers to treat iron ore acid mine drainage. Proceeding of World Environmental and Water Resources Congress. New Mexico. May 20-24: 110-115.

[23] Comba, S., Di Molfetta, A., and Sethi, R., 2011. A Comparison between field applications of nano-, micro-, and millimetric zero-valent iron for the remediation of contaminated aquifers .Water Air Soil Pollut. 215: 595-607.

[24] Cook, S.M., 2009. Assessing the Use and Application of Zero-Valent Iron Nanoparticle Technology for Remediation at Contaminated Sites. Report for USEPA (United state Environmental Protection Agency). Office of Solid Waste and Emergency, Washington, DC. www.clu-in.org/download/studentpapers/zero-valent-iron-cook.pdf.

[25] Costa, A.S., Romo, L.P.C., Arauo, B.R., Lucas, S.C.O., Maciel, S.T.A., Wisniewski Jr., A., and Alexandre, M.R., 2012. Environmental strategies to remove volatile aromatic fractions (BTEX) from petroleum industry wastewater using biomass. Bioresource Technol. 105: 31-39.

[26] Costanza-Robinson, M.S., Carlson, T.D., and Brusseau, M.L., 2013. Vapor-phase transport of trichloroethene in an intermediate-scale vadose-zone system: Retention processes and tracer-based prediction. J. Contam. Hydrol. 145: 82-89.

[27] Cronk, G., Koenigsberg, S., Coughlin, B., Travers, M., and Schlott, D., 2010. Controlled vadose zone saturation and remediation (CVSR) using chemical oxidation, 7th International Conference on Remediation of Chlorinated and Recalcitrant Compounds. May 24-27. Battelle Press, Columbus, OH. 8.

[28] Damm, J.H., Hardacre, C., Kalin, R.M., and Walsh, K.P., 2002. Kinetics of the oxidation of methyl tert-butyl ether (MTBE) by potassium permanganate. Water Res. 36: 3638-3646.

[29] De Nevers, N., 2000. Air Pollution Control Engineering, 2nd edition. McGraw-Hill International, Boston.

[30] DeVaull, G.E., 2007. Indoor vapor intrusion with oxygen-limited biodegradation for a subsurface gasoline source. Environ. Sci. Technol. 41(9): 3241-3248.

[31] DeVaull, G.E., Ettinger, R.A., Salanitro, J.P., and Gustafson, J.B., 1997. Benzene, toluene, ethylbenzene and xylenes (BTEX) degradation in vadose zone soils during vapor transport: first-order rate constants, Proceedings of the Petroleum Hydrocarbons and Organic Chemicals in Ground Water: Prevention, Detection and Remediation Conference, API/NGWA. Ground Water Publishing Company, Westerville, Ohio, 365-379.

[32] Dobaradaran, S., Lutze, H., Mahvi, A.H., and Schmidt, T.C., 2014. Transformation efficiency and formation of transformation products during photochemical degradation of TCE and PCE at micromolar concentrations. Iran. J. Environ. Healt. 12 (16): 1-10.

[33] EPA (Environmental protection agency), 1998. NATO/CCMS Pilot Study: Evaluation of Demonstrated and Emerging Technologies for the Treatment of Contaminated Land and Groundwater (Phase III). Special Session: Treatment Walls and Permeable Reactive Barrier. EPA report: EPA 542-R-98-003.

[34] EPA (Environmental Protection Agency), 1999. Alternative Disinfectants and Oxidants; Guidance Manual. Chapter 5.www.epa.gov/ogwdw/mdbp/pdf/alter/chapt_5.pdf.

[35] EPA (Environmental Protection Agency), 2004. Chemical Oxidation; Chapter XIII. Guidance Manual. www.epa.gov/oust/pubs/tum_ch13.pdf.

[36] EPA (Environmental Protection Agency), 2011. Toxicological Review of Trichloroethylene. CAS No. 79-01-6.

[37] EPA (Environmental Protection Agency), 2012. Petroleum hydrocarbons and chlorinated hydrocarbons differ in their potential for vapour intrusion. Office of Underground Storage Tanks, Washington, D.C. 20460. www.epa.gov/oust/cat/pvi/pvicvi.pdf.

[38] EuroChlor (European Chloroalkali Industry), 2008. Chlorine industry review 2007-2008, Euro Chlor, Bruxelles, BE.

[39] Fairley, J.P., Solomon, M.D., Hinds, J.J., Grader, G.W., Bush, J.H., and Rand, A.L., 2006. Latah county hydrologic characterization project. Final report. www.webs.uidaho.edu/pbac/pubs/HCP_FinalReport.pdf.

[40] Fan, C.Y., Krishnamurthy, S., 1995. Enzymes for enhancing bioremediation of petroleum-contaminated soils: a brief review. J. Air Waste Manage. Assoc. 45: 453-460.

[41] Farhadian, M., Vachelard, C., Duchez, D., and Larroche, C., 2008. In situ bioremediation of monoaromatic pollutants in groundwater: a review. Bioresource Technol. 99: 5296-5308.

[42] Farrell, J., and Reinhard, M., 1994. Desorption of halogenated organics from model solids, sediments, and soil under unsaturated conditions. 1. Isotherms. Environ. Sci. Technol. 28(1): 53-62.

[43] Forsey, S.P., 2004. In Situ Chemical Oxidation of Creosote/Coal Tar Residuals : Experimental and Numerical Investigation. PhD. thesis, University of Waterloo.

[44] Frank F.A., 2011. Vapour Intrusion, Dealing with Contaminated Sites: From Theory towards Practical Application. Published by Spinger.

[45] Frazier, J.D., Fiacco, Jr.R.J., Pac, T., Lewis, R., Flattery, J., Madera, E.P., 2004. Physical distribution of injected oxidants within saturated soils for three injection strategies. Proceedings, Third International Conference on Oxidation and Reduction Technologies for In Situ Treatment of Soil and Groundwater, San Diego, CA, USA, October: 24-28.

[46] Freitas, J.G., 2009. Impacts of Ethanol in Gasoline on Subsurface Contamination. PhD thesis. University of Waterloo, Waterloo Ontario, Canada.

[47] Freitas, J.G., Fletcher, B., Aravena, R., and Baker, J.F., 2010. Methane production and isotopic fingering in ethanol fuel contaminated sites. Groundwater 48: 844-857.

[48] Gardner, K.A., 1996. Permanganate Oxidations of Aromatic Hydrocarbons in Aqueous and Organic Solution. PhD thesis, University of Washington.

[49] Gibert, O., Cortina, J.L., de Pablo, J., and Ayora, C., 2013. Performance of a field-scale permeable reactive barrier based on organic substrate and zero-valent

iron for in situ remediation of acid mine drainage. Environ. Sci. Pollut. Res. 20: 7854-7862.

[50] Gillham, R.W., and O'Hannesin, S.F., 1992. Metal-catalysed abiotic degradation of halogenated organic compounds. In Proc. 1992 IAH conference "Modern Trends in Hydrogeology", Hamilton, Ont., May 10-13.

[51] Gillham, R.W., and O'Hannesin, S.R., 1994. Enhanced degradation of halogenated aliphatics by zero-valent iron. Groundwater 32 (6): 958-967.

[52] Heiderscheidt, J.L., Crimi, M., Siegrist, R.L., and Singletary, M.A., 2008. Optimization of full-scale permanganate ISCO system operation: Laboratory and numerical studies. Groundwater Monit. R. 28(4): 72-84.

[53] Hers, I., Atwater, J., Li, L., and Gilje, R.Z., 2000. Evaluation of vadose zone biodegradation of BTX vapours. J. Contam. Hydro. 46: 233-264.

[54] Hesemann, J.R., and Hildebrandt, M., 2009. Successful unsaturated zone treatment of PCE with sodium permanganate. Remediation J. 19(2): 37-48.

[55] Hinchee, R.E., 1993. Bioventing of Petroleum Hydrocarbons, Handbook of Bioremediation, CRC Press Inc.

[56] Hohener, P., and Ponsin, V., 2014. In situ vadose zone bioremediation. Current Opinion in Biotechnology, 27: 1-7.

[57] Hood, E.D., Thomson, N.R., Grossi, D., Farquhar, G.J., 2000. Experimental determination of the kinetic rate law for the oxidation of perchloroethylene by potassium permanganate. Chemosphere 40: 1383-1388.

[58] Huang, K.C., Hoag, G.E., Chheda, P., Woody, B.A., and Dobbs, G.M., 1999. Kinetic study of oxidation of trichloroethylene by potassium permanganate. Environ. Eng. Sci. 16: 265-274.

[59] Huang, K.C., Hoag, G.E., Chheda, P., Woody, B.A., and Dobbs, G.M., 2001. Oxidation of chlorinated ethenes by potassium permanganate: a kinetics study. Hazard. Mater. 87: 155-169.

[60] Huling, S.G., and B., Pivetz, 2006. In situ chemical oxidation-engineering issue. EPA/600/R-06/072.

[61] Jaky, M., Szammer, J., Simon-Trompler, E., 2000. Kinetics and mechanism of the oxidation of ketones with permanganate ions. J. Chem. Soc. Perkin Trans. 2: 1597-1602.

[62] Jin, Z., Gui-bai, L., and Jun, M., 2003. Effects of chlorine content and position of chlorinated phenols on their oxidation kinetics by potassium permanganate. Environ. Sci. 15: 342-345.

[63] Johnson, R., Pankow, D., Bender, C.P., and Zogorski, J., 2000. Target compounds-to what extent will past releases contaminate community water supply wells? Environ. Sci. Technol. 34: 210A-217A.

[64] Kao, C.M., Huang, K.D., Wang, J.Y., Chen, T.Y., and Chien, H.Y., 2008. Application of potassium permanganate as an oxidant for in-situ oxidation of trichloroethylene-contaminated groundwater: A laboratory and kinetics study. Hazard. Mater. 153: 919-927.

[65] Kang, N., Hua, I., and Rao, P.S., 2004. Production and characterization of encapsulated potassium permanganate for sustained release as an in-situ oxidant. Ind. Eng. Chem. Res. 43(17): 5187-5193.

[66] KDHE (Kansas Department of Health and Environment), 2007. Kansas Vapor Intrusion Guidance; Chemical Vapor Intrusion And Residential Indoor Air. www.kdheks. gov/ ber/ download/Ks_VI_Guidance.pdf

[67] Kim, H.H., Ogata, A., and Futamura, S., 2007. Complete oxidation of volatile organic compounds (VOCs) using plasma-driven catalysis and oxygen plasma. Int. J. Plasma Environ. Sci. Technol. 1: 46-51.

[68] Komárek, M., Vanek, A., and Ettler, V., 2013. Chemical stabilization of metals and arsenic in contaminated soils using oxides; A review. Environ. Pollut. 172: 9-22.

[69] Kotvis, J.A., 2011. Emerging Trend: Vapor intrusion and its impact on real sstate transactions and liability. Presented: Dallas Bar Association Real Property Law Section. Dallas, Texas. www.dallasbar.org/system/files/2011_september_ presentation.pdf?...1.

[70] Kristensen, E., 1995. Aerobic and anaerobic decomposition of organic matter in marine sediment: Which is fastest? Limnol. Oceanogr. 40(8): 1430-1437.

[71] Lahvis, M.A., Baehr, A.L., and Baker, R.J., 1999. Quantification of aerobic biodegradation and volatilization rates of gasoline hydrocarbons near the water table under natural attenuation conditions. Water Resour. Res. 35(3): 753-765.

[72] Langevoort. M. 2009. Multiphase flow and enhanced biodegradation of dense non-aqueous phase liquids. PhD thesis, Utrecht University.

[73] Leal, M., Martínez-Hernández, V., Lillo, J., Meffe, R., and de Bustamante, I., 2013. Zeolite in horizontal permeable reactive barriers for artificial groundwater recharge. Geophysical Research Abstracts, Vol. 15, EGU2013-924: http://meeting organizer.copernicus.org/EGU2013/EGU2013-924.pdf.

[74] Lens, P., Grotenhuis, T., Malina, G., and Tabak, H., 2005. Soil and Sediment Remediation: Mechanisms, Technologies and Applications. Published by IWA Publishing.

[75] Li, H., and Jiao, J., 2005. One-dimensional airflow in unsaturated zone induced by periodic water table fluctuation. Water Resour. Res.41:W04007.

[76] Liang, S.H., Chen, K.F., Wu, C.S., Lin, Y.H., Kao, C.M., 2014. Development of $KMnO_4$-releasing composites for in situ chemical oxidation of TCE-contaminated groundwater. Water Res. 54:149-158.

[77] Liu, S.J., Zhao, Z.Y., Li, J., Wang, J., and Qi, Y., 2013. An anaerobic two-layer permeable reactive bio-barrier for the remediation of nitrate contaminated groundwater. Water res. 47: 5977-5985.

[78] Lundegard, P.D., Johnson, P.C., and Dahlen, P., 2008. Oxygen transport from the atmosphere to soil gas beneath a slab-on-grade foundation overlying petroleum impacted soil. Environ. Sci. Technol. 42(15): 5534-5540.

[79] MacKinnon, L.K., Thomson, N.R., 2002. Laboratory-scale in situ chemical oxidation of a perchloroethylene pool using permanganate. J. Contam. Hydrol. 56: 49-74.

[80] Mackova, M., Dowling, D., and Macek, T., 2006. Focus on biotechnology; Phytoremediation and Rhizoremediation, Published by Springer.

[81] Massmann, J., and Farrier, D.F., 1992. Effects of atmospheric pressure on gas transport in the vadose zone. Water Resour. Res. 28: 777-791.

[82] Mora, V.C., Madueño, L., Peluffo, M., Rosso, J.A., Del Panno, M.T., and Morelli, I.S., 2014. Remediation of phenanthrene-contaminated soil by simultaneous persulfate chemical oxidation and biodegradation processes. Environ. Sci. Pollut. Res. 21:7548-7556.

[83] Moraci, N., and Calabrò, P.S., 2010. Heavy metals removal and hydraulic performance in zero-valent iron/pumice permeable reactive barriers. J. Environ. Manage. 9: 2336-2341.

[84] Mendoza, C., Armstrong, J., Gilmour, S., and Atkinson, D., 1996. Vadose-Zone Remediation of Hydrocarbon-Contaminated Gas Plant Sites in Alberta. Oil and Gas Pools of the Western Canada Sedimentary Basin: Program and Abstracts, 33-33.http://archives.datapages.com/data/ meta/ cspg_sp/data/019/019001/pdfs/33 _firstpage.pdf.

[85] NAS (National Academy of Science), 1971. Chlorinated hydrocarbons: a report by National Research Council (U.S.) Panel on Monitoring Persistent Pesticides in the Marine Environment.

[86] Navarro, A., Chimenos, J.M., Muntaner, D., and Fernandez, A.I., 2006. Permeable reactive barriers for the removal of heavy metals: lab-scale experiments with low-grade magnesium oxide. Ground Water Monit. R. 26(4): 142-152.

[87] Ong, S.K., and Lion, L.W., 1991. Effects of soil properties and moisture on the sorption of trichloroethylene vapor. Water Res. 25(1): 29-36.

[88] Oturan, M.A., and Aaron, J.J., 2014. Advanced oxidation processes in water/waste water treatment: Principles and applications. A Review. Environ. Sci. Technol., DOI: 10.1080/10643389.2013.829765.

[89] Parker, B.L., 2002. Full-scale permanganate remediation of a solvent DNAPL source zone in a sand aquifer. Presented at the EPA Seminar, In Situ Treatment of Groundwater Contaminated with Non-Aqueous Phase Liquids, Chicago, Illinois. http://cluin.org/studio /napl_121002/agenda.cfm.

[90] Pasteris, G., Werner, D., Kaufmann, K., and Hohener, P., 2002. Vapor phase transport and biodegradation of volatile fuel compounds in the unsaturated zone: A large scale lysimeter experiment. Environ. Sci. Technol. 36: 30-39.

[91] Petri, B.G., 2006. Impacts of Subsurface Permanganate Delivery Parameters on Dense Non-aqueous Phase Liquid Mass Depletion Rates. Colorado School of Mines.

[92] Picone, S., 2012. Transport and biodegradation of volatile organic compounds: influence on vapor intrusion into buildings. PhD thesis. Wageningen University, The Netherlands.

[93] Puls, R.W., Powell, R.M., and Paul, C.J., 1995. In situ remediation of ground water contaminated with chromate and chlorinated solvents using zero-valent iron: A field study. 209th ACS National Meeting. April 2-7, Anaheim, California.

[94] Rastkari, N., Yunesian, M., and Ahmadkhaniha, and R., 2011. Exposure assessment to trichloroethylene and perchloroethylene for workers in the dry cleaning industry. Bull Environ. Contam. Toxicol. 86: 363-367.

[95] Rivett, M.O., Wealthall, G.P., Dearden, R.A., and McAlary, T.A., 2011. Review of unsaturated-zone transport and attenuation of volatile organic compound (VOC) plumes leached from shallow source zones. Contam. Hydrol. 123: 130-156.

[96] Robertson, W.D., and Cherry, J.A., 1995. In situ denitrification of septic-system nitrate using reactive porous media barriers: Field trials. Groundwater 33: 99-111.

[97] Romantschuk, M., Sarand, I., Petanen, T., Peltola, R., Jonsson-Vihanne, M., Koivula,T., Yrjala, K., and Haahtela, K., 2000. Means to improve the effect of in situ bioremediation of contaminated soil: an overview of novel approaches. Environ Pollut. 107: 179-185.

[98] Ross, C., Murdoch, L.C., Freedman, D.L., and Siegrist, R.L., 2005. Characteristics of potassium permanganate encapsulated in polymer. J. Environ. Eng.131 (8): 1203-1211.

[99] Rudakov, E.S., Lobachev, V.L., 2000. The first step of oxidation of alkylbenzenes by permanganates in acidic aqueous solutions. Russ. Chem. Bull. 49: 761-777.

[100] Sara, M.N., 2003. Site Assessment and Remediation Handbook, 2nd edition. CRC Press LLC.

[101] Schubert, M., Schmidt, A., Müller, K., and Weiss, H., 2011. Using radon-222 as indicator for the evaluation of the efficiency of groundwater remediation by in-situ air sparging. Environ Radioact. 102:193-199.

[102] Shen, R., Pennell, K.G., Suuberg, E.M., 2014. Analytical modeling of the subsurface volatile organic vapor concentration in vapor intrusion. Chemosphere 95: 140-149.

[103] Sercu, B., Jones, A.D.G., Wu, C.H., Escobar, M.H., Serlin, C.L., Knapp, T.A., Andersen, G.L., and Holden, P.A. 2013. The influence of in situ chemical oxidation on microbial community composition in groundwater contaminated with chlorinated solvents. Microb. Ecol. 65:39-49.

[104] Serrano, A. and Gallego, M., 2004. Direct screening and confirmation of benzene, toluene, ethylbenzene and xylenes in water. J. Chromatography A 1045 (1-2): 181-188.

[105] Smith, J.A., Chiou, C.T., Kammer, J.A., and Kile, D.E., 1990. Effect of soil moisture on the sorption of trichloroethene vapor to vadose-zone soil at picatinny arsenal, New Jersey. Environ. Sci. Technol. 24(5): 676-683.

[106] Siegrist, R.L., Crimi, M., and Simkin, T.J., 2011. Chemical Oxidation for Groundwater Remediation. Springer Science+Business Media, LLC, New York.

[107] Siegrist, R.L., Crime, M., Thomson, N.R., Clayton, W.S., Marley, M.C., 2014, In-situ chemical oxidation. SERDP ESTCP Environm. Remediation Technol. 7: 253-305.

[108] Siegrist, R.L., Urynowicz, M.A., West, O.R., Crimi, M.L., and Lowe, K.S., 2001. Principles and practices of in-situ chemical oxidation using permanganate. Columbus, OH: Battelle Press.

[109] Simon, A., Poulicek, M., Velimirov, B., and Machenzie, F.T., 1994. Comparison of anaerobic and aerobic biodegradation of mineralized skeletal structures in marine and estuarine conditions. Biogeochemistry 25: 167-195.

[110] Sogaard, E.G., 2014. Chemistry of Advanced Environmental Purification Processes of Water; Fundamentals and applications. 1st edition. Elsevier Publisher.

[111] Stroo, H.F., and Ward, C.H., 2010. In Situ Remediation of Chlorinated Solvent Plumes. Springer Science+Business Media, LLC.

[112] Struse, A.M., Siegrist, R.L., Dawson, H.E., and Urynowicz, M.A., 2002. Diffusive transport of permanganate during in situ oxidation. J. Environ. Eng. 128(4): 327-334.

[113] Suarez, M.P., Rifai H.S., 1999. Biodegradation rates for fuel hydrocarbons and chlorinated ethenes in groundwater. Bioremediation J. 3(4): 337-362.

[114] Thiruvenkatachari, R., Vigneswaran, S., and Naidu, R., 2008. Permeable reactive barrier for groundwater remediation. J. Ind. Eng. Chem. 14: 145-156.

[115] Tillman, F.D., and Weaver, J.W., 2005. Review of Recent Research on Vapor Intrusion. United States Environmental Protection Agency, EPA/600/R-05/106, Washington,DC.http://209.190.206.131/download/contaminantfocus/vi/Review%20of%20Recent%20Research.pdf.

[116] TITRC (The Interstate Technology & Regulatory Council), 2005. Technical and Regulatory Guidance for In Situ Chemical Oxidation of Contaminated Soil and Groundwater. 2nd Edition. In Situ Chemical Oxidation Team**.** http://www.itrcweb.org/ Guidance/List Documents?topicID=10&subTopicID=17#.

[117] Truex, M.J., Vermeul, V.R., Mendoza, D.P., Fritz, B.G., Mackley, R.D., Oostrom, M., Wietsma, T.W., and Macbeth, T.W., 2011. Injection of zero-valent iron into an unconfined aquifer using shear-thinning fluids. Ground Water Monit. R. 31(1): 50-58.

[118] Tsitonaki, A., Petri, B., Crimi, M., Mosbæk, H., Siegrist, R.L., and Bjerg, P.L., 2010. In situ chemical oxidation of contaminated soil and groundwater using persulfate: a review. Crit. Rev. Environ. Sci. Technol. 40: 55-91.

[119] Urynowicz, M.A., 2008. In-situ chemical oxidation with permanganate: assessing the competitive interactions between target and nontarget compounds. Soil Sedim. Contam. 17: 53-62.

[120] USDE (United States Department of Energy), 1995. In Situ Bioremediation Using Horizontal Wells. Innovative technology summery report. Office of Environmental Management and Office Technology Development. www.osti.gov/servlets/purl/7102.

[121] USEPA (United States Environmental Protection Agency), 1993. Behavior and Determination of Volatile Organic Compounds in Soil: A Literature Review. EPA/600/R-93/140. http://www.epa.gov/esd/cmb/pdf/voclr.pdf.

[122] USEPA (United States Environmental Protection Agency), 1995. Principles and Practices of Bioventing. EPA/540/R-95/534.

[123] USEPA (United States Environmental Protection Agency), 1998. Permeable Reactive Barrier Technologies for Contaminant Remediation. EPA/600/R-98/125. clu-in.org/ download/rtdf/ prb/reactbar.pdf.

[124] USEPA (United States Environmental Protection Agency), 2002. Draft Guidance for Evaluating the Vapor Intrusion to Indoor Air Pathway from Groundwater and Soils. Washington D.C., Office of Solid Waste and Emergency Response. www.epa.gov/correctiveaction/eis/vapor/complete.pdf.

[125] USEPA (United States Environmental Protection Agency), 2006. In Situ Treatment Technologies for Contaminated Soil, Engineering forum issue paper. EPA 542/F-06/013. www.clu-in.org/download/remed/542f06013.pdf.

[126] USEPA (United States Environmental Protection Agency), 2012. Conceptual Model Scenarios for the Vapor Intrusion Pathway. Office of Solid Waste and Emergency Response EPA 530-R-10-003. www.epa.gov/oswer/vaporintrusion/.../ vi-cms-v11final-2-24-2012.pdf.

[127] Waldemer, R.H., and Tratnyek, P.G., 2006. Kinetics of contaminant degradation by permanganate. Environ. Sci. Technol. 40: 1055-1061.

[128] Wang, W.H., Hoag, G.E., Collins, J.B., and Naidu, R., 2013. Evaluation of surfactant-enhanced in situ chemical oxidation (S-ISCO) in Contaminated Soil. Water Air Soil Pollut. 224:1713.

[129] Wang, L.K., Hung, Y.T., and Shammas, N.K., 2005. Physicochemical treatment process. Handbook of environmental engineering. Volume 3. Humana Press Inc.

[130] Watts, R.J., Foget, M.K., Kong, S.H., Teel, A.L., 1999. Hydrogen peroxide decompos-ition in model subsurface systems. J. Hazard. Mater. 69(2): 229-243.

[131] Waybrant, K.R., Blowes, D.W., and Ptacek, C.J., 1998. Selection of reactive mixtures for use in permeable reactive walls for treatment of mine drainage. Environ. Sci. Technol. 32 (13): 1972-1979.

[132] Wenk, J., Aeschbacher, M., Salhi, E., Canonica, S., von Gunten, U., and Sander, M., 2013. Chemical oxidation of dissolved organic matter by chlorine dioxide, chlorine, and ozone: effects on its optical and antioxidant properties. Environ. Sci. Technol. 47: 11147-11156.

[133] Weiner, E.R., 2000. Applications of Environmental Chemistry: A Practical Guide for Environmental Professionals. CRC Press LLC.

[134] Wise, D.L., Trantolo, D.J., Cichon, E.J., Inyang, H.I., and Stottmeister, U., 2000. Bioremediation of Contaminated Soils. Marcel Dekker, Inc.

[135] Wiedemeier, T.H., Rifai, H.S., Newell, C.J., and Wilson, J.T., 1999. Natural Attenuation of Fuels and Chlorinated Solvents in the Subsurface. John Wiley: New York.

[136] Xu, X., and Thomson, N.R., 2010. Hydrogen peroxide persistence in the presence of aquifer materials. Soil and Sediment Contam.19: 602-616.

[137] Yan, Y.E., and Schwartz, F.W., 1999. Oxidative degradation and kinetics of chlorinated ethylenes by potassium permanganate. J. Contam. Hydrol. 37: 343-365.

[138] Yan, Y.E., and Schwartz, F.W., 2000. Kinetics and mechanisms for TCE oxidation by permanganate. Environ. Sci. Technol. 34: 2535-2541.

[139] Yao, Y., Shen, R., Pennell, K.G., and Suuberg, E.M., 2013. A review of vapor intrusion models. Environ. Sci. Technol. 47: 2457-2470.

[140] Yen, C.H., Chenb, K.F., Kaoc, C.M., Liangc, S.H., and Chend, T.Y., 2011. Application of persulfate to remediate petroleum hydrocarbon-contaminated soil: Feasibility and comparison with common oxidants. J. Hazard. Mater.186: 2097-2102.

[141] Yeh, C.H., Lin, C.W., and Wu., C.H., 2010. A permeable reactive barrier for the bioremediation of BTEX-contaminated groundwater: Microbial community distribution and removal efficiencies. J. Hazard. Mater.178: 74-80.

[142] You, K., and Zhan, H., 2012. Can atmospheric pressure and water table fluctuation be neglected in soil vapor extraction? Adv. Water Resour. 35: 41-54.

[143] You, K., and Zhan, H., 2013. Comparisons of diffusive and advective fluxes of gas phase volatile organic compounds (VOCs) in unsaturated zones under natural conditions. Adv. Water Resour. 52: 221-231.

[144] Yu, K.P., and Lee, G.W.M., 2007. Decomposition of gas-phase toluene by the combination of ozone and photocatalytic oxidation process (TiO_2/UV, TiO_2/UV/O_3, and UV/O3). Appl. Catal. B. Environ. 75: 29-38.

[145] Yuan, B., Li, F., Chen, Y., and Fu, M.L., 2013. Laboratory-scale column study for remediation of TCE-contaminated aquifers using three-section controlled-release potassium permanganate barriers. J. Environ. Sci. 25 (5): 971-977.

[146] Zargar, M., Sarrafzadeh, M.H., Taheri, B., and Keshavarz, A., 2014. Assessment of in situ bioremediation of oil contaminated soil and groundwater in a petroleum refinery: A laboratory soil column study. Petrol. Sci. Technol. 32: 1553-1561.

Chapter 2

Oxidation of volatile organic vapours in air by solid potassium permanganate;

Batch experiments

Published as: Mahmoodlu, M.G., Hartog, N., Hassanizadeh, S.M., Raoof, A., 2013. Oxidation of volatile organic vapours in air by solid potassium permanganate, Chemosphere. 91(11): 1534-1538.

Abstract

Volatile organic compounds (VOCs) may frequently contaminate groundwater and pose threat to human health when migrating into the unsaturated soil zone and upward to the indoor air. The kinetic of chemical oxidation has been investigated widely for dissolved VOCs in the saturated zone. But, so far there have been few studies on the use of in-situ chemical oxidation (ISCO) of vapour phase contaminants. In this study, batch experiments were carried out to evaluate the oxidation of trichloroethylene (TCE), ethanol, and toluene vapours by solid potassium permanganate. Results revealed that solid potassium permanganate is able to transform the vapour of these compounds into harmless oxidation products. The oxidation rates for TCE and ethanol were higher than for toluene. The oxidation process was modeled using a kinetic model, linear in the gas concentration of VOC [NL^{-3}] and relative surface area of potassium permanganate grains (surface area of potassium permanganate divided by gas volume) [L^{-1}]. The second-order reaction rate constants for TCE, ethanol, and toluene were found to be equal to 2.0×10^{-6} cm s^{-1}, 1.7×10^{-7} cm s^{-1}, and 7.0×10^{-8} cm s^{-1}, respectively.

2.1. Introduction

Volatile organic compounds (VOCs) are defined as organic compounds with boiling points (at 1 atm) below 260 ºC (De Nevers, 2000). VOCs have high vapour pressures under normal conditions, so they can easily vaporize into the atmosphere or form vapour plumes in the soil (Kim et al., 2007). VOCs are present in some household products and automobile liquids (Berscheid et al., 2010). Releases of VOCs to the environment have occurred through surface spills, leaking underground storage tanks, and inadequate disposal practices (Berscheid et al., 2010). Small quantities of VOCs may contaminate large volumes of water. When released as free product, VOCs may migrate downward to significant depths through the soil. In addition, VOC vapours can migrate upwards to the surface through diffusion and produce elevated concentrations within indoor air spaces (Berscheid et al., 2010). Exposure to some VOCs might affect central nervous system and internal organs, and might cause symptoms such as headache, respiratory tract irritation, dizziness and nausea, known as the Sick Building Syndrome (SBS) (Yu, and Lee, 2007).

We have chosen TCE, ethanol, and toluene, as model VOCs (target compounds) for chlorinated solvents, biofuel, and mineral oil, respectively, for the reasons explained below.

TCE is one of the most common man-made chemicals found in soil (Albergaria et al., 2012). It has been widely used as a dry cleaning solvent, degreasing agent, and chemical extraction agent. Since TCE is carcinogenic, its movement from contaminated groundwater and soil into the indoor air of overlying buildings is of serious concern (EPA, 2011). Ethanol is being increasingly used in (renewable) fuel alternatives and as replacement for methyl tertiary-butyl ether (MTBE), which, despite helping to accomplish Clean Air Act goals, has caused widespread water contamination problems (Johnson et al., 2000; Capiro et al, 2007). Ethanol can reduce the biodegradation rate of light non-aqueous phase liquid (LNAPL) such as benzene, toluene, ethylbenzene, and xylene isomers (BTEX) in groundwater and soil (Freitas et al., 2010; Mackay et al., 2007). Toluene is found

frequently in indoor environments. Toluene is mainly used as an additive to improve the octane number of gasoline (Yu and Lee, 2007).

One of most common treatment techniques for unsaturated zone polluted with VOCs is soil vapour extraction (SVE). This is a long-term operation and doesn't convert a contaminant to less toxic compounds. A promising alternative is in-situ oxidation of VOC that can lead to favorable results in less time. Oxidation of VOCs may convert hazardous contaminants to harmless compounds. The oxidizing agents most commonly used for the treatment of hazardous contaminants are potassium permanganate, ultraviolet radiation, ozone, chlorine dioxide, hydrogen peroxide, sodium persulfate, and Fenton's reagent (H_2O_2 oxidation in the presence of ferrous iron, Fe^{2+}).

Among these oxidants, potassium permanganate has been receiving increased attention for the treatment of liquids, slurry soils, and sludges polluted with VOCs (Kao et al, 2008). Early laboratory studies have indicated that dissolved potassium permanganate can remediate a variety of organic compounds, chlorinated alkanes (Waldemer, and Tratnyek, 2006), chlorinated ethylenes (Huang et al., 1999; Hood et al., 2000; Yan and Schwartz, 2000; Waldemer and Tratnyek, 2006; Kao et al., 2008; Urynowicz, 2008), oxygenates (Damm et al., 2002; Jaky et al., 2000; Waldemer, and Tratnyek, 2006), BTEX (Gardner,1996; Rudakov and Lobachev, 2000; Waldemer, and Tratnyek, 2006), substituted phenols (Jin et al., 2003; Waldemer, and Tratnyek, 2006) and PAHs (Forsey, 2004), in aqueous phase. However, the potential of solid potassium permanganate to oxidize VOC vapours in unsaturated zone is currently unknown.

In this study, we demonstrate the ability of solid potassium permanganate to oxidize VOC vapours. For this, we performed a series of batch experiments with two objectives: (1) to evaluate the ability of solid potassium permanganate to fully oxidize vapour phase contaminants, (2) to determine kinetic parameters for TCE, ethanol, and toluene oxidation by solid potassium permanganate.

2.2. Material and experimental procedure

We used 4.8×10^{-6}, 3.5×10^{-6}, 2.3×10^{-6} mole of TCE, ethanol, and toluene vapours, respectively. These values were calculated based on 1.5 ml of gas samples (under normal conditions) which were obtained from the headspace of their highly pure liquid phases. Solid potassium permanganate of 99% purity was obtained from Sigma-Aldrich. The required potassium permanganate for complete oxidation of VOCs was calculated based on the following reactions for TCE, ethanol, and toluene, respectively:

$$C_2HCl_{3(g)} + 2KMnO_{4(s)} \rightarrow 2K^+ + 3Cl^- + 2MnO_{2(s)} + H^+ + 2CO_{2(g)} \quad (2.1)$$

$$C_2H_5OH_{(g)} + 4KMnO_{4(s)} + 4H^+ \rightarrow 4K^+ + 4MnO_{2(s)} + 2CO_{2(g)} + 5H_2O \quad (2.2)$$

$$C_6H_5CH_{3(g)} + 12KMnO_{4(s)} + 12H^+ \rightarrow 12K^+ + 12MnO_{2(s)} + 10H_2O + 7CO_{2(g)} \quad (2.3)$$

The required amount of potassium permanganate for oxidizing 4.8×10^{-6} mole of TCE, 3.5×10^{-6} mole of ethanol, and 2.3×10^{-6} mole of toluene were estimated to be 1.25, 2.22, and 4.44 mg, respectively. These were calculated based on reactions in aqueous environment, assuming a full dissolution of crystals. In dissolved form, potassium permanganate may be fully available for oxidation. But, in the solid form only the surface of potassium permanganate grains is in contact with the gas phase. Accordingly, more potassium permanganate is needed to avoid limitation in the oxidation rate. Hence, excess amount of potassium permanganate (2.703 g) was used for each batch.

Potassium permanganate grains were put inside 12-ml transparent glass vials, which were capped with a hard septum to prevent any leakage (Fig. 2.1). VOC vapour was injected using a gas tight syringe (2.5 ml Hamilton, SGE) and 16 mm disposable needles (Φ 0.5 mm, Terumo).

In order to get kinetic parameters, three batch experiments at three different initial amounts of vapour and potassium permanganate were performed for all compounds (Table 2.1). All experiments were carried out in duplicate. For each

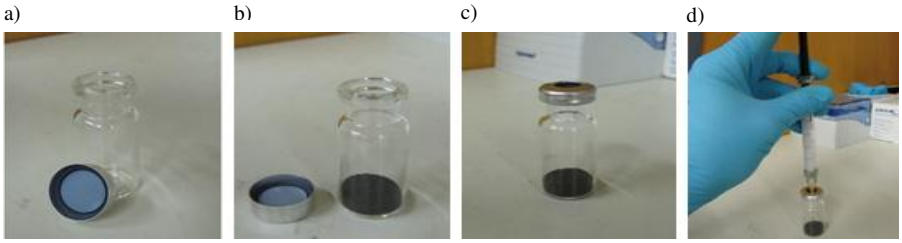

Fig. 2.1: Experimental setup for the batch experiments: a) a 12-ml transparent glass vial, b) a glass vial including dry potassium permanganate grains, c) a glass vial capped by a hard septum, and d) injecting VOC vapour into a capped-glass vial.

Table 2.1: Initial experimental conditions for each compound

Compound	Trial	n_A (mol)	M_{KMnO4}(g)	V^g(cm^3)	A_{KMnO4}(cm^2)	S_0(cm^{-1})
TCE	1	4.8×10^{-6}	2.703	10.5	2703	257.43
	2	2.4×10^{-6}	2.703	10.5	2703	257.43
	3	4.8×10^{-6}	1.351	11.25	1351.5	120.13
Ethanol	1	3.5×10^{-6}	2.703	10.5	2703	257.43
	2	1.75×10^{-6}	2.703	10.5	2703	257.43
	3	3.5×10^{-6}	1.351	11.25	1351.5	120.13
Toluene	1	2.3×10^{-6}	2.703	10.5	2703	257.43
	2	1.15×10^{-6}	2.703	10.5	2703	257.43
	3	2.3×10^{-6}	1.351	11.25	1351.5	120.13

n_A : Initial number of VOC moles, M_{KMnO4} : Mass of solid potassium permanganate, A_{KMnO4}: Surface area of potassium permanganate, V^g: Volume of the gas phase, S_0 : Initial relative surface area.

experiment, we prepared several identical batches and each batch was allocated to a given sampling time.

A control experiment was also performed in duplicate for each compound to ensure that the loss of target compound due to leakage was negligible over the course of the experiments. To prepare a control batch, a 12-ml transparent glass vial was capped with a hard septum. Then VOC vapour was injected into the vial. All experiments were carried out in a vertical rotary shaker, at room temperature, 20 ± 2 ºC, and air humidity of 37 ± 2%, which is also the initial humidity inside the vials.

2.3. Sampling and Measurements

Reaction and control batches were periodically sampled using a gas tight syringe until no detectable concentration was found in the reaction vial. To eliminate the effect of pressure drop due to sampling, each vial was used only once. The concentrations of target compounds, TCE, ethanol, and toluene were measured by a gas chromatograph (GC). Gas samples of 2 ml were taken using the headspace syringe of the GC from each vial. Then, samples were injected into the GC. The GC (Agilent 6850) was equipped with flame ionization detector (FID) and separation was done on an Agilent HP-1 capillary column (stationery phase: 100% dimethylpolysiloxane, length: 30 m, ID: 0.32 mm, film thickness: 0.25 μm).

Specific surface area of potassium permanganate was measured using 10-point Brunauer-Emmett-Teller (BET) method by a Nova 3000 from Quantachrome. Performance of this machine was controlled using reference 173 from Community Bureau of Reference. Samples were degassed at 120 ℃ overnight before measurements. The relative surface area was calculated as the surface area per volume of gas (Table 2.1).

To calculate the amount of the potassium permanganate consumption, at end of experiment potassium permanganate grains were dissolved in deionized (DI) water and its concentration was measured using a UV-Spectrophotometer (UV-1800, Shimadzu) at a wavelength of 525 nm.

2.4. Oxidation Study

Fig. 2.2 depicts the normalized concentration (C/C_0) of the target compounds as a function of time, where C denotes the observed concentration of the target compound for a given time and C_0 is the initial concentration of the target compound. Oxidation of target compounds shows an exponential trend, as indicated by the fitted formula in the graph (Fig. 2.2). These results also show that solid potassium permanganate was able to rapidly oxidize the vapour phase of TCE and ethanol. Toluene was also degraded but less rapidly. No VOC intermediates or

reaction products were found in vapour samples. During the experiment, potassium permanganate crystals turned into dark color, which is the color of a coating layer of produced manganese dioxide (MnO_2).

2.5. Data analysis: Kinetics

Since the results of control experiments showed a negligible change in the concentration VOC over the course of the experiments, the adsorption of VOC vapours to glass and septum or reduction in the VOC concentration due to leakage was disregarded. We assumed the adsorption of VOC vapours to the reaction products (e.g. manganese dioxide) in the batches containing solid potassium permanganate (reactive batch) to be negligible. Hence, the oxidation was the main process to reduce the concentration of VOC in the reactive batches.

Since the oxidation of three reactants showed an exponential trend, we assumed that the kinetics follow a first-order reaction rate. We also assumed that only surface of solid potassium permanganate reacts with compounds. So, to a proper calculation of the reaction rate coefficient, we should have an equation that involves the physical properties of potassium permanganate, such as the surface area and mass of potassium permanganate. Such an equation may be written as:

$$\frac{dC^g}{dt} = -k^g C^g S \tag{2.4}$$

where k^g denotes the reaction rate constant in the gas phase, C^g is the vapour concentration of compound [NL^{-3}], t is time [T], and S is the relative surface area of solid potassium permanganate [L^{-1}], which is defined as:

$$S = \frac{A_{KMnO4}}{V^g} \tag{2.5}$$

where A_{KMnO4} is the surface area of the potassium permanganate [L^2] and V^g is the volume of the gas phase [L^3].

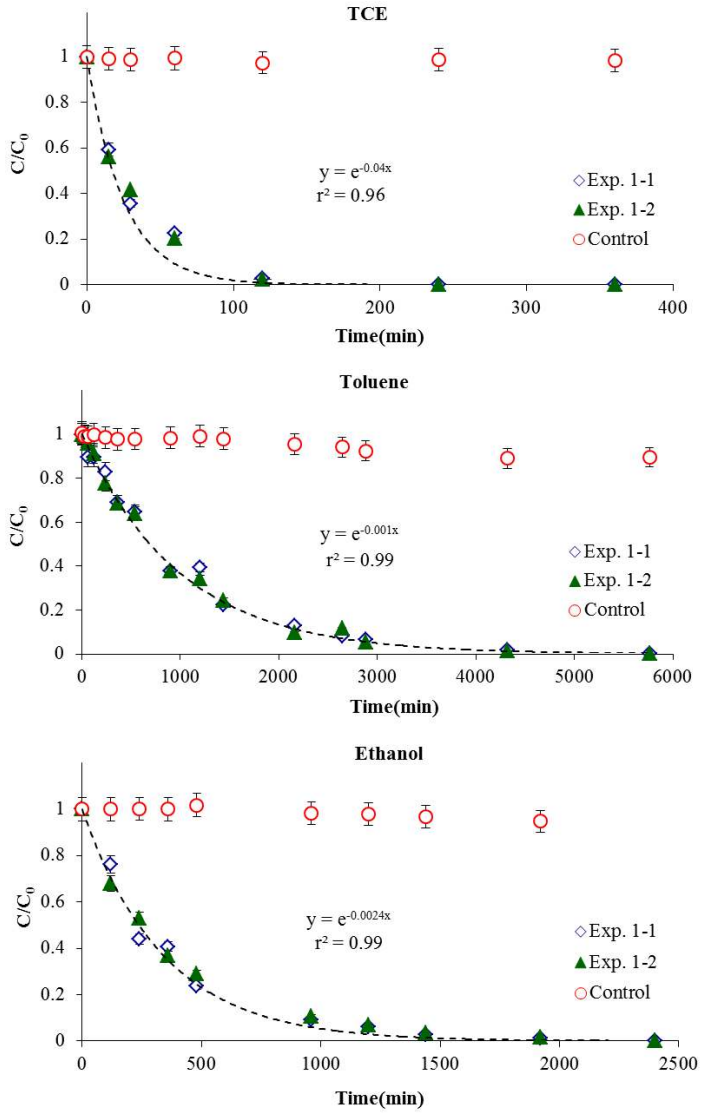

Fig. 2.2: Oxidation of TCE, ethanol, and toluene vs. time for Experiment 1 (Exp. x-y: x denotes the number of the experiment and y is the experiment repetition).

First, we assumed the relative surface area not to alter significantly during the course of the reaction. To validate this assumption, we determined the amount of potassium permanganate that was consumed, at the end of the experiment. This was done by dissolving potassium permanganate grains which were used in the experiments in DI water and then using a spectrophotometer to determine its mass. We compared this to the initial mass and the result showed that there was no significant consumption of solid potassium permanganate during our experiments. With S set equal to S_0, Equation 2.4 can be solved to obtain:

$$\frac{1}{S_0}\ln\frac{C^g}{C_0^g} = -k^g t \tag{2.6}$$

where S_0 denotes the initial relative surface area of potassium permanganate [L^{-1}].

According to Equation 2.6, plot of $1/S_0 \ln C^g / C_0^g$ versus time should yield a straight line. Then, the reaction rate constant k^g can be obtained from the slope of this line. We used all data from Experiment 1, 2, and 3 to estimate k^g for each compound. Fig. 2.3 shows that the plots of $1/S_0 \ln C^g / C_0^g$ versus time for all compounds. The square of linear correlation coefficients (r^2) obtained for TCE, ethanol, and toluene were 0.96, 0.99, and 0.99, respectively. Results suggested that the oxidation of the target compounds can be modeled by Equation 2.6 as long as sufficient relative surface area of potassium permanganate is available. This also confirmed the validity of our assumption that the reduction in VOC vapours due to the adsorption process can be negligible over the course of the experiments. The reaction rate constants for target compounds are given in Table 2.2.

We compared results of our experiments with the oxidation of VOCs in aqueous phase reported in the literature (Waldemer, and Tratnyek, 2006). We found that the oxidation process in both phases follows a pseudo first-order model. This comparison also revealed that the oxidation rates for VOCs in vapour phase are much smaller than for aqueous phase. However, in both phases, the reaction rate for TCE is higher than for ethanol and toluene.

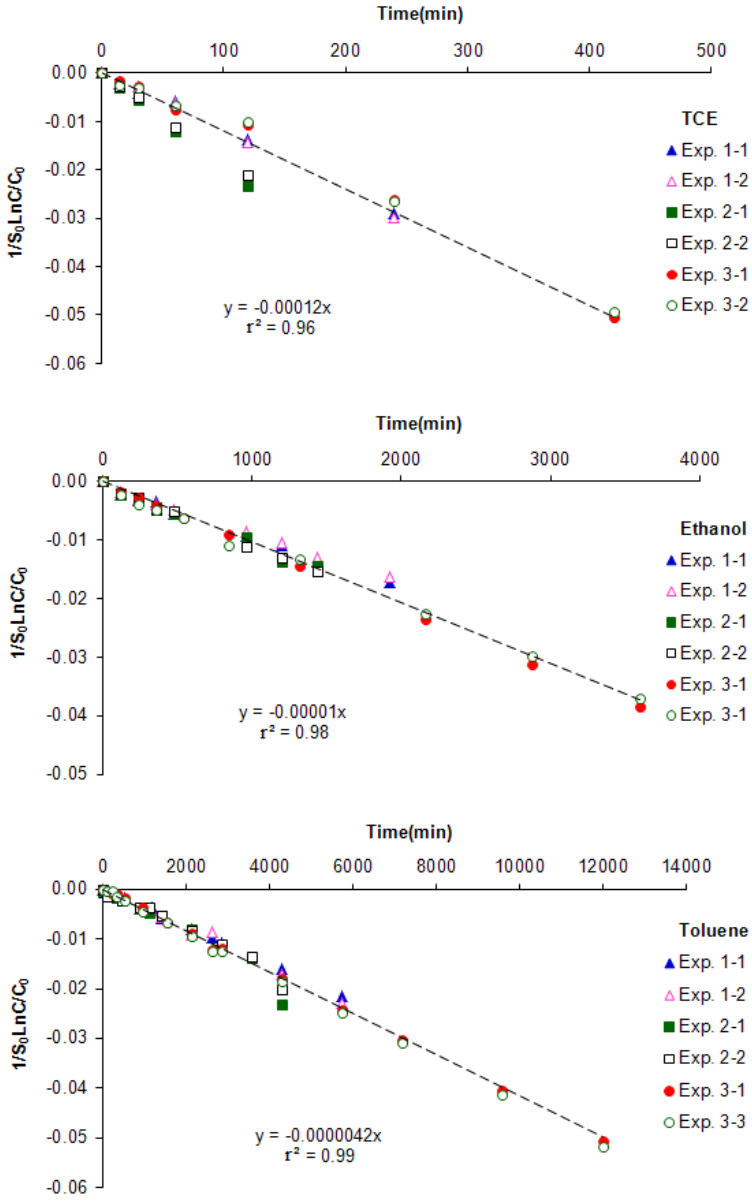

Fig. 2.3: Plot of $1/S_0 \ln C^g/C_0^g$ (denoted by y) vs. time (denoted by x) for evaluating k following Equation 2.6.

Table 2.2: Reaction rate constants for oxidation of TCE, ethanol, and toluene in the vapour phase at 20 ºC

Compound	**k^g (cm s^{-1})**	**r^2**
TCE	2.0×10^{-6}	0.96
Ethanol	1.7×10^{-7}	0.98
Toluene	7.0×10^{-8}	0.99

r^2: The square of the correlation coefficient

As mentioned above, as a result of oxidation, manganese dioxide is produced and coats the grains. This may affect the efficiency of oxidation process. To analyze the effect of surface coating, we accounted for the reduction of the relative surface area during the experiment. This was done by supplementing Equation 2.4 with an equation relating the relative surface area to the manganese dioxide concentration. This resulted in the following equation:

$$\frac{dC^g}{dt} = -k^g C^g [S_0 - \frac{\varphi}{\gamma}(C_0^g - C^g)] \qquad (2.7)$$

where φ is the number of moles of manganese dioxide produced per mole of target compound (based on stoichiometry reaction) and γ is the coating factor (number of moles of produced manganese dioxide per area of potassium permanganate grains) [NL^{-2}].

The numerical solution of Equation 2.7 was fitted to the TCE experimental data. Results showed a maximum reduction of around 4% in the relative surface area. This confirms the validity of our assumption that there is a negligible change in the relative surface area of potassium permanganate during our TCE experiments. Although the largest amount of manganese dioxide was produced during oxidation of ethanol and toluene (based on stoichiometry reaction), there was still a large

excess of the relative surface area during the ethanol and toluene experiment (based on the amount of potassium permanganate we used). Moreover, we calculated the amount of used potassium permanganate for all three compounds. On all cases, this was found to be small fraction of initial amount (around 4%).

2.6. Conclusions

In this study, we investigated the kinetic parameters of both chlorinated and non-chlorinated hydrocarbon vapours by solid potassium permanganate under room temperature and humidity conditions. Results showed that potassium permanganate is able to oxidize the vapour of TCE and ethanol, and toluene. We also found that TCE and ethanol in vapour phase can be rapidly oxidized by solid potassium permanganate. However, toluene was degraded slower. A linear kinetic oxidation model, based on the concentration of VOC in gas and a constant relative surface area, effectively predicted the rate of TCE, ethanol, and toluene oxidation. Results revealed that the reaction rate constants for TCE, ethanol, and toluene are 2.0×10^{-6} cm s^{-1}, 1.7×10^{-7} cm s^{-1}, and 7.0×10^{-8} cm s^{-1}, respectively. Results also showed that the amount of used potassium permanganate for all three compounds was small fraction of initial amount (around 4%).

These findings will be helpful in designing a horizontal permeable reactive barrier with solid potassium permanganate in unsaturated zone for vapour intrusion. The performance of such methodology may be affected by moisture content, pH, and temperature of the soil matrix. Also, one has to consider the health effects of by-product gases such as ethane (Pant and Pant, 2010) and methane (Freitas et al., 2010) that can be produced under anaerobic biodegradation of TCE and ethanol, respectively.

2.7. References

[1] Albergaria, J.T., Alvim-Ferraz, M.dc.M., and Delerue-Matos, C., 2012. Remediation of sandy soils contaminated with hydrocarbons and halogenated hydrocarbons by soil vapour extraction. Environ. Manage. 104: 195-201.

[2] Berscheid, M., Burger, K., Hutchison, N., Muniz-Ghazi, H., Renzi, B., Ruttan, P., and Sterling, S., 2010. Proven Technologies and Remedies Guidance: Remediation of Chlorinated Volatile Organic Compounds in Vadose Zone Soil. California Department of Toxic Substances Control. 154 pp.

[3] Capiro, N.L., Stafford, B.P., Rixey, W.G., Bedient, P.B., and Alvarez, P.J.J., 2007. Fuel-grade ethanol transport and impacts to groundwater in a pilot-scale aquifer tank. Water Res. 41: 656-664.

[4] Damm, J.H., Hardacre, C., Kalin, R.M., and Walsh, K.P., 2002. Kinetics of the oxidation of methyl tert-butyl ether (MTBE) by potassium permanganate. Water Res. 36: 3638-3646.

[5] De Nevers, N., 2000. Air Pollution Control Engineering, 2nd edition, McGraw-Hill International, Boston.

[6] EPA (Environmental Protection Agency), 2011. Toxicological Review of Trichloroethylene. CAS No. 79-01-6. www.epa.gov/iris/toxreviews/0199tr/0199tr.pdf.

[7] Forsey, S.P., 2004. In Situ Chemical Oxidation of Creosote/Coal Tar Residuals: Experimental and Numerical Investigation. Ph.D. Thesis, University of Waterloo.

[8] Freitas, J.G., Fletcher, B., Aravena, R., and Baker, J.F., 2010. Methane production and isotopic fingering in ethanol fuel contaminated sites. Groundwater 48: 844-857.

[9] Gardner, K.A., 1996. Permanganate Oxidations of Aromatic Hydrocarbons in Aqueous and Organic Solution. PhD Thesis, University of Washington.

[10] Hood, E.D., Thomson, N.R., Grossi, D., and Farquhar, G.J., 2000. Experimental determination of the kinetic rate law for the oxidation of perchloroethylene by potassium permanganate, Chemosphere 40: 1383-1388.

[11] Huang, K.C., Hoag, G.E., Chheda, P., Woody, B.A., and Dobbs, G.M., 1999. Kinetic study of oxidation of trichloroethylene by potassium permanganate. Environ. Eng. Sci. 16: 265-274.

[12] Jaky, M., Szammer, J., and Simon-Trompler, E., 2000. Kinetics and mechanism of the oxidation of ketones with permanganate ions, J. Che. Soc., Perkin Trans. 2: 1597-1602.

[13] Jin, Z., Gui-bai, L., and Jun, M., 2003. Effects of chlorine content and position of chlorinated phenols on their oxidation kinetics by potassium permanganate, Environ. Sci. 15: 342-345.

[14] Johnson, R., Pankow, D., Bender, C.P., and Zogorski, J., 2000. Target compounds-to what extent will past releases contaminate community water supply wells?. Environ. Sci. Technol. 34: 210A-217A.

[15] Kao, C.M., Huang, K.D., Wang, J.Y., Chen, T.Y., and Chien, H.Y., 2008. Application of potassium permanganate as an oxidant for in-situ oxidation of trichloroethylene-contaminated groundwater: A laboratory and kinetics study. Hazard. Mater. 153: 919-927.

[16] Kim, H.H., Ogata, A., and Futamura, S., 2007. Complete oxidation of volatile organic compounds (VOCs) using plasma-driven catalysis and oxygen plasma. Int. J. Plasma Environ. Sci. Technol. 1: 46-51.

[17] Mackay, D., De Sieyes, N., Einarson, M., Feris, K., Pappas, A., Wood, I., Jacobson, L., Justice, L., Noske, M., Wilson, J., Adair, C., and Scow, K., 2007. Impact of ethanol on the natural attenuation of MTBE in a normally sulfate-reducing aquifer. Environ. Sci. Technol. 41: 2015-2021.

[18] Pant, P., and Pant, S., 2010. A review: Advances in microbial remediation of trichloroethylene (TCE). Environ. Sci. 22: 116-126.

[19] Rudakov, E.S., and Lobachev, V.L., 2000. The first step of oxidation of alkylbenzenes by permanganates in acidic aqueous solutions, Russ. Chem. Bull. 49: 761-777.

[20] Urynowicz, M.A., 2008. In-situ chemical oxidation with permanganate: assessing the competitive interactions between target and nontarget compounds. Soil & Sediment Contam. 17: 53-62.

[21] Waldemer, R.H., and Tratnyek, P.G., 2006. Kinetics of contaminant degradation by permanganate. Environ. Sci. Technol. 40: 1055-1061.

[22] Yan, Y.E., and Schwartz, F.W., 2000. Kinetics and mechanisms for TCE oxidation by permanganate. Environ. Sci. Technol. 34: 2535-2541.

[23] Yu, K.P., and Lee, G.W.M., 2007. Decomposition of gas-phase toluene by the combination of ozone and photocatalytic oxidation process (TiO_2/UV, TiO_2/UV/O_3, and UV/O_3). Appl. Catal. B: Environ. 75: 29-38.

Chapter 3

Evaluation of the kinetic oxidation of aqueous volatile organic compounds by permanganate; Batch experiments

Published as: Mahmoodlu, M.G., Hassanizadeh, S.M., and Hartog, N., 2014. Evaluation of the kinetic oxidation of aqueous volatile organic compounds by potassium permanganate. Science of the Total Environment. 485-486: 755-763.

Abstract

The use of permanganate solutions for in-situ chemical oxidation (ISCO) is a well-established groundwater remediation technology, particularly for targeting chlorinated ethenes. The kinetics of oxidation reactions is an important ISCO remediation design aspect that affects the efficiency and oxidant persistence. The overall rate of the ISCO reaction between oxidant and contaminant is typically described using a second-order kinetic model while the second-order rate constant are determined experimentally by means of a pseudo first order approach. However, earlier studies of chlorinated hydrocarbons have yielded a wide range of values for the second-order rate constants. Also, there is limited insight in the kinetics of permanganate reactions with fuel-derived groundwater contaminants such as toluene and ethanol. In this study, batch experiments were carried out to investigate and compare the oxidation kinetics of aqueous trichloroethylene (TCE), ethanol, and toluene in an aqueous potassium permanganate solution. The overall second-order rate constants were determined directly by fitting a second-order model to the data, instead of typically used the pseudo-first-order approach. The second-order reaction rate constants ($M^{-1}s^{-1}$) for TCE, toluene, and ethanol were 8.0×10^{-1}, 2.5×10^{-4}, and 6.5×10^{-4}, respectively. Results showed that the inappropriate use of the pseudo-first-order approach in several previous studies produced biased estimates of the second-order rate constants. In our study this error was expressed as a function of the extent (P/N) in which the reactant concentrations deviated from the stoichiometric ratio of each oxidation reaction. The error associated with the inappropriate use of the pseudo-first-order approach is negatively correlated with the P/N ratio and reached up to 25% of the estimated second-order rate constant in some previous studies of TCE oxidation. Based on our results, a similar relation is valid for the other volatile organic compounds studied.

3.1. Introduction

Groundwater contamination with volatile organic compounds (VOCs) is a major environmental problem at sites (formerly) occupied by large-scale chemical industries or small scale users such as dry-cleaners or fuel stations (Rivett et al., 2011; Schubert et al., 2011). These compounds are also present in some household products and automobile liquids (Berscheid et al., 2010). VOCs are groundwater contaminants of widespread concern because of (1) very large volumes that are sometimes released into the environment, (2) their toxicity, and (3) the fact that some VOCs, once they have reached groundwater, tend to persist and migrate to drinking water wells or upward by diffusion through the unsaturated zone to indoor spaces. Exposure to some VOCs may cause damage to the central nervous system and internal organs and may lead to symptoms such as headache, respiratory tract irritation, dizziness and nausea, known as the Sick Building Syndrome (Yu and Lee, 2007).

Of the different VOCs present, we selected for our study TCE, toluene, and ethanol as the model VOCs (target compounds) for chlorinated solvents, mineral oil, and biofuel, respectively. TCE has been widely used as a dry cleaning solvent, degreasing product and chemical extraction agent. Inappropriate TCE disposal has produced widespread groundwater contamination. Since TCE is carcinogenic, its movement from contaminated groundwater and soil into the indoor air of overlying buildings is a serious concern (EPA, 2011). Similarly, toluene, an additive to improve the octane number of gasoline, is one of the main organic compounds found frequently in indoor environments. Toluene is listed as one of the six major classes of indoor VOCs (aromatic, aldehyde, alkane, ketone, alcohol, and chlorocarbon) (Yu and Lee, 2007). Exposure to toluene may cause irritation of the eye, nasal and mucous membranes, and the respiratory tract (Yu and Lee, 2007).

More recently, ethanol is being used increasingly in (renewable) fuel alternatives and as a replacement for methyl tertiary-butyl ether (MTBE), which, despite helping to accomplish Clean Air Act goals, has caused widespread water contamination (Johnson et al., 2000; Capiro et al., 2007). Also, the presence of

ethanol in groundwater can reduce the biodegradation rates of benzene, toluene, ethylbenzene, and xylene isomers (BTEX) in groundwater and soil (Mackay et al., 2007; Freitas et al., 2010). Extended exposure to ethanol can damage liver, kidneys, and the central nervous system (Yu and Lee, 2007). A need hence exists to improve our understanding of the oxidation and fate of ethanol in contaminated groundwater.

In-situ chemical oxidation (ISCO) is one of the technologies available for in-situ remediation of VOC-contaminated groundwater. Chemical oxidation technology is a potent soil remedial option that can effectively eliminate an extensive range of VOCs (Yen et al., 2011). The oxidizing agents most commonly used for the treatment of hazardous contaminants are permanganate, ozone, hydrogen peroxide, and Fenton's reagent. Of these oxidants, potassium permanganate has received much attention for the treatment of liquid, slurry soils, and sludges polluted with VOCs. Potassium permanganate is often used as an ISCO agent for the following five reasons: (1) its oxidation potential (E_0 = 0.5-1.7 V), (2) its ability to oxidize a variety of organic chemicals (Powers et al., 2001; Siegrist et al., 2001; Struse et al., 2002; Hønning et al., 2004; Mumford et al., 2004; Mumford et al., 2005; Urynowicz, 2008), (3) its effectiveness over a wide range of pH values, (4) its relatively low cost, and (5) its significantly higher stability in the subsurface as compared to other chemical oxidants (Huang et al., 1999; Bryant et al., 2001).

Depending upon the soil matrix and groundwater composition, permanganate in an aquifer may be stable for as long as several weeks (Siegrist et al., 2001; Cave et al. 2007). The injection of dissolved potassium permanganate into plumes to remediate contaminated groundwater has been used for the in-situ treatment of chlorinated hydrocarbons (Damma et al., 2002). Moreover, since oxidation reactions with permanganate proceed by electron transfer rather than more rapid free radical processes, as with Fenton's reagent, potassium permanganate appears amenable to application in low permeability soils (Kao et al., 2008). Permanganate reacts with organic compounds to produce manganese dioxide (MnO_2) as well as carbon dioxide (CO_2) or intermediate organic compounds (Yin and Herbert, 1999) of the form:

$$R_{(aq)} + MnO_{4(aq)}^{-} \rightarrow MnO_{2(s)} + CO_{2(g)} \qquad \text{or} \qquad R_{ox} + \text{others} \tag{3.1}$$

where R denotes an organic contaminant and R_{ox} is an oxidized intermediate organic compound.

A number of processes such as cleaving, hydroxylation, and hydrolysis lead to the production of intermediates and eventually to carbon dioxide and water. The permanganate ion is especially useful in oxidizing organics that have carbon-carbon single and double bonds (for example, chlorinated ethylenes, aldehyde groups, or hydroxyl groups) (Lee et al., 2003).

The full oxidation of TCE, toluene, and ethanol by permanganate follows Equations 3.2 to 3.4, respectively. Permanganate breaks down TCE to CO_2 and Cl^{-}, while ethanol and toluene are transformed into CO_2 and H_2O. In all reactions, MnO_4^{-} reduces to manganese dioxide which is a solid precipitate at circumneutral pH values. Moreover, in the absence of reductants, permanganate can react with water and produce manganese dioxide particles (Kao et al., 2008) as given by Equation 3.5. However, this reaction typically takes place at very low rates.

$$C_2HCl_{3(aq)} + 2KMnO_{4(aq)} \rightarrow 2K^{+} + 2MnO_{2(s)} + 3Cl^{-} + 2CO_{2(g)} + H^{+} \tag{3.2}$$

$$C_6H_5CH_{3(aq)} + 12KMnO_{4(aq)} + 12H^{+} \rightarrow 12K^{+} + 12MnO_{2(s)} + 10H_2O_{(aq)} + 7CO_{2(g)} \tag{3.3}$$

$$C_2H_5OH_{(aq)} + 4KMnO_{4(aq)} + 4H^{+} \rightarrow 4K^{+} + 4MnO_{2(s)} + 2CO_{2(g)} + 5H_2O_{(aq)} \tag{3.4}$$

$$4MnO_{4(aq)}^{-} + 2H_2O_{(aq)} \rightarrow 3O_{2(g)} + 4MnO_{2(s)} + 4OH^{-} \tag{3.5}$$

For the design and monitoring of an ISCO remediation approach, the kinetics of oxidation reactions is an important aspect that may affect the efficiency and oxidant persistence. ISCO using potassium permanganate solution is a well-established remediation technology, particularly for targeting chlorinated ethenes (Huang et al., 2001; Waldemer and Tratnyek, 2006; Urynowicz, 2008). However, the earlier studies of chlorinated ethenes have yielded a wide range for the estimated

second-order rate constants. In large part these estimates were derived using the pseudo-first order experimental approach that requires one of the reactants to be present in significant excess (Huang et al., 2001; Siegrist et al. 2001; Waldemer and Tratnyek, 2006; Urynowicz, 2008). Also, there is still limited insight in the kinetics of permanganate reactions with fuel-derived VOC groundwater contaminants such toluene (Rudakov and Lobachev, 2000; Waldemer and Tratnyek, 2006) and ethanol (Barter and Littler, 1967). In this study we therefore determined kinetic parameters for the oxidation of three dissolved VOCs (TCE, toluene and ethanol) by permanganate. For this purpose we performed a series of batch experiments with three objectives: (1) to determine the oxidation kinetic parameters of TCE, toluene, and ethanol by aqueous permanganate, (2) to establish a suitable kinetic reaction rate model, and (3) to estimate errors caused by the inappropriate use of the pseudo first-order model.

3.2. Materials and Methods

3.2.1. Materials

Chemicals used in this study included TCE, ethanol, and toluene (99% purity, Sigma-Aldrich, Merck and ACROS, respectively), potassium permanganate (99% purity, Sigma-Aldrich), sodium bicarbonate (99.7% purity, Merck), ammonium chloride (99.8% purity, Merck) and oxalic acid (99% purity, Merck). Stock solutions of aqueous-phase TCE, ethanol, and toluene were individually prepared in 2-liter glass vessels by dissolving the chemicals in deionized (DI) water. The vessels were vigorously shaken and allowed to equilibrate overnight. Then, they were preserved at 8°C for further use. Potassium permanganate solutions of desired concentrations were prepared by dissolving solid potassium permanganate in DI water. To prevent the photodecomposition of permanganate, the stock solutions were covered by aluminum foil.

Two separate buffer solutions of pH 9.0 and 6.0 were prepared. This was performed by adding the required amounts of either sodium bicarbonate or

ammonium chloride to DI water. A solution of oxalic acid was prepared by dissolving an appropriate amount of oxalic acid in DI water.

3.2.2. Sampling and analyses

During the batch experiments, aqueous samples of 1.5 ml were periodically taken from the kinetic (including both reactant) and control batches using a 2.5 ml gas tight syringe (SGE Analytical Science, Australia). The aqueous sample was injected to a 10-ml transparent glass vial. 100 µL of oxalic acid (0.5 mol) was immediately added to each sample to prevent any further oxidation of the VOC compounds. Then, the sample was capped with a magnetic cap and hard septum (Magnetic Bitemall; Red lacquered, 8mm center hole; Pharma-Fix-Septa, Silicone blue/PTFE grey; Grace Alltech). Batches were sampled until no detectable VOC concentration was found in the kinetic batches.

Concentrations of the target compounds were measured with a gas chromatograph (GC) (Fig. 3.1). The GC (Agilent 6850) was equipped with flame ionization detector (FID) and separation was done on an Agilent HP-1 capillary column (stationery phase: 100% dimethylpolysiloxane, length: 30 m, ID: 0.32 mm, film thickness: 0.25 µm). A temperature programmed run was used to analyze the samples. The concentration of VOC compounds was determined using a headspace method as used in previous studies (e.g. Snow, 2002; Przyjazny and Kokosa, 2002; Almeida and Boas, 2004; Sieg et al. 2008). The limits of quantification (LOQ) were calculated by using a signal-to-noise ratio of 10:1 (Kubinec et al., 2005).

To measure the concentration of permanganate, the samples were diluted immediately after collection and centrifuged (Heraeus/Kendro Biofuge) for 4 min at 13000 rpm to settle suspended manganese dioxide particles. The aqueous concentration of permanganate was measured subsequently using a UV-Spectrophotometer (UV-1800, Shimadzu) at a wavelength of 525 nm (Fig.3.2). TCE oxidation was also monitored by measuring the production of chloride. Chloride concentrations were determined by ion chromatography (e.g. Huang et al., 1999; Morales et al., 2000; He and Zhao, 2005; Tyrrell et al. 2009). The ion

chromatograph (Dionex DX-120) was equipped with a 4-mm Dionex IonPac™ AS22 capillary column. During the experiments, acidity was measured using a pH meter (HANNA, HI 8314).

3.2.3. Experimental and simulation procedure

The oxidation of target compounds with potassium permanganate was investigated in 120-ml glass vial reactors at room temperature (21 ± 1 °C). All experiments were carried out using a basic orbital laboratory shaker (IKA KS 260 B). Experiments were conducted using different combinations of the initial concentrations of the target compounds and potassium permanganate (Table 3.1). For two experiments, the initial concentration of the potassium permanganate was identical, while different initial concentration of the target compounds. For two other experiments, the initial concentration of permanganate was different, but with identical initial concentration of the target compounds.

We also prepared a series of control batches containing stock solutions of either the VOC or potassium permanganate. Control experiments were performed for each compound under identical conditions to ensure that the loss of target compound or permanganate due to reaction with water, photodecomposition or adsorption to the rubber stopper was negligible over the course of experiments.

Additional experiments for each compound were performed with the pH buffer to determine the effect of pH on the kinetics of oxidation of target compounds by permanganate. All experiments were performed in duplicate.

The second-order rate constants were derived by fitting a second-order rate model to the batch data. The obtained kinetic parameters for TCE, toluene, and ethanol were compared with literature values derived mostly using pseudo-first-order approaches (Table 3.2). The second-order rate constants were also estimated using the pseudo-first order experimental approach. Then, the error due to the inappropriate use of pseudo-first-order reaction rate was estimated by comparing k

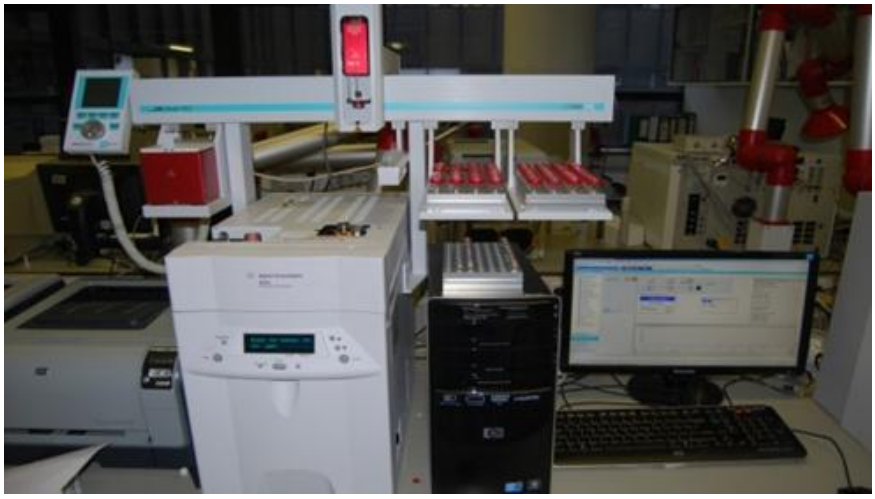

Fig. 3.1: Gas chromatograph (Agilent 6850) for measuring concentrations of the target compounds.

Fig. 3.2: A UV-Spectrophotometer (UV-1800, Shimadzu) for measuring concentrations of potassium permanganate.

Table 3.1: Experimental conditions for the three target compounds.

Compound	Experiment	$[VOC]_0$ (mmol)	$[KMnO_4]_0$ (mmol)	~P/N
TCE	1	42.0×10^{-3}	17.0×10^{-2}	2.0
	2	42.0×10^{-3}	3.4×10^{-1}	4.0
	3	85.0×10^{-3}	17.0×10^{-1}	10.0
	4	42.0×10^{-3}	17.0×10^{-1}	20.0
	5	21.0×10^{-3}	17.0×10^{-1}	40.5
Toluene	1	15.0×10^{-1}	100.0	5.5
	2	65.0×10^{-2}	100.0	12.8
	3	32.5×10^{-2}	100.0	25.6
	4	32.5×10^{-2}	200.0	51.3
	5	16.2×10^{-2}	100.0	51.3
Ethanol	1	40.0	200.0	1.25
	2	40.0	400.0	2.5
	3	30.0	400.0	3.33
	4	10.0	400.0	10.0
	5	2.5	200.0	20.0

Here, P is the initial concentration of potassium permanganate to initial concentration of a VOC and N is the number of moles of potassium permanganate in the stoichiometric reaction

of the pseudo-first-order reaction rate model with the value of second-order reaction rate model. Estimated errors were plotted versus the P/N value for data from the present study and TCE data from the literature (Huang et al., 1999; Huang et al., 2001; Kao et al., 2008; Urynowicz, 2008). All data points in figures are shown with 5% error bar.

3.2.4. Kinetics of VOC oxidation

The stoichiometric reaction for a target compound can be written in the following form:

Table 3.2: Second-order rate constants and corresponding experimental conditions for oxidation of target compounds with potassium permanganate.

VOC	[VOC] (mmol)	[$KMnO_4$] (mmol)	pH	T (°C)	~P/N	Method	k ($M^{-1}s^{-1}$)	Reference
TCE	8.0×10^{-2}	3.2×10^{-1}	6.0 - 8.0	RT	1.0	NA	7.9×10^{-1} (DI water), 8.5×10^{-1} (In tap water)	Vella and Veronda (1993)
	8.0×10^{-3}	7.0×10^{-1}	8.0	RT	21.85	NA	4.2×10^{-1}	Tratnyek et al. (1998)
	3.1×10^{-2} - 8.3×10^{-2}	3.7×10^{-1} - 1.2	4.0 - 8.0	21.0	3.0 - 3.6	First-order model	$6.7 \times 10^{-1} \pm 3.0 \times 10^{-2}$	Yen and Schwartz (1999)
	1.0×10^{-1}	6.3	4.0 - 8.0	21.0	15.75	First-order model	6.5×10^{-1} - 6.8×10^{-1}	Yen and Schwartz (2000)
	$1.4 \times 10^{-1} \pm 7.0 \times 10^{-2}$	$1.9 \pm 7.0 \times 10^{-2}$	7.0	20.0	3.4	First-order model	$8.0 \times 10^{-1} \pm 1.2 \times 10^{-1}$	Huang et al. (2001)
	NA	NA	6.9	20.0	NA	First-order model	8.9×10^{-1}	Siegrist et al. (2001)
	1.0 - 4.0	1.0×10^{-1}	7.0	25.0	*6.25×10^{-3} - 2.5×10^{-2}	First-order model	$7.6 \times 10^{-1} \pm 3.0 \times 10^{-2}$	Waldemer and Tratnyek (2006)
	3.8×10^{-2} - 1.5×10^{-1}	7.6×10^{-2} - 7.6×10^{-1}	6.3	25.0	0.5 - 12.5	Second-order model	8.0×10^{-1}	Kao et al. (2008)
	2.9×10^{-1}	6.3	NA	20.0	10.85	First-order model	9.5×10^{-1}	Urynowicz (2008)
	2.1×10^{-2} - 8.5×10^{-2}	3.4×10^{-1} - 1.7	4.3 - 7.0	20.0	2.0 - 40	First-order model Second-order model	6.7×10^{-1} ($r^2 = 0.99$) 8.0×10^{-1} ($r^2 = 0.99$)	This study
Toluene	4.0	1.0×10^{-1}	7.0	25.0	*1.67×10^{-4}	First-order model	83.2×10^{-5}	Waldemer and Tratnyek (2006)
	NA	NA	5.0 - 7.0	20.0	NA	First-order model	23.0×10^{-5}	Rudakov and Lobachev (2000)
	NA	NA	5.0 - 7.0	30.0	NA	First-order model	61.0×10^{-5}	Rudakov and Lobachev (2000)
	16.2×10^{-2} -1.5	100-200	7.0-8.5	20.0	25.7 - 51.2	First order model Second-order model	18.8×10^{-5} ($r^2 = 0.96$) 25.0×10^{-5} ($r^2 = 0.99$)	This study
Ethanol	171.5	9.2	4.6	20.0	*3.35×10^{-3}	First-order model	16.7×10^{-4}	Barter and Littler (1967)
	171.5	9.2	4.6	30.0	*3.35×10^{-3}	First-order model	40.3×10^{-4}	Barter and Littler (1967)
	2.5 - 80.0	200 - 400	7.0 - 7.8	20.0	1.25 - 20	First-order model Second-order model	53.3×10^{-5} ($r^2 = 0.96$) 65.0×10^{-5} ($r^2 = 0.99$)	This study

NA: Not available, RT: Room temperature, * Concentration of the target compound was kept constant, r^2: The square of linear correlation coefficient.

$$A + NB \rightarrow \text{Products} \tag{3.6}$$

where A and B denote the target compound and potassium permanganate, respectively, and N here is the number of moles of potassium permanganate in the stoichiometric reaction.

As shown by the stoichiometric reaction, full oxidation of one mole of a target compound requires N moles of potassium permanganate. Thus, the consumption of permanganate and target compounds are related by:

$$\Delta C_B = N\Delta C_A \tag{3.7}$$

where C_A denotes the concentration of the compound (M), C_B is the concentration of potassium permanganate (M), and ΔC denotes the consumed concentration of reactants (M).

Typically, second-order reaction rate constants for the oxidation of VOC compounds by permanganate have been obtained using a pseudo-first-order approach by assuming that either the contaminant or permanganate concentration is constant (Waldemer and Tratnyek, 2006; Urynowicz, 2008). However, the general form of a second-order reaction rate equation, as a function of the target compound and potassium permanganate concentrations in the aqueous phase, can be written as follows:

$$\frac{dC_A}{dt} = -kC_A C_B \tag{3.8}$$

where k denotes the reaction rate constant and t represents the time (s).

We now reformulate Equation 3.8 in terms of consumed fraction of reactants, $X_A(=(C_{A0}-C_A)/C_{A0})$ and $X_B(=(C_{B0}-C_B)/C_{B0})$. Here, C_{A0} is the initial

concentration of target compound (M). From Equation 3.7 and the definition of $P(=C_{B0}/C_{A0})$, we have: $X_B=NX_A/P$. Substitution of these definitions into Equation 3.8 and rearranging yields the following equation:

$$\frac{dX_A}{dt} = kC_{A0}(1-X_A)(P-NX_A) \tag{3.9}$$

Integration of Equation 3.9 gives the following general formula for the variation of X_A with time:

$$\frac{1}{C_{A0}(P-N)} \ln\left[\frac{(P-NX_A)}{P(1-X_A)}\right] = kt \qquad \text{where} \qquad P \geq N \tag{3.10}$$

According to Equation 3.10, a plot of $1/C_{A0}(P\text{-}N)$ ln $[(P\text{-}NX_A)/P\ (1\text{-}X_A)]$ vs. time should yield a straight line, with its slope being the second-order reaction rate constant k.

The solution for X_B follows from Equation 3.10 by substituting $X_A= PX_B/N$ to obtain:

$$\frac{P}{C_{B0}(P-N)} \ln\left[\frac{N(1-X_B)}{(N-PX_B)}\right] = kt \qquad \text{where} \qquad N>PX_B \tag{3.11}$$

The assumption for the commonly used pseudo first-order approach of constant concentration of one of the reactants is only valid if the amount of the target compound or permanganate is sufficiently high to neglect any change in the concentration during the course of an experiment (Huang et al., 2001; Siegrist et al. 2001; Urynowicz, 2008; Waldemer and Tratnyek, 2006). If permanganate is in excess, this means that P/N is much larger than unity. Therefore, Equation 3.10 for such conditions may be simplified to yield:

$$\frac{1}{C_{B0}} \ln \frac{C_A}{C_0} = -kt \qquad \text{where} \qquad P>>N \qquad (3.12)$$

To estimate k using the pseudo first-order approach, Equation 3.12 can be used with a constant concentration of permanganate, equal to its initial value.

3.3. Oxidation of VOC compounds

The oxidation of VOC compounds by permanganate was monitored until VOC concentrations were below detection. Fig. 3.3 depicts the normalized concentration (C/C_0) of the VOC compounds as a function of time. The experiments lasted from less than an hour for TCE to up to a week for toluene, with experimental durations for ethanol oxidation being intermediate. Concentration of the target compounds in the controls did not decrease during the experiments. Since no additional peaks were observed in the chromatogram of the samples, we concluded that the VOCs were fully mineralized according to Equations 3.2 to 3.4. Experiments were conducted with excess potassium permanganate using varying initial reactant concentration ratios that deviated from the stoichiometry of the reactions (Table 3.1).

The extent of the deviations was expressed as the ratio of the initial molar concentration of potassium permanganate over the required stoichiometric concentration (i.e., P/N). As illustrated in Fig. 3.3, oxidation rates increased for larger values of P/N.

Both the VOC and permanganate concentrations were found to decrease as expected based on the stoichiometry of full oxidation according to reactions 3.2 to 3.4. Also, for TCE, approximately 97.5% of the chloride ions for the TCE experiments with an initial concentration of 0.042 (mmol) were recovered during the TCE oxidation stage (Fig. 3.4). This also indicated that TCE was completely

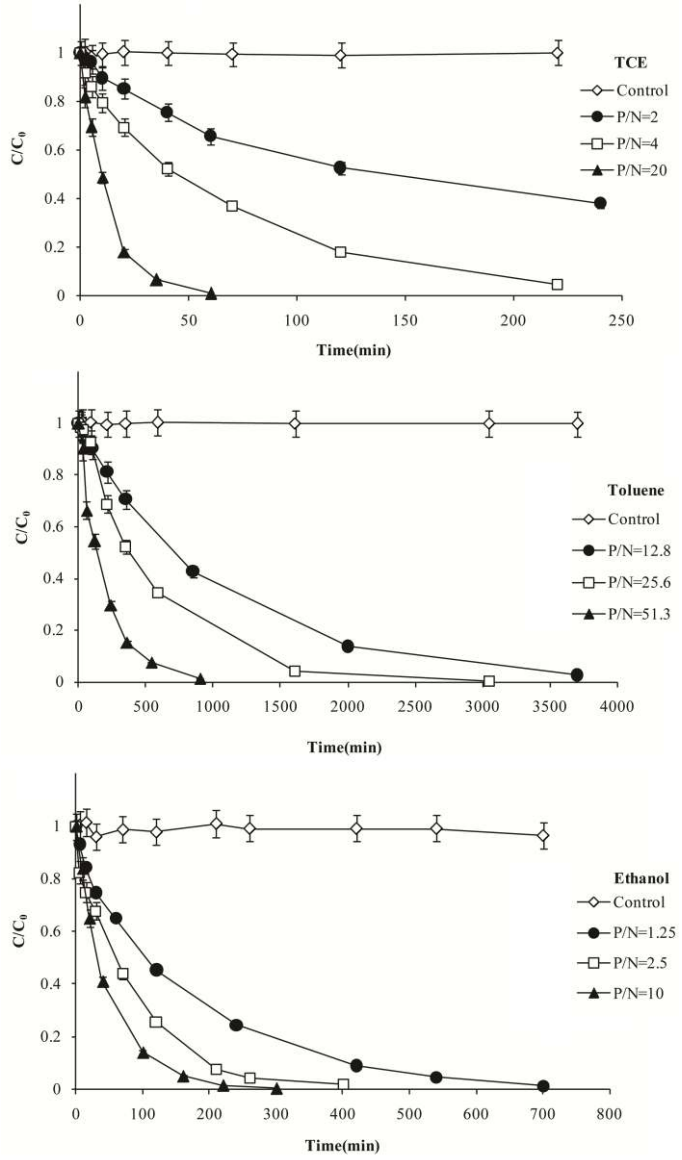

Fig. 3.3: Oxidation of TCE, toluene, and ethanol vs. time for three different P/N ratios.

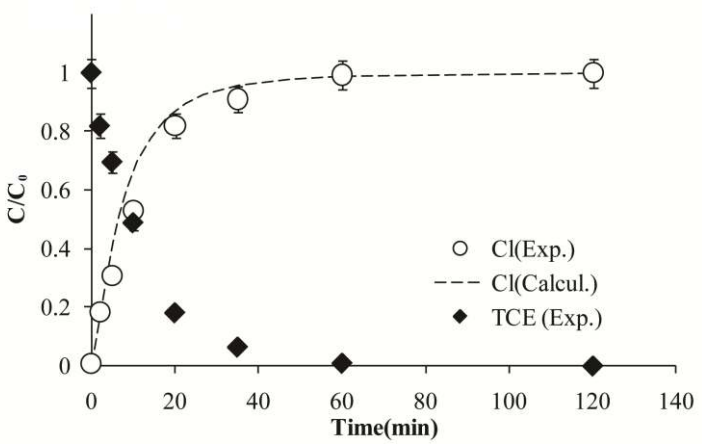

Fig. 3.4: Normalized concentration of TCE and chloride ion vs. time for Experiment 3.4.

oxidized to produce CO_2, H^+, and Cl^-. The measured Cl^- concentration in all TCE experiments closely followed the calculated value based on the stoichiometric reaction (Equation 3.4).

Results revealed that the measured consumed fractions of permanganate agreed with values calculated based on stoichiometric reactions (Fig. 3.5). This means that the consumption of permanganate was only due to the oxidation of target compounds, and that decomposition reactions with water were negligible during the experiments.

3.4. Kinetics analysis of data

We used Equation 3.10 and all data from Experiments 1 to 5 (Table 3.1), to estimate k for each compound. Fig. 3.6 shows that the plots of $1/C_{A0}$ (P-N) ln $[(P-NX_A)/(P(1-X_A)]$ vs. time for all compounds. The square of linear correlation coefficients (r^2) values of the regressions obtained for TCE, toluene, and ethanol

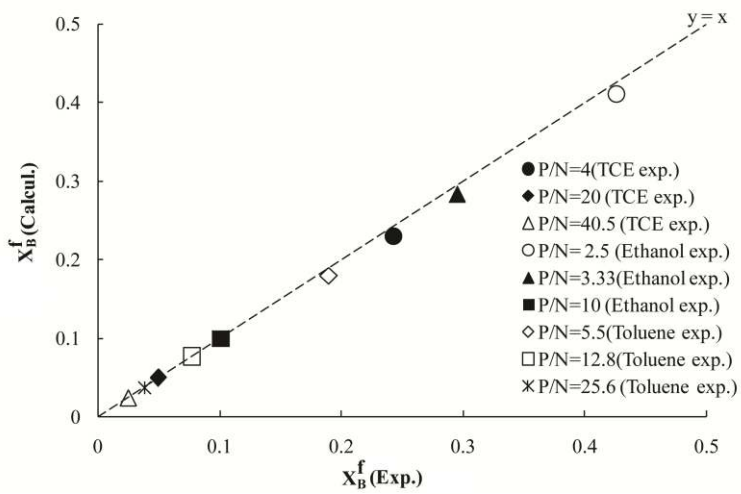

Fig. 3.5: Final consumed fraction of potassium permanganate ($X_B^f = C_B^f / C_{B0}$) for different P/N values.

were 0.990, 0.987 and, 0.971, respectively. The corresponding reaction rate constants are given in Table 3.2. Results showed that the reaction rate constant for TCE was higher than for ethanol and toluene, consistent with the study by Waldemer and Tratnyek (2006).

We also used Equation 3.11 to estimate k again; this time based on the consumed fraction of permanganate (X_B). Fig. 3.7 depicts plots of P/C_{B0} (P-N) ln $[N(1-X_B)/(N-PX_B)]$ vs. time for all target compounds. Results show that Equation 3.11 can simulate very effectively the consumption of permanganate during oxidation of the target compounds. Reaction rate constants ($M^{-1}s^{-1}$) based on Equation 3.11 were found to be 7.83×10^{-1}, 2.60×10^{-4}, and 6.67×10^{-4} for TCE, toluene, and ethanol, respectively. For the calculations we used all available data for the degradation of potassium permanganate.

We applied Equation 3.12 to all data from experiments 1 to 5 for each compound. Fig. 3.8 shows plots of $1/C_{B0} \ln C_A/C_0$ versus time for all compounds. Values of k were calculated from the slope of the line for each compound. The r^2

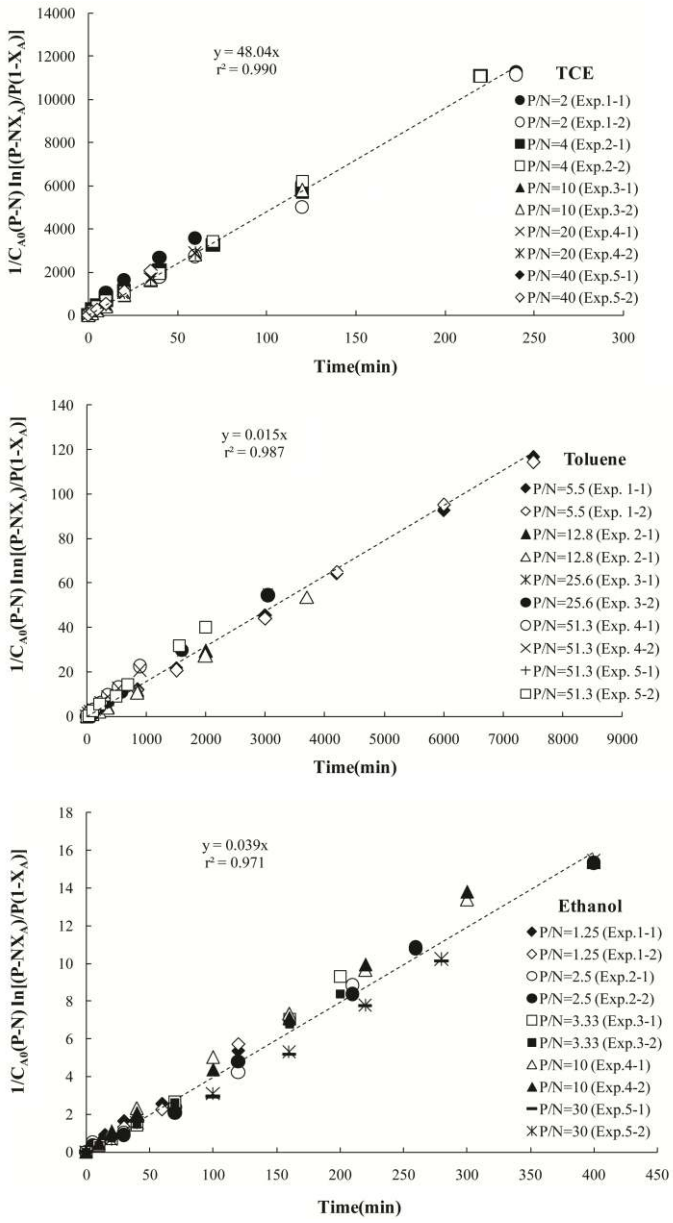

Fig. 3.6: Plots of $1/C_{A0}(P\text{-}N)\ln[(P\text{-}NX_A)/P(1\text{-}X_A)]$ vs. time for the target compounds, corresponding to Equation 3.10 (Exp. x-y: x denotes the number of the experiment and y is the experiment repetition).

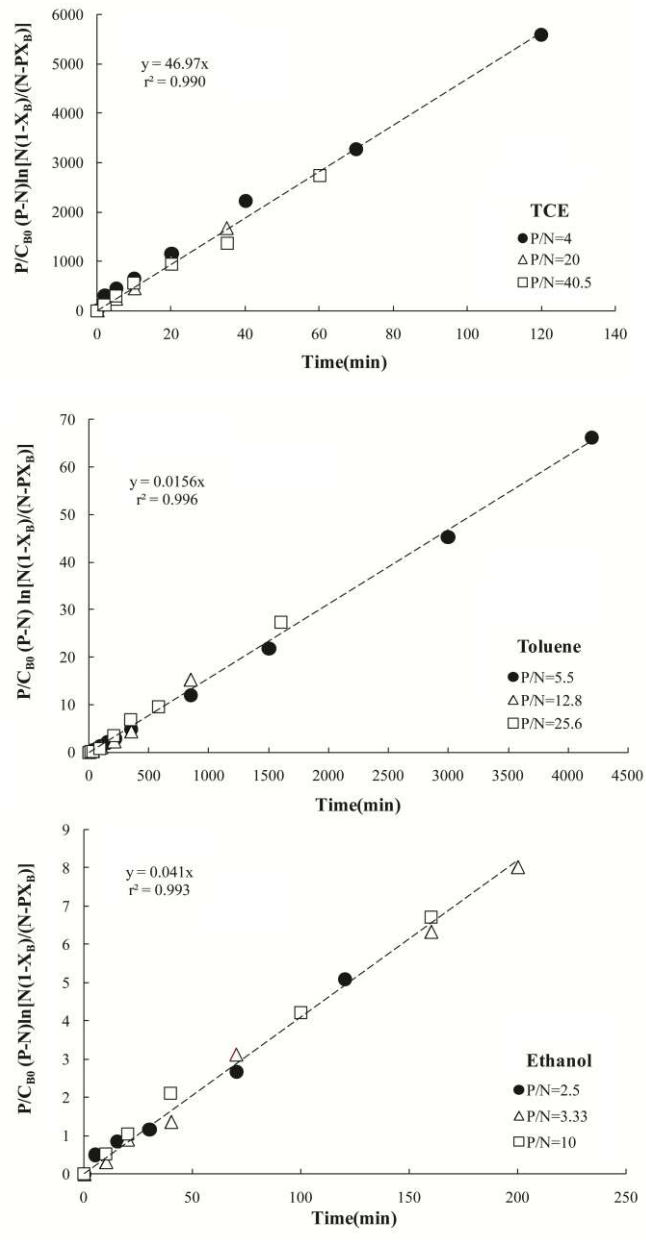

Fig. 3.7: Plot of $P/C_{B0}(P-N)\ \ln[N(1-X_B)/(N-PX_B)]$ vs. time for target compounds based on Equation 3.11.

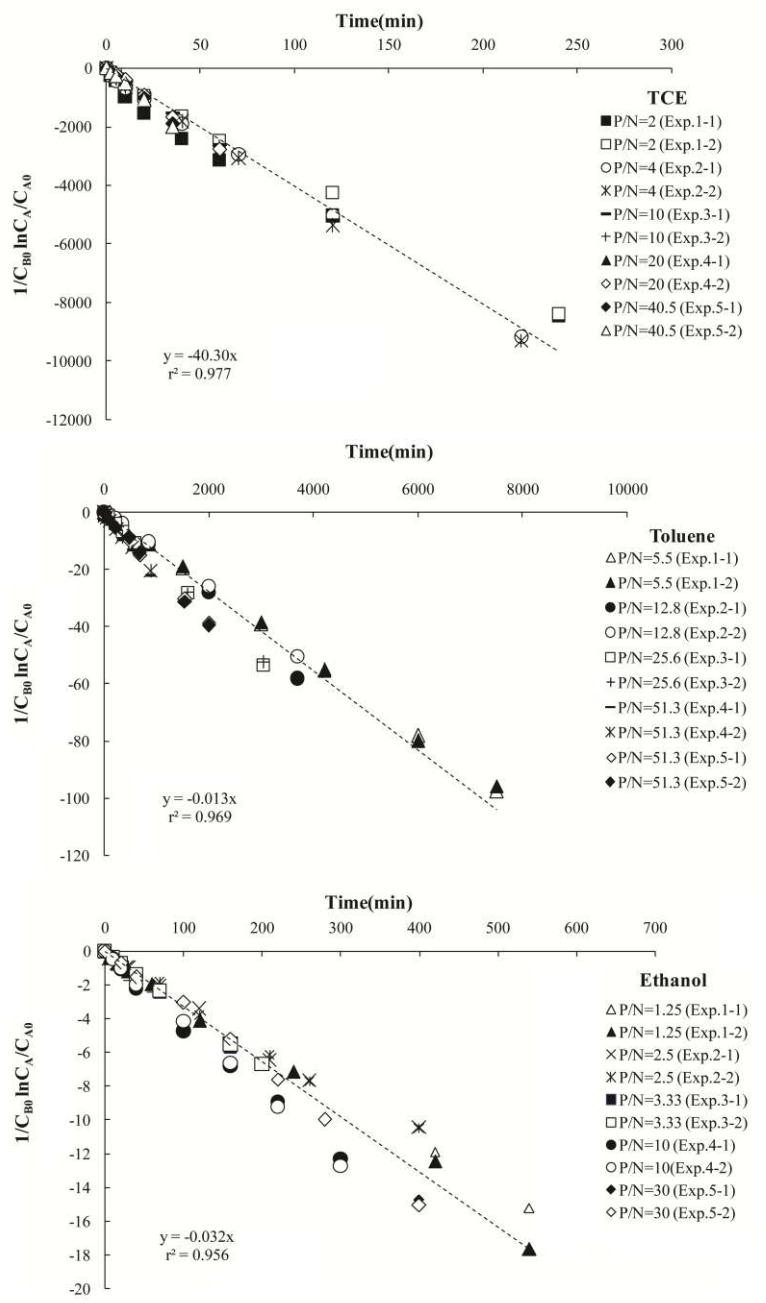

Fig. 3.8: Plots of $1/C_{B0} \ln C_A/C_0$ vs. time for the target compounds, corresponding to Equation 3.12.

values for the pseudo-first order approach were smaller than those for the second-order model, having values of 0.977, 0.969, and 0.956 for TCE, toluene, and ethanol, respectively.

Comparison of simulation results obtained with the two models revealed that the oxidation reaction of the target compounds was better represented by the second-order model, rather than the pseudo-first order model. This indicates that the permanganate abundances (P/N up to 50) were insufficient to ignore changes in the initial permanganate concentrations. Reaction rate constants derived using the second-order model hence should be considered more appropriate.

With increasing stoichiometric abundance of one of the reactants, the error associated with assuming a constant initial concentration in the pseudo-first-order approach is expected to decrease. To assess the influence of reactant abundance on the error in estimating second-order rate constants with a pseudo-first order approach, Equations 3.10 and 3.12 were used to determine k for each experiment (Experiments 1 to 5) individually. We subsequently estimated the error by comparing k of a pseudo-first-order reaction rate model with the value of second-order reaction rate model. Results show that the errors were negatively correlated with the P/N, with the largest error corresponding to the lowest ratio of P/N ratio (Fig. 3.9). Moreover, for the largest values of P/N, the errors became smaller, but never zero since the consumption of excess reactant is never really zero. However, with a stoichiometric excess of P/N > 40, the error (using the pseudo-first-order model to estimate the second-order rate constant) fell below 5%.

Literature has shown a range of estimated second-order rate constants, mainly using the pseudo-first order approach (Table 3.2). As these studies used varying degrees of reactant excess, we investigated to what extent this range was influenced by errors due to the inappropriate use of the pseudo-first order approach. For this purpose we fitted the second-order and pseudo first-order models to literature data for TCE oxidation (Huang et al., 1999; Huang et al., 2001; Kao et al., 2008; Urynowicz, 2008) and calculated the difference between the k values of the two models for different P/N values (Fig. 3.9). Results confirmed that the

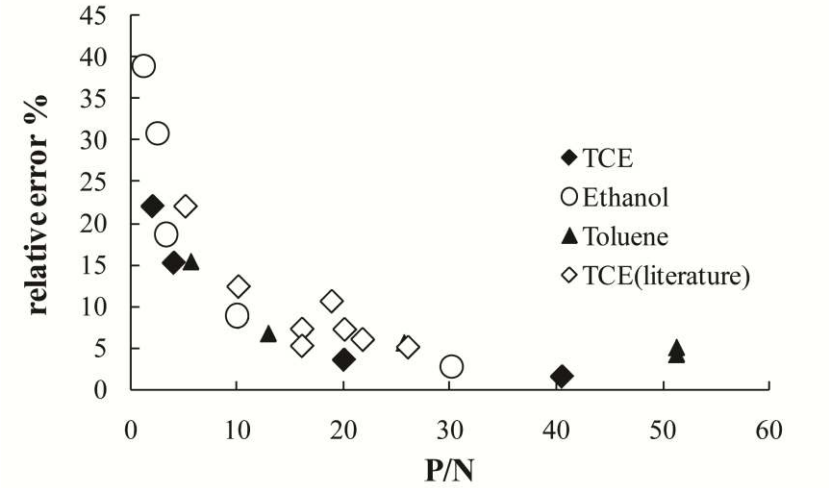

Fig. 3.9: Relative errors in k using the pseudo first-order reaction rate model versus the P/N value.

magnitude of errors was negatively correlated with P/N ratio, similar to the analysis of our own data (Fig. 3.9).

In Table 3.2, the reported estimates for the second-order reaction rate constants for the oxidation of target compounds by permanganate and their corresponding experimental conditions are presented. Evidently, a wide range of the second-order reaction rate constant values are reported for TCE oxidation. Those values varied between 4.2×10^{-1} and 11.9×10^{-1} $M^{-1}s^{-1}$ for different conditions (Huang et al., 2001; Kao et al., 2008; Siegrist et al., 2001; Waldemer and Tratnyek, 2006). Our value for the TCE reaction rate constant, 8.0×10^{-1} $M^{-1}s^{-1}$, was identical to the value obtained by Kao et al., (2008), who also used the second-order modeling approach. Hence, despite different experimental conditions, the calculated value of the TCE reaction rate constant in our study was consistent with this literature value for the second order rate constant.

Several studies provided data on the oxidation of toluene by permanganate (Rudakov and Lobachev, 2000; Waldemer and Tratnyek, 2006). A comparison of all available reaction rate constants for toluene and their corresponding

experimental conditions showed that our value of 2.5×10^{-4} $M^{-1}s^{-1}$ is at the low end of the reported range. The estimation method used to determine the second-order reaction rate constant (either the pseudo-first-order or second order modeling approach) can be a reason for this difference.

For the second-order reaction rate constant of ethanol oxidation by permanganate, only two values could be found in the literature (Table 3.2). Those values are higher than the value obtained in our study (6.5×10^{-4} $M^{-1}s^{-1}$ at ~20 ºC). In the study by Barter and Littler (1967), the ethanol concentration was kept in excess (P/N <<1), which should yield a very low error using the pseudo-first-order approach, equivalent to a P/N of 298. However, their study was conducted at much lower pH values of about of 3.0 to 4.0, while our experiments were performed at groundwater relevant pH's in the range of 7.0 to 7.8. Higher oxidation rates at lower pH's may be explained by the overall reaction equation (Equation 3.4), which shows a net 1:1 proton demand for each mole of permanganate consumed. A similar pH dependency may be expected for the oxidation of toluene (Equation 3.3). Changes in pH during our toluene and ethanol oxidation experiments were however limited, and did not affect the reaction rates. The results of our experiments showed, the pH decreased from 7.0 down to 4.3 during TCE oxidation, but increased to 7.8 and 8.6 for ethanol and toluene oxidation, respectively. As shown by Equations 3.2 to 3.4, the oxidation of TCE produced H^+, which caused a decrease in pH, while ethanol and toluene oxidation produced OH^-, which caused an increase in pH.

Since groundwater pH values are commonly around 7.0, an experiment was performed at this pH value for each compound (Fig. 3.10). Results produced the same reaction rate constants, thus showing that the pH does not have a significant effect on the reaction rate constant within the range of pH values from 4.3 to 7.0, 7.0 to 8.5, and 7.0 to 7.8 for TCE, toluene, and ethanol, respectively. These results are consistent with those by Waldemer and Tratnyek (2006) and Kao et al. (2008) who found that the pH did not significantly affect the TCE reaction rate within this pH range.

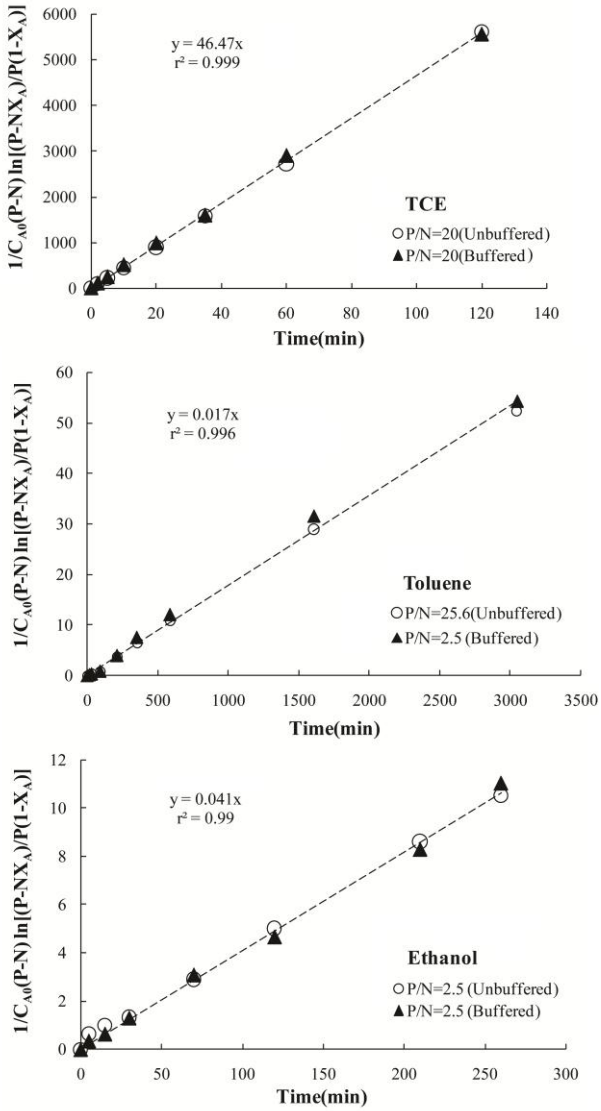

Fig. 3.10: Comparison of the oxidation of target compounds in buffered and unbuffered experiments based on Equation 3.10.

3.5. Conclusions

In this study, the kinetics of the oxidation of dissolved chlorinated hydrocarbon (TCE) and non-chlorinated hydrocarbons (toluene and ethanol) by permanganate were investigated at room temperature (~20 ºC). Results showed that the oxidation rate of ethanol and toluene by permanganate were lower compared to TCE. Rather than employing the common pseudo-first-order kinetic analysis, we used a more realistic and accurate second-order formulation for the oxidation of target compounds by permanganate. The reaction rate constants based on the second-order model for TCE, toluene, and ethanol were found to be 8.0×10^{-1} (M^{-1} s^{-1}), 2.5×10^{-4} ($M^{-1}s^{-1}$), and 6.5×10^{-4} ($M^{-1}s^{-1}$), respectively.

Our results further revealed that the reaction rate constants of TCE, toluene, and ethanol are independent of pH within the range of 4.3 to 7.0, 7.0 to 8.5, and 7.0 to 7.8, respectively. For TCE, this dependency had been reported previously in the literature (Kao et al., 2008; Waldemer and Tratnyek, 2006). The oxidation of toluene and ethanol is however expected to increase with increasing acidity.

The degree of reactant excess (P/N value) was found to strongly influence the accuracy of the pseudo-first-order approach. In general, the reaction rate constant obtained from the pseudo-first-order model is smaller than the second-order rate constant. The difference is larger for P/N ratios. The relative difference is around 5% to 25%. So, the inappropriate use of the pseudo-first-order model shows a significant deviation from the actual second-order reaction rate constant. Neglecting these errors may have a significant effect on design, modeling, and performance of an ISCO remediation plan. Errors in k can also affect the desired injection rate of potassium permanganate solution to the contaminated site and the desirable concentration of potassium permanganate in the injected solution.

Despite the slower oxidation kinetics of ethanol and toluene in comparison to TCE, their reaction rates, correspond to half-lives of one to several hours, are still fast enough for the field application of permanganate to remediate these compounds.

3.6. References

[1] Almeida, C.M.M., and Boas, L.V., 2004. Analysis of BTEX and other substituted benzenes in water using headspace SPME-GC-FID: method validation. J. Environ. Monit. 6: 80-88.

[2] Barter, R.M., and Littler, J.S., 1967. Hydride ion transfer in oxidations of alcohols and ethers. Chem. Soc. B: 205-210.

[3] Berscheid, M., Burger, K., Hutchison, N., Muniz-Ghazi. H., Renzi, B., Ruttan, P., and Sterling, S., Proven, 2010. Technologies and Remedies Guidance: Remediation of Chlorinated Volatile Organic Compounds in Vadose Zone Soil. California Department of Toxic Substances Control. http://www.dtsc.ca.gov/ sitecleanup/upload/cVOC_040110.pdf.

[4] Bryant, D., Battey, T., Coleman, K., Mullen, D., Oyelowo, L., 2001. Permanganate in-situ chemical oxidation of TCE in a fractured bedrock aquifer. Proceeding of the First International Conference on Oxidation and Reduction Technologies for In-Situ Treatment of Soil and Groundwater; 2001 June 25-29; Niagara Falls, Ontario, Canada.

[5] Capiro, N.L., Stafford, B.P., Rixey, W.G., Bedient, P.B, Alvarez, P.J.J., 2007. Fuel-grade ethanol transport and impacts to groundwater in a pilot-scale aquifer tank. Water. Res. 41: 656-64.

[6] Cave, L., Hartog, N., Al, T., Parker, B., Mayer, K.U., Cogswell S., 2007. Electrical monitoring of in situ chemical oxidation by permanganate. Ground water Monit. R 27(2): 77-84.

[7] Damma, J.H., Hardacreb, C., Kalina, R.M., Walsha, K.P., 2002. Kinetics of the oxidation of methyl tert-butyl ether (MTBE) by potassium permanganate. J. Water Res. 36: 3638-46.

[8] EPA (Environmental Protection Agency), 2011. Toxicological review of trichloroethylene. CAS No. 79-01-6. http://www.epa.gov/iris/toxreviews/0199tr/ 0199tr.pdf.

[9] Freitas, J.G., Fletcher, B., Aravena, R., and Baker, J.F, 2010. Methane production and isotopic fingering in ethanol fuel contaminated sites. Groundwater; 48: 844-857.

[10] He, F., and Zhao, D., 2005. Preparation and characterization of a new class of starch-stabilized bimetallic nanoparticles for degradation of chlorinated hydrocarbons in water. Environ. Sci. Technol. 39: 3314-3320.

[11] Hønning, J., Broholm, M.M., and Larsen, T.H., 2005. Oxidation kinetics and consumption of potassium permanganate in moraine clay, Third International Conferences on Oxidation and Reduction Technologies for In-Situ Treatment of Soil and Groundwater (ORT-3); 2004 October 24-28; San Diego, US. Ontario: Redox Technologies, Inc.

[12] Huang, K.C., Hoag, G.E., Chheda, P., and Woody, B.A., 1999. Dobbs GM. Kinetic study of oxidation of trichloroethylene by potassium permanganate. Environ. Eng. Sci. 16: 265-274.

[13] Huang, K.C., Hoag, G.E., Chheda, P., Woody BA, and Dobbs. G.M., 2001. Oxidation of chlorinated ethenes by potassium permanganate: a kinetics study. Hazard. Mater. 87: 155-169.

[14] Johnson, R., Pankow, D., Bender, C.P., Price, C.V., and Zogorski, J., 2000. MTBE: to what extent will past releases contaminate community water supply wells?. Environ. Sci. Technol. 34: 210-217.

[15] Kao, C.M., Huang, K.D., Wang, J.Y., Chen, T.Y., and Chien, H.Y., 2008. Application of potassium permanganate as an oxidant for in-situ oxidation of trichloroethylene-contaminated groundwater: A laboratory and kinetics study. Hazard. Mater. 153: 919-927.

[16] Kubinec, R., Adamuscin, J., Jurdakova, H., Foltin, M., Ostrovsky, I., Kraus, A., and Sojak, L., 2005. Gas chromatographic determination of benzene, toluene, ethylbenzene and xylenes using flame ionization detector in water samples with direct aqueous injection up to 250 µl. J Chromatogr A 1084: 90-94.

[17] Lee, E.S., Seol, Y., Fang, Y.C., and Schwartz, F.W., 2003. Destruction efficiencies and dynamics of reaction fronts associated with the permanganate oxidation of trichloroethylene. Environ. Sci. Technol. 37: 2540-2546.

[18] Mackay, D., De Sieyes, N., Einarson, M., Feris, K., and Pappas, A., Wood, I., Jacobson, L., Justice, L., Noske, M., Wilson, J., Adair, C., and Scow, K., 2007. Impact of ethanol on the natural attenuation of MTBE in a normally sulfate-reducing aquifer. Environ. Sci. Technol. 41: 2015-2021.

[19] Morales, J.A., de Graterol, L.S., and Mesa, J., 2000. Determination of chloride, sulfate and nitrate in groundwater samples by ion chromatography. J. Chromatogr A 884(1-2): 185-190.

[20] Mumford, K.G., Lamarche, C.S, and Thomson, N.R., 2004. Natural oxidant demand of aquifer materials using the push-pull technique. Environ. Eng. 130: 1139-1146.

[21] Mumford, K.G., Thomson, N.R., and Allen-King, R.M., 2005. Bench-scale investigation of permanganate national oxidant demand kinetics. Environ. Sci. Technol. 39: 2835-2840.

[22] Powers, S.E., Rice, D., and Dooher, B., Alvarez P.J.J., 2001. Will ethanol-blended gasoline affect groundwater quality?. Environ. Sci. Technol. 35: 26A-30A.

[23] Przyjazny, A., and Kokosa, J.M., 2002. Analytical characteristics of the determination of benzene, toluene, ethylbenzene and xylenes in water by headspace solvent microextraction. J. Chromatogr A 977 (2):143-153.

[24] Rivett, M.O., Wealthall, G.P., Dearden, R.A., and McAlary, T.A., 2011. Review of unsaturated-zone transport and attenuation of volatile organic compound (VOC) plumes leached from shallow source zones. Contam. Hydrol. 123:130-156.

[25] Rudakov, E.S., Lobachev, V.L., 2000. The first step of oxidation of alkylbenzenes by permanganates in acidic aqueous solutions. Russ. Chem. Bull 49: 761-777.

[26] Schubert, M., Schmidt, A., Müller, K., and Weiss, H., 2011. Using radon-222 as indicator for the evaluation of the efficiency of groundwater remediation by in-situ air sparging. Environ. Radioactiv. 102: 193-199.

[27] Sieg, K., Fries, E., and Püttmann, W., 2008. Analysis of benzene, toluene, ethylbenzene, xylenes and *n*-aldehydes in melted snow water via solid-phase

dynamic extraction combined with gas chromatography/mass spectrometry. J. Chromatogr A 1178(1-2): 178-186.

[28] Siegrist, R.L., Urynowicz, M.A., West, O.R., Crimi, M.L., and Lowe, K.S., 2001. Principles and practices of in-situ chemical oxidation using permanganate. Columbus, OH: Battelle Press.

[29] Snow, N.H., 2002. Head-space analysis in modern gas chromatography. Trace-Trend Anal Chem 21: 608-17.

[30] Struse, A.M., Siegrist, R.L., Dawson, H.E., and Urynowicz, M.A., 2002. Diffusive transport of permanganate during in-situ oxidation. Environ. Eng. 128: 327-334.

[31] Tyrrell, É., Shellie, R.A., Hilder, E.F., Pohl, C.A., 2009. Haddad PR. Fast ion chromatography using short anion exchange columns. J. Chromatogr A 1216(48): 8512-8517.

[32] Urynowicz, M.A., 2008. In-situ chemical oxidation with permanganate: assessing the competitive interactions between target and nontarget compounds. Soil & Sediment Contam. 17: 53-62.

[33] Vella, P.A., and Veronda, B., 1993. Oxidation of trichloroethylene: A comparison of potassium permanganate and Fenton's reagent. Proceedings of the Third International Symposium on Chemical Oxidation, Technology for the Nineties; 1993 February 17-19; Vanderbilt University, Nashville, US. Lancaster: Technomic Publishing Company.

[34] Waldemer, R.H., Tratnyek, P.G., 2006. Kinetics of contaminant degradation by permanganate. Environ. Sci. Technol. 40: 1055-1061.

[35] Yan, Y.E., and Schwartz, F.W., 1999. Oxidative degradation and kinetics of chlorinated ethylenes by potassium permanganate. Contam. Hydrol. 37: 343-365.

[36] Yan, Y.E., and Schwartz, F.W., 2000. Kinetics and mechanisms for TCE oxidation by permanganate. Environ. Sci. Technol. 34: 2535-2541.

[37] Yen, C.H., Chen, K.F., Kao, C.M., Liang, S.H., and Chen, T.Y., 2011. Application of persulfate to remediate petroleum hydrocarbon-contaminated soil: feasibility and comparison with common oxidants. Hazard. Mater. 186(2-3): 2097-2102.

[38] Yin, Y., and Herbert, E.A., In-Situ Chemical Treatment. Technology Evaluation Report. Ground-Water Remediation Technologies Analysis Center. Pittsburgh PA. http://clu-in.info/download/toolkit/inchem.pdf.

[39] Yu, K.P., and Lee, G.W.M., 2007. Decomposition of gas-phase toluene by the combination of ozone and photocatalytic oxidation process (TiO_2/UV, TiO_2/UV/O_3, and UV/O_3). Appl. Catalysis B: Environ. 75: 29-38.

Chapter 4

Oxidation of trichloroethylene, toluene, and ethanol vapours by a partially saturated permeable reactive barrier; Column experiments and modeling

Published as: Mahmoodlu, M.G., Hassanizadeh, S.M., Hartog, N., Raoof, A., 2014. Oxidation of trichloroethylene, toluene, and ethanol vapours by a partially saturated permeable reactive barrier. J. Contam. Hydrol. 164:193-208.

Abstract

The mitigation of volatile organic compound (VOC) vapours in the unsaturated zone largely relies on the active removal of vapour by ventilation. In this study we considered an alternative method involving the use of solid potassium permanganate to create a horizontal permeable reactive barrier for oxidizing VOC vapours. Column experiments were carried out to investigate the oxidation of trichloroethylene (TCE), toluene, and ethanol vapours using a partially saturated mixture of potassium permanganate and sand grains. Results showed a significant removal of VOC vapours due to the oxidation. We found that water saturation has a major effect on the removal capacity of the permeable reactive layer (PRL). We observed a high removal efficiency and reactivity of potassium permanganate for all target compounds at the highest water saturation (S^w=0.6). A change in pH within the reactive layer reduced oxidation rate of VOCs. The use of carbonate minerals increased the reactivity of potassium permanganate during the oxidation of TCE vapour by buffering the pH. Reactive transport of VOC vapours diffusing through the PRL was modelled, including the pH effect on the oxidation rates. The model accurately described the observed breakthrough curve of TCE and toluene vapours in the headspace of the column. However, miscibility of ethanol in water in combination with produced water during oxidation made the modelling results less accurate for ethanol. A linear relationship was found between total oxidized mass of VOC vapours per unit volume of PRL and initial water saturation. This behaviour indicates that pH changes control the overall reactivity and longevity of the PRL during oxidation of VOCs. Results suggest that field application of a horizontal permeable reactive barrier can be a viable technology against upward migration of VOC vapours through the unsaturated zone.

4.1. Introduction

During the past few decades, the migration of volatile organic compounds (VOCs) by diffusion from contaminated soil or groundwater into overlying buildings has received considerable attention (McHugh et al. 2013; Provoost et al., 2009). Human health risks of VOCs are typically dominated by the extent of exposure through inhalation of indoor air. The health risks from VOC vapour inhalation are much greater than those from drinking comparably contaminated water on volumetric base (KDHE, 2007). Hence, methods to diminish or prevent vapour intrusion into buildings are of great public interest.

A number of techniques exist for treating unsaturated zone contaminated with VOCs. Despite their successful use, they all suffer from several shortcomings. For example, soil vapour extraction requires long-term operation and does not convert the contaminants to less toxic compounds (Cho et al., 2002). Bioventing is an in-situ bioremediation technology that degrades VOCs. However, performance of this method can be affected by soil permeability and water content restrictions. Moreover, the method is not effective for aerobic biodegradation of many chlorinated hydrocarbons (Hinchee, 1993; USEPA, 1995). In-situ chemical oxidation (ISCO) of VOCs has been well developed as a remediation technology of dissolved VOCs in groundwater (Heiderscheidt et al., 2008; Li and Schwartz, 2004; Tsitonaki et al., 2010; Yuan et al., 2013). However, only a few studies have applied ISCO to the unsaturated zone using permanganate (Hesemann and Hildebrandt, 2009) or other oxidants (Cronk et al., 2010). In these studies, the oxidant was mostly introduced as an aqueous solution, thus effectively saturating the unsaturated zone. By contrast, our recent study showed that dry solid potassium permanganate granules were able to oxidize TCE, toluene, and ethanol (target compound) vapours, according to the following overall reaction equations (Mahmoodlu et al., 2013a):

$$C_2HCl_{3(g)} + 2KMnO_{4(s)} \rightarrow 2K^+ + 2MnO_{2(s)} + 3Cl^- + 2CO_{2(g)} + H^+ \quad (4.1)$$

$$C_6H_5CH_{3(g)} + 12KMnO_{4(s)} + 2H_2O \rightarrow 12K^+ + 12OH^- + 12MnO_{2(s)} + 7CO_{2(g)} \quad (4.2)$$

$$C_2H_5OH_{(g)} + 4KMnO_{4(s)} \rightarrow 4K^+ + 4OH^- + 4MnO_{2(s)} + 2CO_{2(g)} + H_2O \quad (4.3)$$

VOC vapour oxidation presented in our earlier study occurred through the exposure of VOC vapour to excess amounts of solid potassium permanganate. As a result, any potential long-term effects on the reactivity of potassium permanganate through the accumulation of reaction products, such as manganese dioxide (MnO_2) and pH changes, could not be assessed. Also, the experiments were performed at low moisture conditions with only ambient air providing initial humidity. While the study confirmed the potential of using permanganate for permeable reactive barriers in the unsaturated zone, it remained unclear how water content and chemical evolution would affect the reactivity of a PRL. In this study we therefore performed a series of column experiments to (1) evaluate the ability of solid potassium permanganate as a horizontal permeable reactive layer (HPRL) to oxidize the vapour of three VOCs under various degrees of water saturation, (2) investigate the impact of the accumulations of by-products on the long-term reactivity of potassium permanganate, and (3) numerically simulate the migration and oxidation process of each target compound diffusing through the PRL.

4.2. Materials and methods

4.2.1. Materials

The contaminants (target compounds) used in this study were pure TCE, toluene, and ethanol (from Sigma-Aldrich, Merck, and ACROS, respectively). Solid potassium permanganate of 99% purity was obtained from Sigma-Aldrich and well mixed with sand to create a PRL. The sand used in this study originated from a river bed in Papendrecht (Filcom Company, The Netherlands) and was sieved to retain sizes of 0.5-1 mm. The porosity of sand was estimated to be approximately 0.35.

Since the mean size of potassium permanganate grains was almost equal to the sand mean grain size, we assumed the same porosity for potassium permanganate.

Two additional TCE experiments were conducted to test the effect of pH buffering by adding sodium bicarbonate ($NaHCO_3$) (≥99.0%, Merck) and calcium carbonate ($CaCO_3$) (≥99.0%, Merck). Deionized (DI) water was used to adjust the required initial water saturation in the PRL, and to investigate the effect of adding water on the reactivity of PRL.

A glass cylinder of 5.0 cm length and 4.0 cm internal diameter, capped by a steel stainless lid, was used to construct the experimental columns. The columns were divided into two parts by means of a glass filter (P0, $\phi = 0.3$, Robu & Schott, ISO 4793), which was fused to the inner wall of the columns. HPRLs consisting of a combination of solid potassium permanganate, sand, and DI water, was placed on top of the glass filters, through which VOC vapour could diffuse from below (Fig. 4.1).

4.2.2. Sampling and Measurements

During the experiments, gas samples of 1.5 ml were periodically taken from the headspace of the reactive and control columns using a 2.5 ml gas-tight syringe (SGE Analytical Science, Australia). To eliminate the effect of a pressure drop due to sampling, the same volume of air (1.5 ml) was simultaneously injected in the upper part of the column through a separate valve (Injecting air valve). The gas sample subsequently was injected into a 10-ml transparent glass vial which was capped with a magnetic cap and hard septum (Magnetic Bitemall; Red lacquered, 8 mm center hole; Pharma-Fix-Septa, Silicone blue/PTFE grey; Grace Alltech). Sampling vials were immediately placed into the tray of a gas chromatograph (GC). Gas samples of 2.0 ml were taken by an autosampler using the headspace syringe of the GC from each vial. Samples were next injected into the GC. The GC (Agilent 6850) was equipped with a flame ionization detector (FID). Separation was done on an Agilent HP-1 capillary column (stationery phase: 100% dimethylpolysiloxane, length: 30 m, ID: 0.32 mm, film thickness: 0.25 μm). A temperature programmed

run was used to analyze the samples. VOC concentrations were determined using a headspace method as employed in previous studies (e.g. Almeida and Boas, 2004; Przyjazny and Kokosa, 2002; Sieg et al. 2008; Snow, 2002). The limits of quantification (LOQ) were calculated by using a signal-to-noise ratio of 10:1 (Kubinec et al., 2005).

To measure the total organic carbon (TOC) content, the sand (D_0=0.5-1 mm) was grinded before the experiment and sieved to a particle size fraction of < 250 μm. Measurements were next carried out using Fisons Instruments analyzer (NA 1500 NCS) with a cycle time of 180 s and a source temperature of 190 $^{\circ}$C.

4.2.3. Experimental procedure

Mixtures of potassium permanganate grains (20 g) and sand (10 g) with different water saturation (0.0, 0.2, 0.4, and 0.6) were used to create the PRLs. First, potassium permanganate and the sand grains were placed into a small plastic container and shaken for 10 minutes in order to obtain a homogeneous mixture. This mixture subsequently was wetted with DI water required to obtain the desired water saturation. In order to obtain homogeneity, the wetted mixture was shaken for 15 minutes. The mixture was next placed on the glass filter of each column described above. This created a PRL of about 1.0 cm thick with a surface area 13.2 cm^2. The columns were immediately capped with a vapour-tight stainless steel lid. Finally, 2.5 ml of the pure phase of a particular VOC was introduced via the lower level valve into the bottom of the column (Fig. 4.1). To prevent the pressure to increase due to the injection of pure phase of the target compounds, the same volume of air (2.5 ml) was withdrawn from the lower part of the column before injection. Preliminary observations of the ethanol oxidation during high-water saturation experiments showed that the ethanol pool was depleted. Hence, for the ethanol experiments when the pool was about depleted, we injected an additional volume 2.5 ml of pure ethanol into the bottom of the column.

To prevent any photodecomposition of potassium permanganate, all columns were wrapped in aluminum foil. A series of control experiments with 30 g

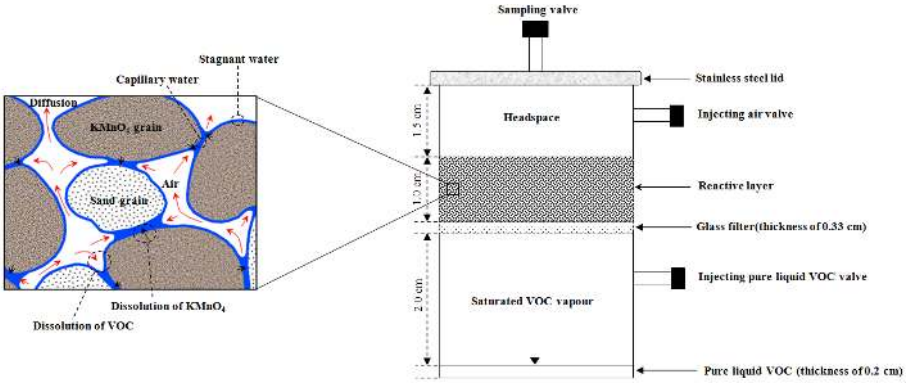

Fig. 4.1: Schematic view of the column experiments and the main processes during the migration of VOC vapour through a PRL.

sand, no potassium permanganate, and identical water saturations was carried out for all target compounds. All experiments were conducted in a fume cabinet at room temperature (22 ± 1 ºC) in duplicate. We assumed that the temperature and pressure inside the columns remained constant and were equal to room temperature and atmospheric pressure, respectively.

Two separate additional experiments were conducted for TCE, in which 1.0 g of dry basic salts was added to the PRL, in order to buffer proton production. For one experiment, we used sodium bicarbonate and in the other experiment calcium carbonate.

For the TCE experiments, we further tested the effect of adding water during the experiments on the reactivity of the PRL. The water was added to the PRL in two different ways. In one case, we made an instantaneous injection of 1.0 ml DI water to the PRL using a syringe (SGE Analytical Science, Australia). In other experiment, the same amount of DI water injected continuously at a rate of approximately 2.1×10^{-3} ml min^{-1}, using a syringe pump (KDS Model 100 Series).

4.3. Processes and equations

Fig. 4.1. shows a schematic of experimental column setup. The columns contained four domains. The first domain consists of a pool of VOC liquid. The second domain comprises the air space above the liquid pool and below the PRL. The third domain is the PRL consisting of potassium permanganate and sand with its water and air phases. The fourth domain is the headspace above the PRL.

For our simulations we assumed that the composition of the liquid pool and the air space above the liquid pool did not change with time. This assumption was certainly valid for TCE and toluene since the liquid did not deplete and the concentration in the air space above it quickly reached its equilibrium value (corresponding to its vapour pressure) because of rapid diffusion. For ethanol, this assumption was only weakly valid since its partial pressure changed with time due to full miscibility of ethanol with water in the column. The water evaporated from the PRL, diffused down and dissolved in the ethanol pool, and vice versa. This resulted in a lower ethanol fraction within the liquid phase (<100%), and thus decreasing its partial pressure over time. Assuming equilibrium between water in the PRL and the ethanol pool, we calculated the mole fraction of ethanol in the mixture (ethanol and water). Based on the calculated mole faction of ethanol in the non-ideal mixture (Kuhn et al., 2009), the partial pressure of ethanol was estimated to be approximately 80% of its vapour pressure.

Diffusion in the headspace above the PRL was thought to be fast enough to consider this domain as a well-mixed zone (i.e., with no vertical concentration gradients). However, to take into account the storage of VOC mass within the headspace, and also for the purpose of specifying well-defined boundary conditions, we chose to include this domain in our modelling.

The main processes taking place in the PRL are: (1) upward diffusion of VOC vapours in the air phase, (2) dissolution of VOC vapour into the water phase, (3) dissolution of solid potassium permanganate into the water phase, and (4) oxidation of dissolved VOC by dissolved permanganate in water (Fig. 4.1).

We assumed that there was no change in air pressure and temperature in the column. We hence neglected the advection term in the transport equations. Based on the very small amount of TOC (0.05 %) in sand and its oxidation in the presence of potassium permanganate (Mumford et al., 2005) in the reactive experiment, we also assumed the adsorption of VOC to the sand grains to be negligible. Hence, the governing transport equation for a target compound in the gas phase of PRL and headspace, assuming a one-dimensional transport, can be written as:

$$\theta^g \frac{\partial C_A^g}{\partial t} = \theta^g D_{e,A}^g \frac{\partial^2 C_A^g}{\partial x^2} - r_A^{diss} \quad ; \text{ A= TCE, toluene, ethanol} \tag{4.4}$$

where θ^g denotes the air content [-], A denotes the target compound, C_A^g is the concentration in air [NL^{-3}], $D_{e,A}^g$ is the effective gas diffusion coefficient [L^2T^{-1}], and r_A^{diss} is the rate of dissolution in water. The latter term is absent in the headspace, and θ^g is hence equal to 1.0.

Boundary conditions for Equation 4.4 are a constant concentration of the target compound ($C_A^g(t, x=0) = C_{A0}^g$) at the lower boundary of the PRL and no-flux at the top of the headspace. The simulation further implies continuity fluxes across the interface between the PRL and the headspace. The value of C_{A0}^g for TCE and toluene was taken equal to the vapour pressure of the target compounds. However, C_{A0}^g for ethanol was taken to be 80% of its vapour pressure. Initial concentrations of the target compound were equal to zero throughout the domain, i.e., $C_A^g(x, t=0) = 0$.

Several literature studies show that for VOCs with high vapour pressures, vapour diffusion dominates the migration of VOCs through unsaturated soil

(USEPA, 1993; Berscheid et al., 2010; Shen et al., 2014). The rate of vapour diffusion is obviously slower in soil than in free air. The effective gas diffusion is influenced by the pore space tortuosity, which itself depends on porosity and the volumetric air content (USEPA, 1993; Raoof and Hassanizadeh, 2013). The effective gas diffusion coefficient of VOC vapour in the PRL was expressed as follows (Millington and Quirk, 1961; Pennell et al., 2009; Yao et al., 2013):

$$D^{g}_{e,A} = D^{g}_{A} \frac{\theta^{g\frac{10}{3}}}{\phi^{2}} \tag{4.5}$$

where D^{g}_{A} is the molecular diffusion coefficient of the target compound in free air [L^2T^{-1}] and ϕ denotes the porosity of the porous medium.

The dissolution of the VOC compounds into water was modelled as a linear kinetic process expressed as (Yoshii et al., 2012):

$$r^{diss}_{A} = k^{diss}_{A} a_i \left(\frac{C^{g}_{A}}{H_{C,A}} - C^{w}_{A}\right) \tag{4.6}$$

where k^{diss}_{A} is the dissolution rate constant [LT^{-1}], a_i is the specific air-water interfacial area, $H_{C,A}$ denotes Henry's constant, and C^{w}_{A} is the concentration of the target compound in soil water of the PRL [NL^{-3}].

The dependence of the dissolution rate on the specific air-water interfacial area, a_i, has been reported by various researchers (Cho et al., 2005; Costanza and Brusseau, 2000; Hoeg et al., 2004; Kim et al., 2001). The specific air-water interfacial area is known to depend on water saturation as well as on capillary pressure (Hassanizadeh and Gray, 1993; Joekar-Niasar et al., 2010; Raoof et al.,

2013). However, for the purpose of this study we assumed that a_i depends only on water saturation, S^w, according to the following equation (Zhang et al., 2012):

$$a_i = a_{i0} S^w (1 - S^w)^{\sigma} \tag{4.7}$$

where σ is a fitting parameter and a_{i0} is the specific interfacial area corresponding to residual saturation (Zhang et al., 2012).

Regarding the spread of target compounds in soil water, we assumed one-dimensional diffusive transport. The governing equation for the aqueous phase, which pertains to only the PRL, is hence:

$$\theta^w \frac{\partial C_A^w}{\partial t} = \theta^w D_{e,A}^w \frac{\partial^2 C_A^w}{\partial x^2} + r_A^{diss} - r_A^{oxid} \tag{4.8}$$

where θ^w is the water content [-], r_A^{oxid} is the oxidation rate and $D_{e,A}^w$ is the effective diffusion coefficient in water.

Boundary conditions for Equation 4.8 are a zero flux at both the bottom and top of the PRL. We further assumed that the target compounds are initially absent in water, i.e., $C_A^w(x, t=0) = 0$.

The effective diffusion coefficient of the target compound assumed to be given by a similar equation as for air (Pennell et al., 2009; Yao et al., 2013):

$$D_{e,A}^w = D_A^w \frac{\theta^{w\frac{10}{3}}}{\phi^2} \tag{4.9}$$

where D_A^w denotes the molecular diffusion coefficient of the target compound in water [L^2T^{-1}].

Dissolved permanganate is known to be able to oxidize a variety of VOCs in water (Kao et al., 2008; Mahmoodlu et al., 2014; Waldemer and Tratnyek, 2006). Mahmoodlu et al. (2014) proposed a second-order equation for the oxidation rate of VOCs in the aqueous phase, given as a function of the target compound and potassium permanganate concentrations. For unsaturated conditions, the oxidation rate can be written as:

$$r_A^{oxid} = kC_A^w C_B^w \theta^w \tag{4.10}$$

where k denotes the reaction rate coefficient in the aqueous phase [$N^{-1}T^{-1}$], B denotes potassium permanganate, and C_B^w is the concentration of dissolved permanganate in water [NL^{-3}].

Potassium permanganate commonly dissolves quickly in soil water up to its solubility of 64 g l^{-1} at 20 °C (USEPA, 1999). Since we used an excess amount of potassium permanganate, the consumption of potassium permanganate due to oxidizing VOCs was neglected. We hence equated the maximum concentration of permanganate in water equal to the solubility of potassium permanganate, $C_{B,max}^w$.

Preliminary analysis of the experimental results showed that oxidation rate ceased after a certain period of time. Our results suggested that this was due to a decrease in the pH during the TCE experiment, and an increase in the pH during the toluene and ethanol experiments, as expressed by their stoichiometric reaction equations (Equations 4.1 to 4.3). In order to model this effect, we allowed for a dependency of k on pH, according to the following equations:

$$k_{TCE} = \kappa_{TCE}(pH - \omega_{TCE})^{\beta_{TCE}} \tag{4.11}$$

$$\frac{\partial H^+}{\partial t} = \zeta_{TCE} r_{TCE}^{oxid} \tag{4.12}$$

in which κ_{TCE} denotes the reaction rate constant in water [$N^{-1}T^{-1}$] as determined with batch experiments (Mahmoodlu et al., 2013b), ω_{TCE} and β_{TCE} are fitting parameters obtained as part of the simulation results, and H^+ denotes the proton concentration [NL^{-3}]. The parameter ζ_{TCE} in Equation 4.12 is the number of moles of protons produced during oxidation of TCE. According to Equation 4.1, its value is equal to unity.

Similar relationships were employed for the reaction rate coefficients of toluene and ethanol as follows:

$$k_A = \kappa_A (\omega_A - pH)^{\beta_A} \quad ; \quad A= \text{toluene, ethanol} \tag{4.13}$$

$$\frac{\partial OH^-}{\partial t} = \zeta_A r_A^{oxid} \tag{4.14}$$

where κ_A denotes the reaction rate constant in water [$N^{-1}T^{-1}$] as determined previously (Mahmoodlu et al., 2013b), ω_A and β_A are fitting parameters, OH^- denotes the molar concentration of hydroxide ions, and ζ_A is the number of moles of hydroxide ions consistent with the stoichiometric reaction ($\zeta_{toluene} = 12$ and $\zeta_{ethanol} = 4$).

The above set of coupled equations was solved simultaneously using COMSOL Multiphysics (Rolle et al., 2012; Müller et al., 2013).

4.4. Results and discussion

4.4.1. Oxidation process and water saturation effect

Fig. 4.2 depicts normalized concentrations (C/C_0) of the target compounds in the control experiments as a function of time for different initial water saturations. Here, C denotes the observed concentration of VOC vapour in the headspace and C_0 is the maximum observed concentration of VOC vapour in the lower part of the column above the liquid pool. The latter was found to correspond to the vapour pressure of the particular VOC. The results in Fig. 4.2 indicate that the concentration of the target compounds in the headspace increased gradually with time up to the maximum observed concentrations. Results of the control experiments showed that an increase in water saturation retarded vapour migration through the partially saturated sand layer (Fig. 4.2). A likely explanation is the effect of water saturation on the effective diffusion coefficient of the VOCs. Literature shows that vapour diffusion is very sensitive to water saturation, with more rapid vapour movement when the medium is drier. Tillman and Weaver (2005) found that with a 10% increase water saturation, the effective vapour diffusion coefficient of TCE decreased by three orders of magnitude. Another explanation for the effect of water saturation is the partitioning of VOC due to its dissolution in water. This caused a retardation of the VOCs (particularly ethanol) and hence longer residence times in the partially saturated sand during the control experiments.

A comparison of the control and reactive experiments revealed that the PRL was very effective in oxidizing VOC vapours. This can be clearly seen in Fig. 4.4, where the build-up of VOC concentrations in the headspace is much slower for the columns with a PRL than in the control columns. The PRL is far more effective at higher water saturation degrees. This is because oxidation occurs in the water phase with the oxidation capacity being higher at higher water saturations. Moreover, the larger volume of water provides a large reservoir for the dissolving vapours.

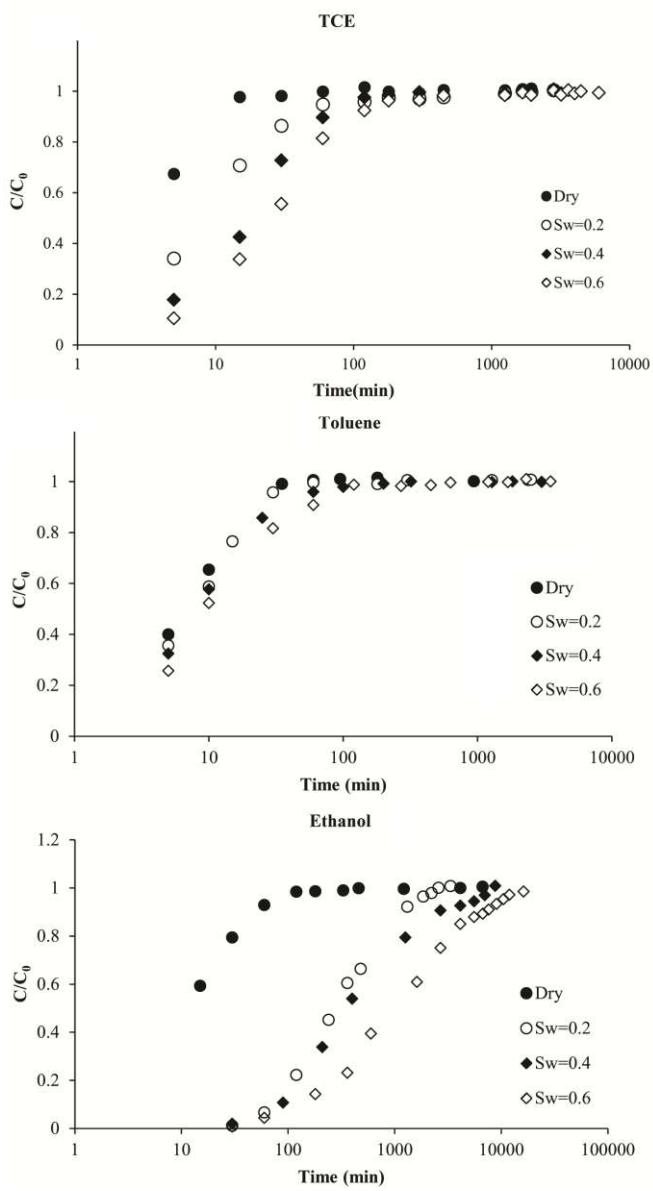

Fig. 4.2: Effect of water saturation on VOC vapours diffusing through the partially saturated sand.

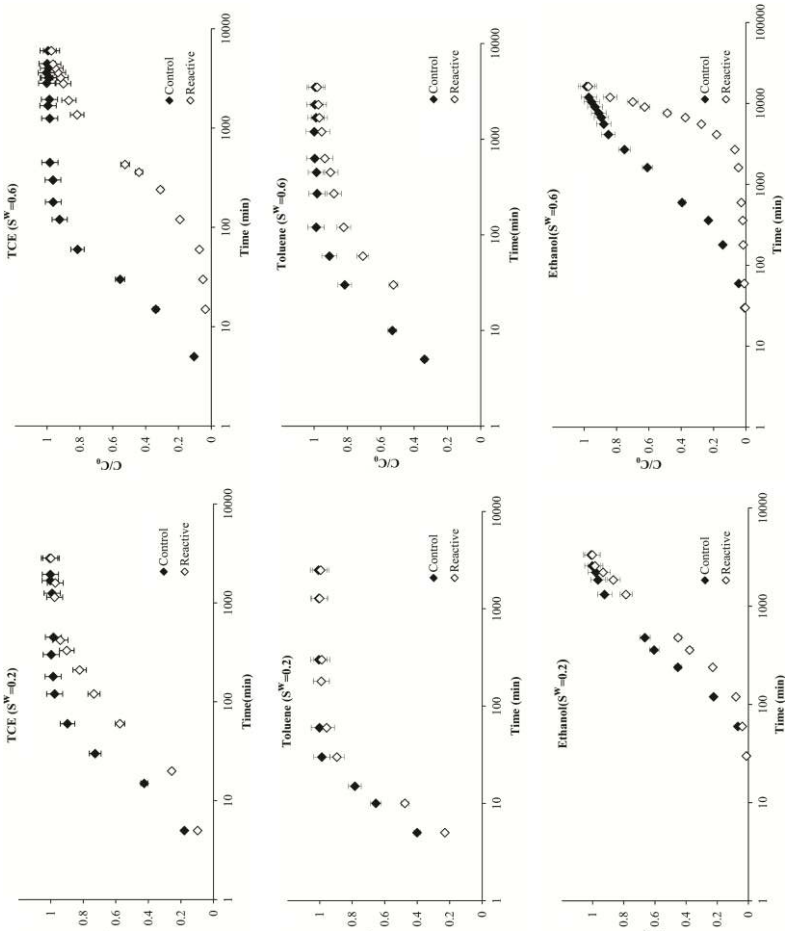

Fig. 4.3: Concentration of VOC vapours diffusing through the PRL for two different water saturations.

4.4.2. Reactivity of potassium permanganate

Our experimental results revealed that the reactivity of the PRL decreased during the course of the experiments. We found that water saturation has a strong effect on the reactivity of potassium permanganate. The PRL at the highest water saturation (i.e., $S_w = 0.6$) was found to be more reactive. As shown by Equations 4.1 to 4.3, the accumulation of by-products, particularly when limited amounts of water are present, may explain the decrease in reactivity of the PRL. Two main by-products might have affected the reactivity of potassium permanganate: protons or OH^- ions and manganese dioxide (Equations 4.1 to 4.3). Highly acidic or basic conditions would decrease the oxidation rate. Furthermore, under normal conditions, manganese dioxide would precipitate on the potassium permanganate grains and reduce their reactive surface.

The accumulation of by-products in the water phase could not be monitored during the experiment. However, we expected that the accumulation of protons in the TCE oxidation experiment (Equation 1), would result in highly acidic conditions for the closed system. Produced protons would react directly with permanganate and generate permanganic acid (Forsey, 2004; Housecroft and Sharpe, 2005) as follows:

$$MnO_4^- + H^+ \rightarrow HMnO_4 \qquad (4.15)$$

This reaction occurs under very acidic condition (Housecroft and Sharpe, 2005). Since monitoring of the pH in the water phase was not possible during our experiments, the pH values were estimated based on stoichiometric reactions. Our calculations for the TCE oxidation experiments showed that the pH could have decreased to about 1.25. Literature shows that manganese dioxide is increasingly soluble under very acidic conditions (Kao et al., 2008). Therefore, the formation of manganese dioxide precipitates and subsequent coating of the reactive surface of permanganate is not a likely reason for reductions in the TCE oxidation rate. We hence conclude that the reactivity of potassium permanganate during the oxidation

of TCE decreased because of the acidic conditions created in the water phase during the TCE column experiments.

To control the inhibitory effect of acidity on the reactivity of potassium permanganate during the oxidation of TCE vapour, two separate experiments were performed using two basic salts under the highest water saturation (S^w=0.6). In one experiment, we added sodium bicarbonate to the initial PRL. In another experiment, calcium carbonate was employed. Their dissolution in water and the pH buffering capacity were triggered by the proton production due to TCE oxidation. In line with the hypothesis that pH exerted the main control on the oxidation rates, results suggests that the addition of both carbonates positively affected the reactivity of the PRL in TCE oxidation experiments (Fig. 4.4). However, the overall effect was still relatively small.

The effect of the accumulated by-products on the reactivity of the PRL should be reduced by adding water. Therefore, in two sets of complementary experiments, we added water to both the reactive and control TCE experiment. In the first set of experiments, we expected to observe the lowest reactivity of the PRL.

In this case, 1.0 ml of water was injected instantaneously into the PRL using a syringe. Results showed that the concentration of TCE vapour in the headspace initially decreased rapidly, but then increased gradually up to a maximum (Fig. 4.5). Results for the TCE control experiment showed only a minor reduction in the TCE vapour concentration of the headspace due to dissolution process. In the second set of experiments, after reaching steady- state conditions, water was injected continuously (at a rate of around 2.1×10^{-3} ml min^{-1}) into the PRL using a syringe pump (Fig 4.6). As shown in Fig. 4.7, the concentration of TCE vapour in the headspace decreased gradually until the pump was turned off. The increase in the reactivity of the PRL due to added water is attributed to a reduction in the proton concentrations. This allows the reaction to continue until protons accumulated again to previous levels.

Similar to the TCE oxidation experiment, the reactivity of the PRL towards toluene and ethanol decreased during the experiments. However, in contrast to the TCE oxidation experiment, and in accordance with Equations 4.2 and 4.3, the

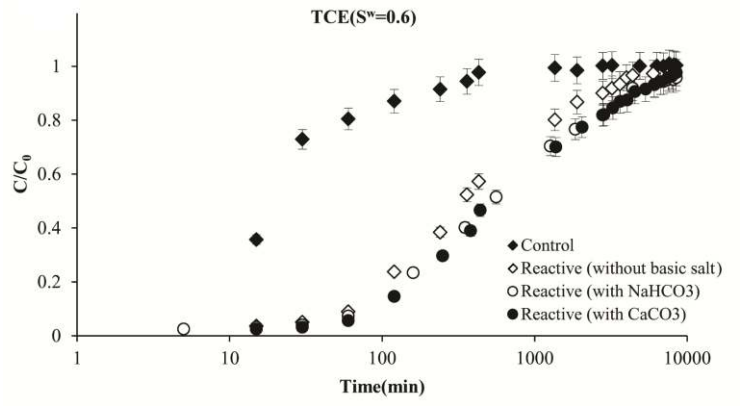

Fig. 4.4: Effect of $NaHCO_3$ and $CaCO_3$ on the reactivity of the PRL during TCE oxidation.

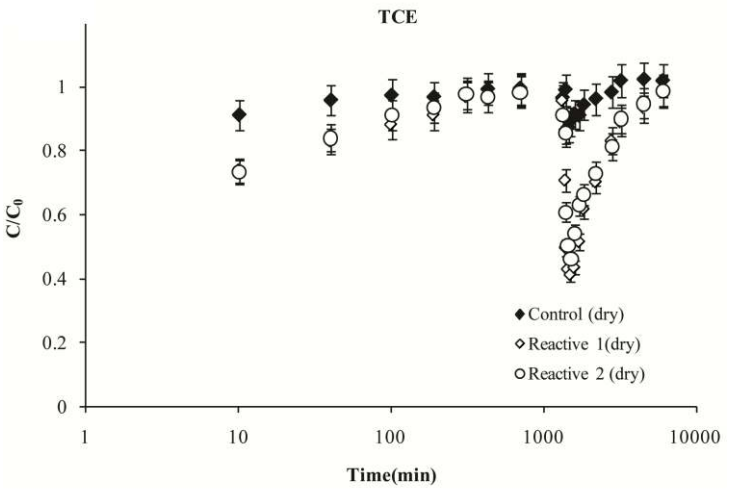

Fig. 4.5: Effect of adding more water to the PRL on the reactivity of the PRL during TCE oxidation. 1.0 ml DI water was injected through the upper valve. Reactive 1 and 2 represent two replicates of the reactive experiment including a dry PRL.

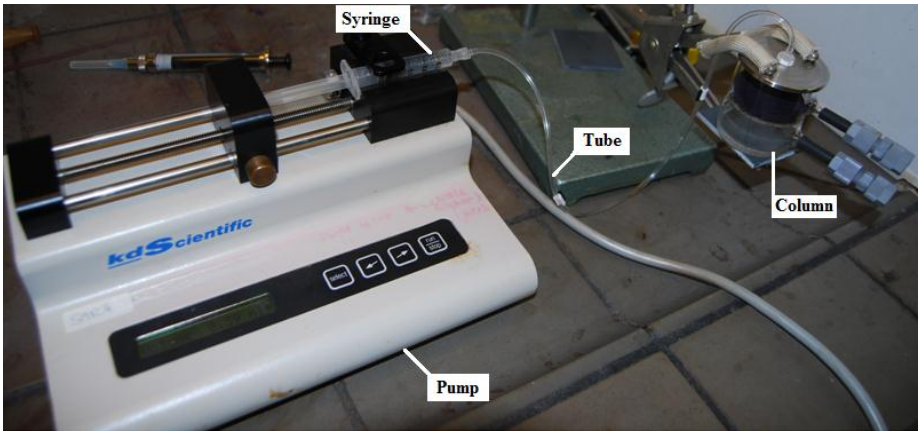

Fig. 4.6: Experimental setup for adding more water to the PRL using a syringe pump.

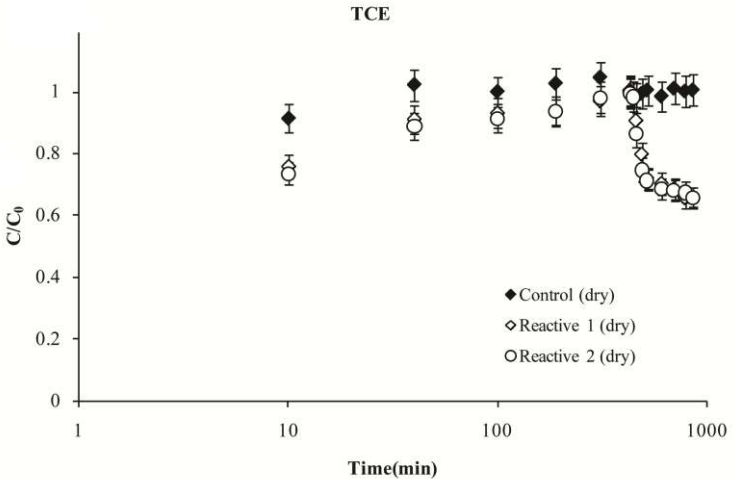

Fig. 4.7: Effect of adding more water to the reactive layer on the reactivity of the PRL during TCE oxidation. Continuous injection of 1.0 ml DI water (at a rate of about 2.1×10^{-3} ml min^{-1}) by a syringe pump.

produced hydroxide ion increased the pH in the water phase (Mahmoodlu et al. 2013b).

Oxidation rate of aromatic rings have been shown to decrease with increasing basicity of the water phase (Forsey, 2004; Lobachev et al., 1997; Rudakov and Loachev, 1994). We hence expected the oxidation rate of toluene to decrease during the toluene experiments (as basicity increased). As shown by Equation 4.2, the oxidation of 1.0 mole toluene by potassium permanganate produces 12.0 mole hydroxide ion and consumes 2.0 mole water. We hence can expect a rapid rise in pH and consequently a decrease in the toluene oxidation rate by potassium permanganate in the PRL.

Literature studies also show a dependency of the ethanol oxidation rate on proton ion (Sen Gupta et al., 1989). The oxidation rate of ethanol hence should increase with acidity and conversely. The stoichiometric reaction of ethanol shows that the oxidation of 1.0 mole ethanol by potassium permanganate produces 4.0 moles hydroxide ion (Equation 4.3). However, the reaction also produces one mole of water, which should temper the concentration of produced hydroxide ions and consequently a slower increase in pH of the PRL. Thus, a slow increase in pH may have caused the lower reactivity of potassium permanganate during the oxidation of ethanol.

4.4.3. Simulation results

Simulations showed that the concentration of the target compounds below the PRL reached equilibrium immediately. Hence, we simulated only the PRL and the headspace domains using Equations 4.4 and 4.8. All input parameters are given in Table 4.1. Simulation results together with experimental data are shown in Figs. 4.8 to 4.10. While there is good agreement between the simulation results and the experimental data for TCE and toluene, a discrepancy occurs for the ethanol experiments, which increases at the higher water saturations (Fig. 4.10). A likely reason is that the assumed concentration of ethanol vapour in the air space below the PRL (C^{g}_{A0}) was too low. In the simulations, we set C^{g}_{A0} equal to 80% of the

Table 4.1: Experimental conditions and modeling parameters of column experiments.

Parameter	VOC	Value	References
[a] Initial porosity, ϕ, (-)	-	3.5×10^{-1}	-
Water content, θ^{w},(-)	-	7.0×10^{-2} ,1.4×10^{-1} and 2.1×10^{-1}	-
Volume of the headspace (m^3)	-	20.7×10^{-6}	-
Volume of the reactive layer (m^3)	-	13.2×10^{-6}	-
Solubility of $KMnO_4$, $C^{W}_{B,max}$,(mol m^{-3}) at 20°C	-	4×10^{2}	USEPA (1999)
Initial specific air-water interfacial area a_{i0} (m^{-1})	-	4.0	Zhang et al.(2012)
Fitting parameter in σ Equation 4.7 (-)		6.0	-
Henry's constant of VOCs , $H_{C,A}$, (-)	TCE	4.3×10^{-1}	Fan and Scow (1993)
	Toluene	2.8×10^{-1}	Fan and Scow (1993)
	Ethanol	2.4×10^{-4}	ITRC (2011)
Reaction rate constant of VOCs in water, κ_A , ($M^{-1} s^{-1}$)	TCE	8.0×10^{-1}	
	Toluene	2.5×10^{-4}	Mahmoodlu et al. (2013b)
	Ethanol	6.5×10^{-4}	
Molecular diffusion of VOCs in air , D^{g}_{A} , ($m^2 s^{-1}$)	TCE	7.9×10^{-6}	Estivill et al. (2007)
	Toluene	7.6×10^{-6}	Hers et al. (2000)
	Ethanol	1.1×10^{-5}	Green and Perry (2007)
Molecular diffusion of VOCs in water, D^{W}_{A} , ($m^2 s^{-1}$)	TCE	9.1×10^{-10}	Fogler (2006) and Lewis et al. (2009)
	Toluene	9.4×10^{-10}	Hers et al. (2000)
	Ethanol	1.2×10^{-9}	Green and Perry(2007)
Dissolution rate coefficient of VOC vapours in water, k^{diss}_{A} , (m s^{-1})	TCE	8.0×10^{-5}	[b]Measured
	Toluene	1.3×10^{-5}	
	Ethanol	1.0×10^{-4}	
Fitting parameter β in Equations 4.11 and 4.13 (-)	TCE	2.0	-
	Toluene	3.0	-
	Ethanol	3.0	-
Fitting parameter ω in Equations 4.11 and 4.13 (-)	TCE	1.25	-
	Toluene	14.0	-
	Ethanol	14.0	-
[c] ζ (-)	TCE	1.0	
	Toluene	12.0	Based on stoichiometric reaction
	Ethanol	4.0	
[d] η (mol m^{-3})	TCE	44.74	-
	Toluene	13.21	-
	Ethanol	196.57	-

[a]Porosity of the PRL, [b]Additional batch experiments were performed to estimate the dissolution rate coefficient of VOCs, [c]Number of mole of proton (for TCE) or hydroxide (for toluene and ethanol) produced during the oxidation of VOCs; according to Equations 1 to 3. [d]Fitting parameter,

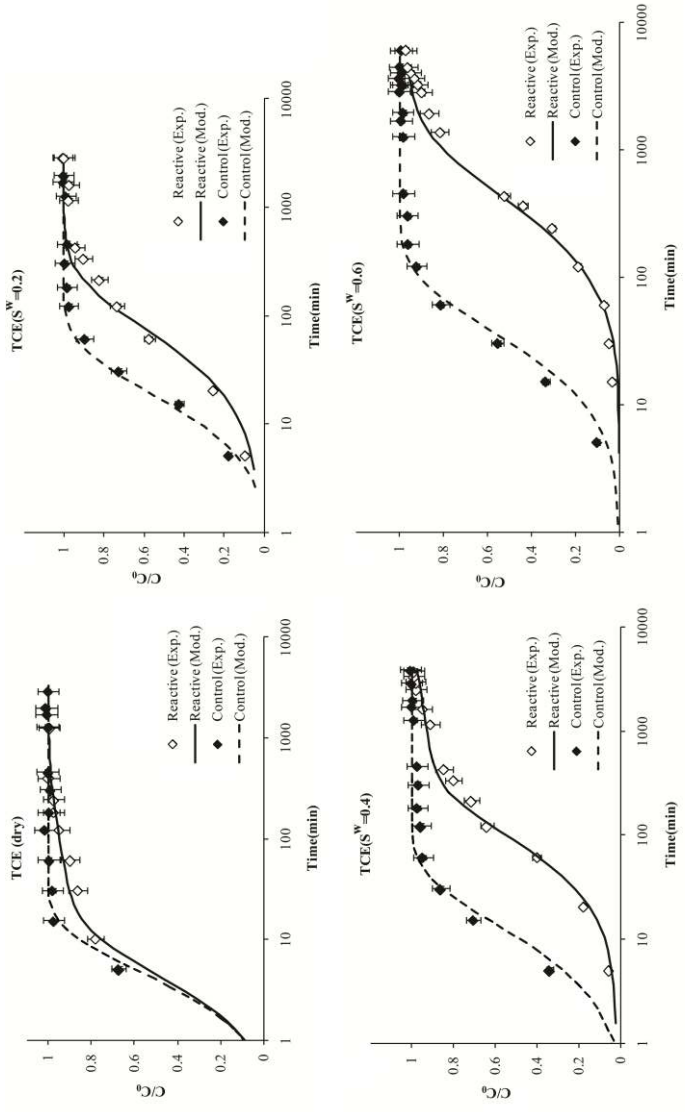

Fig. 4.8: Comparison of measured and simulated breakthrough curves of TCE vapour in the headspace at various water saturations.

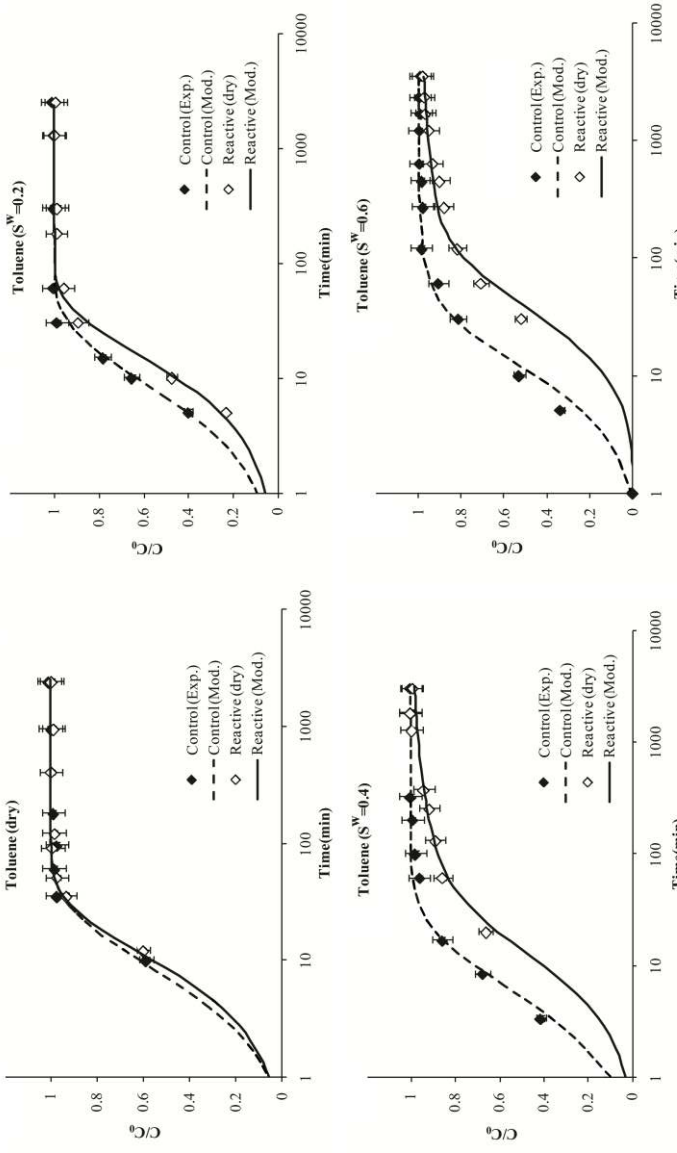

Fig. 4.9: Comparison of measured and simulated breakthrough curves of toluene vapour in the headspace at various water saturations.

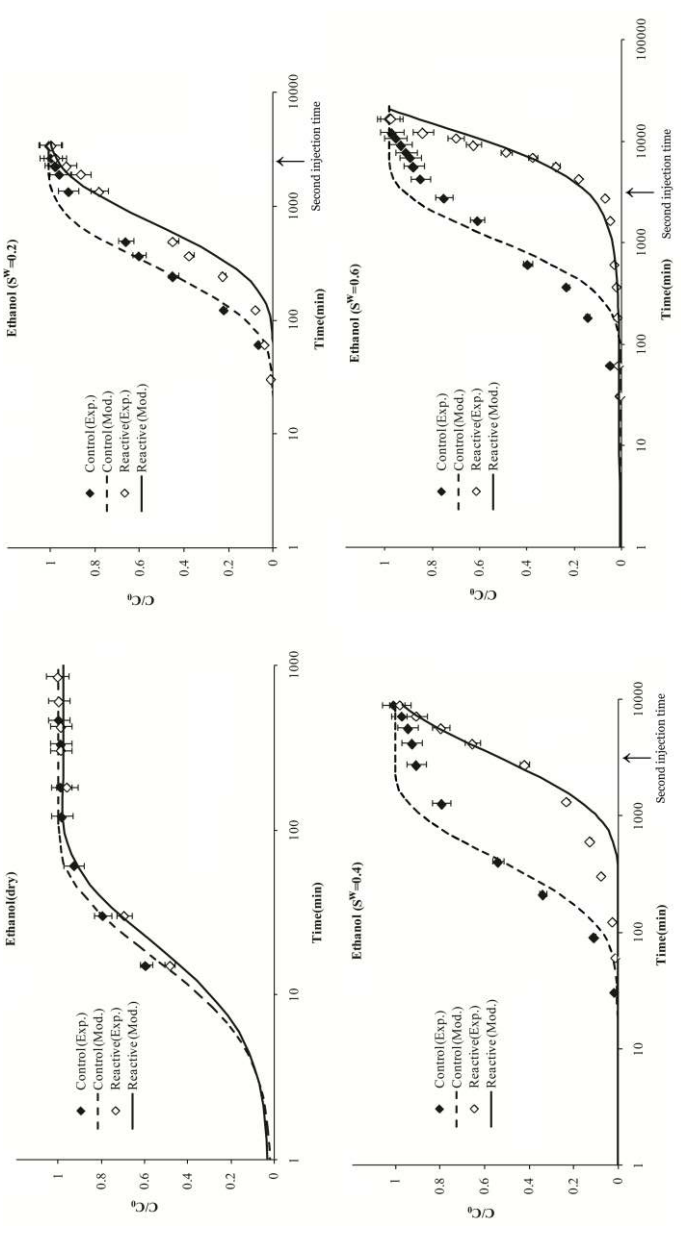

Fig. 4.10: Comparison of measured and simulated breakthrough curves of ethanol vapour in the headspace at various water saturations.

ethanol vapour pressure (see Section 3) to account for dissolution of water vapour in the ethanol pool. This effect was not present initially but became significant only after a long time. This may have resulted in the discrepancy between experimental data and simulation results.

As explained in Sections 3 and 4.2, we expected the change in pH to be the main reason for the decrease in the oxidation rate of the target compounds during the experiments. Modelling results confirmed the controlling effect of pH. The oxidation rate became zero at relatively long times, with the concentrations of all target compounds in the headspace reaching the corresponding concentrations of the control experiments (Figs. 4.9 to 4.11).

We used the simulations to estimate the total mass of VOC vapours entering the layer of both the reactive and control experiments at different water saturation degrees at the end of each experiment. We next estimated the total oxidized mass of VOC as the total mass entering the layer at the end of a reactive experiment minus the mass entering the layer of the corresponding control experiment. The calculated total oxidized mass was normalized using the volume of PRL and plotted in Fig. 4.11 as a function of its initial water saturation. This figure shows a linear increase in the total oxidized mass of VOCs with an increase in initial water saturation. Although the results are based on a 1D-homogeneous diffusion model, they support the assumption that the reaction rate is hampered by the change in pH of the water phase during the oxidation of VOCs. This linear relationship can be expressed by:

$$m_A^{oxid} = \eta S^w \tag{4.16}$$

where m_A^{oxid} denotes the oxidized mass of VOCs per unit volume of PRL [NL^{-3}] and η is a fitting parameter given in Table 4.1 for each VOC.

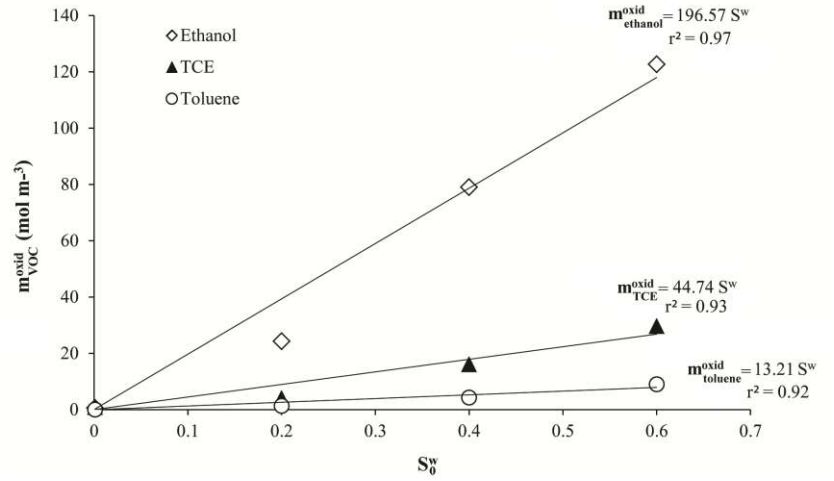

Fig. 4.11: Effect of initial water saturation (S_0^w) on total consumed mass of VOCs per volume of the PRL (m_{VOC}^{oxid}). The mass ratio of potassium permanganate to sand was equal to 2.0 and the thickness of the PRL was 0.01 m.

4.4.4. Longevity of the reactive permeable barrier

The current experiments were performed under very idealized conditions. Field conditions generally involves many environmental factors such as pH, temperature, soil organic matter, soil type, heterogeneity, and soil moisture conditions, which are not considered here. Nevertheless, our results provide an indication of the reactive capacity of a permeable reactive barrier. There are two major differences between a field situation and our experimental setup: 1) the thickness of the permeable layer in the field can be at least 100 times larger, and 2) the concentration of contaminants in the gas phase reaching the layer will be much lower than in our experiments. These two factors are critical when determining the most effective application of potassium permanganate in the field.

In order to obtain a rough estimate of the longevity of a horizontal permeable reactive barrier consisting of potassium permanganate and sand under

field conditions, we considered a hypothetical field situation with a building located above VOC-contaminated groundwater (Fig. 4.12). We considered a horizontal permeable reactive barrier with a thickness of 1.0 m, consisting of solid potassium permanganate and sand (with the mass ratio of potassium permanganate to sand equal to 2.0), and at a typical water saturation of 0.40. We assumed the initial concentrations of TCE and toluene in groundwater to be 1% value of their solubilities in water. However, for ethanol we considered groundwater with a volumetric ratio of 10% ethanol (e.g., as reported by Freitas (2009) for North America). The reactive barrier was assumed to be constructed 2.0 m above the groundwater table (Fig. 4.12). Assuming that VOC vapours are transported to the reactive layer by diffusion only, the continuous mass fluxes reaching the PRL could be calculated. Then, using the correlation equation (i.e., Equation 4.16), we calculated the life time of the permeable reactive barrier. All parameter values and results are given in Table 4.2. Calculations showed that the PRL would be able to oxidize TCE, toluene, and ethanol vapours for a period of 247, 227, and 785 days, respectively. Obviously, the longevity of a horizontal permeable reactive barrier is affected by many environmental factors. Nevertheless, this rough estimate of the longevity shows that horizontal permeable reactive barrier could be a viable option for preventing VOC vapours to reach indoor space. In fact, these estimates are based on experimental results that suffered from water limitations in a sealed column. This caused the built up of reaction products that negatively affected the reactivity of the permeable reactive barrier. The absence or preventionof limitations in water availability during field applications could further enhance the effectiveness of a HPRL to mitigate vapour intrusion risks. This could be a focus of future studies.

4.5. Conclusions

In this study we investigated the possibility of using solid potassium permanganate in a partially water saturated horizontal permeable reactive barrier for

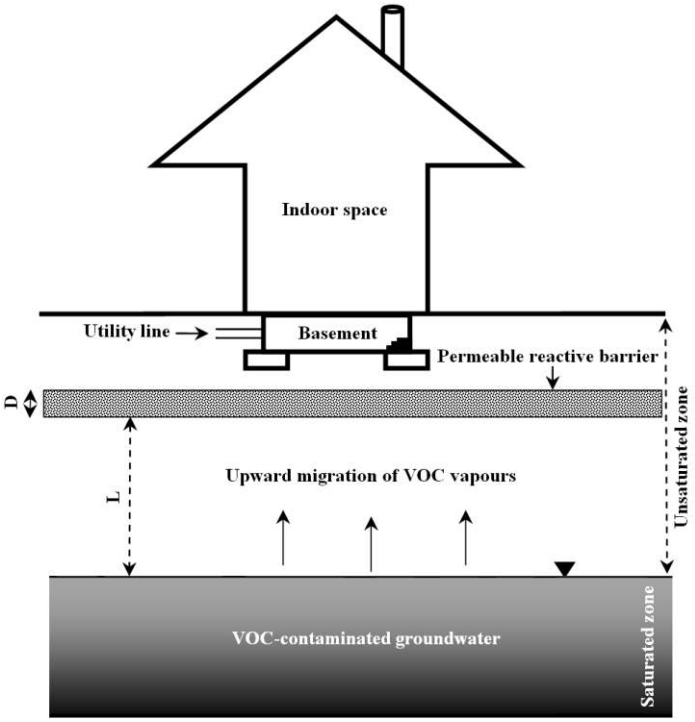

Fig. 4.12: A conceptual model for preventing vapour intrusion using a horizontal permeable reactive barrier.

Table 4.2: Longevity of a partially saturated permeable reactive barrier consisting of potassium permanganate grains and sand in the unsaturated zone.

VOC	[a]C^g (mol m^{-3})	[b]S^w (-)	Flux (mol m^{-2} s^{-1})	[c]m_A^{oxid} (mol m^{-3})	Longevity (day)
TCE	4.1×10^{-2}	0.4	8.4×10^{-7}	17.9	247
Toluene	1.4×10^{-2}	0.4	2.7×10^{-7}	5.3	227
Ethanol	1.7×10^{-1}	0.4	1.2×10^{-6}	78.6	758

[a]Concentration of TCE and toluene in gas phase calculated based on 1% of their solubility in water, but for the estimation of ethanol concentration in air, we assumed a solution of 10% ethanol and 90% water. The ratio of initial mass of potassium permanganate to initial mass of sand is equal to 2.0 and the thickness of permeable reactive barrier is equal to 1.0 m, [b]Water saturation, [b]Oxidized mass of VOCs per unit volume of the PRL.

oxidizing VOC vapours. Results of the control experiments revealed that the upward migration of VOC vapours was affected by the degree of water saturation. In addition to increasing tortuosity, an increase in water saturation retarded the migration of VOC vapours through dissolution of VOCs (particularly ethanol) in water phase of the layer. Results of the reactive experiments showed that water saturation had a strong effect on the removal capacity of the reactive layer. We observed a high removal efficiency and reactivity of the layer for all target compounds at the highest water saturation ($S^w = 0.6$). The change in pH of the water phase during the oxidation of VOCs was found to be the main reason for a reduction in the oxidation rate of the PRL.

The developed model for reactive vapour transport, which included pH-dependent oxidation rates, was able to satisfactorily simulate the experimental data for toluene and TCE. For ethanol was found increasing discrepancy between the simulation results and experimental data with increasing water contents. This was attributed to the fact that, due to the high solubility of ethanol in water, the vapour concentration of the air apace between the ethanol pool and the reactive layer varied with time. We did not account for these variations. Instead, we assumed a constant ethanol vapour concentration to correspond to 80% of the saturated vapour. To improve the simulations for ethanol, the variation of the ethanol vapour concentration with time at the inlet boundary should be accounted for. This would require simulating additional processes, such as the evaporation of ethanol from the liquid pool, evaporation of water from the PRL and its partitioning into the ethanol pool, and estimating the equilibrium vapour concentration of the air phase below the PRL. We were not able to monitor these processes in our current setup. Moreover, the effect of the accumulated by-products and possible interactions with each other on the oxidation rate of ethanol should be considered.

Simulation results revealed that the total oxidized mass of ethanol vapour was higher than TCE and toluene for identical water saturations, despite a larger oxidation rate constant for TCE than for ethanol and toluene (Waldemer and Tratnyek, 2006; Mahmoodlu et al., 2013b). This is due to the fact that TCE and

toluene oxidation is affected by a change in pH of the water phase during their oxidation than ethanol.

A rough estimate of the field scale longevity of a PRL suggests that horizontal permeable reactive barriers can provide a viable option for preventing VOC vapours to reach the land surface. However, the performance of such a methodology can be affected by various environmental factors such as pH, soil organic matter, minerals, temperature, soil type, heterogeneity, and particularly the presence of soil water.

4.6. References

[1] Almeida, C.M.M., and Boas, L.V., 2004. Analysis of BTEX and other substituted benzenes in water using headspace SPME-GC-FID: method validation. Environ. Monit. 6: 80-88.

[2] Berscheid, M., Burger, K., Hutchison, N., Muniz-Ghazi, H., Renzi, B., Ruttan, P., and Sterling, S., 2010. Proven Technologies and Remedies Guidance: Remediation of Chlorinated Volatile Organic Compounds in Vadose Zone Soil.California Department of Toxic Substances Control. http://www.dtsc.ca.gov/ sitecleanup/upload/cVOC_040110.pdf, 2010.

[3] Cho, J., Annabel, M.D., and Rao, P.S.C., 2005. Measured mass transfer coefficients in porous media using specific interfacial area. Environ. Sci. Technol. 39: 7883-7888.

[4] Cho, H.J., Jr, R.J.F., and Daly, M. H., 2002. Soil vapour extraction and chemical oxidation to remediate chlorinated solvents in fractured crystalline bedrock: Pilot study results and lessons learned. Remediation 12(2): 35-50.

[5] Costanza, M., and Brusseau, A., 2000. Contaminant vapor adsorption at the gas-water interface in soils. Environ. Sci. Technol. 34(1): 1-11.

[6] Cronk, G., Koenigsberg, S., Coughlin, B., Travers, M., Schlott, D., 2010. Controlled Vadose Zone Saturation and Remediation (CVSR) Using Chemical Oxidation, 7th International Conference on Remediation of Chlorinated and

Recalcitrant Compounds. May 24-27, 2010. Battelle Press, Columbus, OH. 8 pp, 2010.

[7] Estivill, I.S., Hargreaves, D.M., Puma, G.L., 2007. Evaluation of the intrinsic photocatalytic oxidation kinetics of indoor air pollutants. Environ. Sci. Technol. 41(6): 2028-2035.

[8] Fan, S., Scow, K.M., 1993. Biodegradation of trichloroethylene and toluene by indigenous microbial populations in soil. App. Environ. Microbiol. 59(6): 1911-1918.

[9] Fogler, H.S., 2006. Elements of Chemical Reaction Engineering, Fourth ed. Boston, MA: Prentice Hall.

[10] Forsey, S.P., 2004. In situ Chemical Oxidation of Creosote/Coal Tar Residuals: Experimental and Numerical Investigation. PhD thesis, University of Waterloo, Waterloo Ontario, Canada.

[11] Freitas, J.G., 2009. Impacts of ethanol in gasoline on subsurface contamination. PhD thesis. University of Waterloo, Waterloo Ontario, Canada.

[12] Green, D.W., and Perry, R.H., 2007. Perry's Chemical Engineers' Handbook, eighth ed. McGraw-Hill. ISBN:0-07-142294-3.

[13] Hassanizadeh, S.M., and Gray, W.G., 1993. Thermodynamic basis of capillary pressure in porous media. Water. Resour. Res. 29: 3389-3405.

[14] Heiderscheidt, J.L., Crimi, M., Siegrist, R.L., and Singletary, M.A., 2008. Optimization of full-scale permanganate ISCO system operation: Laboratory and numerical studies. Groundwater Monit. R. 28(4): 72-84.

[15] Hers, I., Atwater, J., Li, L., Gilje, R.Z., 2000. Evaluation of vadose zone biodegradation of BTX vapours. Contam. Hydro. 46: 233-264.

[16] Hesemann, J.R. Hildebrandt, M. 2009. Successful unsaturated zone treatment of PCE with sodium permanganate. Remediation 19(2): 37-48.

[17] Hinchee, R.E., 1993. Bioventing of Petroleum Hydrocarbons, in Handbook of Bioremediation, CRC Press Inc.

[18] Hoeg, S., Scholer, H.F., Warnatz, J., 2004. Assessment of interfacial mass transfer in water-unsaturated soils during vapor extraction. Contam. Hydrol. 74: 163-95.

[19] Housecroft, C.E., and Sharpe, A.G., 2005. Inorganic Chemistry, Second ed. Harlow: Prentice Hall.

[20] ITRC (Interstate Technology & Regulatory Council), 2011. Biofuels: Release Prevention, Environmental Behavior, and Remediation. BIOFUELS-1. Washington, D.C.: Interstate Technology & Regulatory Council, Biofuels Team. www.itrcweb. org.

[21] Joekar-Niasar,V., Hassanizadeh, S.M., and Dahle., H.K., 2010. Non-equilibrium effects in capillarity and interfacial area in two-phase flow: Dynamic and pore-network modeling. J. Fluid Mech. 655, 38-71.

[22] Kao, C.M., Huang, K.D., Wang, J.Y., Chen, T.Y., and Chien, H.Y., 2008. Application of potassium permanganate as an oxidant for in-situ oxidation of trichloroethylene-contaminated groundwater: A laboratory and kinetics study. J. Hazard. Mater. 153: 919-927.

[23] KDHE (Kansas Department of Health and Environment), 2007. Chemical Vapor Intrusion and Residential Indoor Air: Kansas Vapor Intrusion Guidance www.kdheks.gov/ber/download/Ks_VI_Guidance.pdf.

[24] Kim, H., Annable, M.D., Rao, P.S.C., 2001. Gaseous transport of volatile organic chemicals in unsaturated porous media: effect of water-partitioning and Air-Water Interfacial Adsorption. Environ. Sci. Technol. 35: 4457-4462.

[25] Kubinec, R., Adamuscin J., Jurdakova, H., Foltin, M., Ostrovsky, I., Kraus, A., and Sojak, L., 2005. Gas chromatographic determination of benzene, toluene, ethylbenzene and xylenes using flame ionization detector in water samples with direct aqueous injection up to 250 µl. J. Chromatogr A 1084: 90-94.

[26] Kuhn, H., Försterling, H.D., and Waldeck, D.H., 2009. Principles of Physical Chemistry, Second ed. John Wiley & Sons, Inc.

[27] Lewis, S., Lynch, A., Bachas, L., Hampson, S., Ormsbee, L., and Bhattacharyya, D., 2009. Chelate-modified fenton reaction for the degradation of trichloroethylene in aqueous and two-phase systems. Environ. Eng. Sci. 26(4): 849-59.

[28] Li, X.D., Schwartz, F.W., 2004. DNAPL remediation with in situ chemical oxidation using potassium permanganate.II. Increasing removal efficiency by

dissolving Mn oxide precipitates. J. Contam. Hydro. 68: 269-287.

[29] Lobachev, V.L., Radakov E.S., Zaichuk E.V., 1997. Kinetics, kinetic isotope effects, and substrate selectivity of alkybenzene oxidation in aqueous permanganate solutions: VI. Reaction with MnO_3^+. Kinet. Catal. 38(6):745-761.

[30] Mahmoodlu, M.G., Hartog, N., Hassanizadeh, S.M., and Raoof, A., 2013. Oxidation of volatile organic vapours in air by solid potassium permanganate. Chemosphere 91 (11): 1534-1538.

[31] Mahmoodlu, M.G., Hassanizadeh, S.M., Hartog, N., 2013b. Evaluation of the kinetic oxidation of aqueous volatile organic compounds by permanganate. Sci. Total Environ. 485-86: 755-63.

[32] McHugh, T.E., Beckley, L., and Bailey, D., 2013. Influence of shallow geology on volatile organic chemical attenuation from groundwater to deep soil gas. Groundwater Monit. R 33(3): 92-100.

[33] Millington, R.J., Quirk, J.P., 1961. Permeability of porous solids. Trans Faraday Soc. 57:1200-1207.

[34] Müller, D., Francke, H., Blöcher, G., and Shao, H.B., 2013. Simulation of reactive transport in porous media: A benchmark for a COMSOL-PHREEQC-Interface. Conference Proceedings of COMSOL Conference. Rotterdam, The Netherlands. www.comsol.com/paper/download/182397/maaller_abstract.pdf.

[35] Mumford, K.G, Thomson, N.R. and Allen-King R., 2005. Bench-scale investigation of permanganate natural oxidant demand kinetics. Environ. Sci. Technol. 39: 2835-2840.

[36] Pennell, K.G., Bozkurt, O. and Suuberg, E., 2009. Development and application of a three-dimensional finite element vapor intrusion model. J. Air & Waste Manage Assoc. 59, 447-460.

[37] Provoost, J., Reijnders, L., Swartjes, F., Bronders, J., Seuntjens, P., and Lijzen, J., 2009. Accuracy of seven vapour intrusion algorithms for VOC in groundwater. Soils Sediments 9, 62-73.

[38] Przyjazny A., Kokosa J.M., 2002. Analytical characteristics of the determination of benzene, toluene, ethylbenzene and xylenes in water by headspace solvent microextraction. J. Chromatogr A 977(2): 143-153.

[39] Raoof, A., Hassanizadeh, S.M., 2013. Saturation-dependent solute dispersivity in porous media: Pore-scale processes. Water Resour. Res. 49(4): 1943-1951.

[40] Raoof, A., Nick, H.M., Hassanizadeh, S.M., and Spiers, C.J., 2013. PoreFlow: A complex pore-network model for simulation of reactive transport in variably saturated porous media. Comput. Geosci. 61: 160-174.

[41] Rolle, M., Hochstetler, D., Chiogna, G., Kitanidis, P.K., and Grathwohl, P., 2012. Experimental investigation and pore-scale modeling interpretation of compound-specific transverse dispersion in porous media. Transp. Porous Med. 93: 347-362.

[42] Rudakov, E.S., and Loachev, V.L., 1994. Kinetics, kinetic isotope effects, and substrate selectivity of alkylbenzene oxidation in aqueous permanganate solutions: I Reactions with MnO_4^- G anion. Kinet. Catal. 35 (2): 175-179.

[43] Sen Gupta, K.K., Adhikari, M., and Sen Gupta, S., 1989. Kinetics of oxidation of ethanol by potassium permanganate in perchloric acid medium. React. Kinet. Catal. Lett. 38 (2): 313-318.

[44] Shen, R., Pennell, K.G., and Suuberg, E.M., 2014. Analytical modeling of the subsurface volatile organic vapor concentration in vapor intrusion. Chemosphere 95: 140-149.

[45] Sieg, K., Fries, E., and Püttmann, W., 2008. Analysis of benzene, toluene, ethylbenzene, xylenes and *n*-aldehydes in melted snow water via solid-phase dynamic extraction combined with gas chromatography/mass spectrometry. J. Chromatogr A 1178 (1-2): 178-186.

[46] Snow, N.H., 2002. Head-space analysis in modern gas chromatography. Trace-Trend Anal. Chem. 21: 608-617.

[47] Tillman, F.D., and Weaver, J.W., 2005. Review of Recent Research on Vapor Intrusion. United States Environmental Protection Agency, EPA/600/R-05/106,Washington, DC. http://209.190.206.131/ download/contaminantfocus/vi/ Review%20of%20Recent%20Research.pdf.

[48] Tsitonaki, A., Petri, B., Crimi, M., Mosbæk, H., Siegrist, R.L. Bjerg, P.L.,

2010. In Situ Chemical Oxidation of Contaminated Soil and Groundwater Using Persulfate: a review. Crit. Rev. Environ. Sci. Technol. 40: 55-91.

[49] USEPA (United States Environmental Protection Agency), 1993. Behavior and Determination of Volatile Organic Compounds in Soil: A Literature Review. EPA/600/R-93/140. http://www.epa.gov/esd/cmb/pdf/voclr.pdf.

[50] USEPA (United States Environmental Protection Agency) 1995. Principles and Practices of Bioventing. EPA/540/R-95/534.

[51] USEPA (United States Environmental Protection Agency), 1999. Alternative Disinfectants and Oxidants Guidance Manual. EPA 815-R-99-014. http://www. epa.gov/ ogwdw/mdbp/alternative_disinfectants_guidance.pdf.

[52] Waldemer R.H., Tratnyek P.G., 2006. Kinetics of contaminant degradation by permanganate. Environ. Sci. Technol. 40: 1055-1061.

[53] Yao, Y., Shen, R., Pennell, K.G., and Suuberg, E.M., 2013. A review of vapor intrusion models. Environ. Sci. Technol. 47: 2457-2470.

[54] Yoshii, T., Niibori, Y., Mimura, H., 2012. Some fundamental experiments on apparent dissolution rate of gas phase in the groundwater recovery processes of the geological disposal system. WM2012 Conference, February 26 - March 1, Phoenix, Arizona, USA.

[55] Yuan, B., Li, F., Chen, Y., and Fu, M.L., 2013. Laboratory-scale column study for remediation of TCE-contaminated aquifers using three-section controlled-release potassium permanganate barriers. Environ. Sci. 25(5): 971-77.

[56] Zhang, Q., Hassanizadeh, S. M., Raoof, A., van Genuchten, M.Th., and Roels, S.M., 2012. Modeling virus transport and remobilization on during transient partially saturated flow. Vadose Zone J.11(2).

Chapter 5

Evaluation of a horizontal permeable reactive barrier for oxidation of VOC vapours under unsaturated conditions;

Column experiments and modeling

Abstract

Permeable reactive barriers are increasingly used to treat contaminant plumes by transforming the contaminants into environmentally acceptable forms in the saturated zone. In this study, we considered a horizontal permeable reactive barrier (HPRB) in the unsaturated zone for oxidizing volatile organic compound (VOC) vapours under unsaturated conditions. We therefore performed column experiments to investigate the ability of a HPRB containing solid potassium permanganate mixed with clean sand in a 1:1 mass ratio in the unsaturated zone to oxidize the vapour of trichloroethylene (TCE), toluene, and ethanol migrating upward from contaminated saturated zone. Results revealed a significant removal of VOC vapours due to oxidation process. An increase in the HPRB thickness was found to effectively reduce TCE concentration in the headspace of the experimental setup. Results showed that the location of the HPRB relative to the water table had a strong effect on the removal efficiency of VOC vapours. Inserting the HPRB far above the water table caused a more rapid change in the pH within the HPRB, leading to lower oxidation rates of TCE and toluene. While the HPRB located close to the water table was far more effective. A reactive vapour transport model that included the effect of pH on the oxidation rate could satisfactorily simulate the TCE and toluene experimental data for the setup with the HPRB far above the water table. While the simulations of ethanol vapour could ignore the pH effect on the oxidation rate due to production of water and subsequent dilution of the hydroxide ion concentration during oxidation. For the setup with the HPRB close to the water table, the experimental data for all target compounds could also be modeled without the pH effect on oxidation. This is because the high background water content and possible diffusion of proton or/and hydroxide mainly downwards to higher water saturation area neutralized the effect of pH on the oxidation rate and subsequent leading to a higher removal efficiency and reactivity of the HPRB for all VOCs. However, the higher water contents near the water table may increase the dissolution of potassium permanganate into water and its subsequent diffusion away from the HPRB. Furthermore, nearness to the water table may increases the risk of

occasionally saturating the HPRB due to groundwater level fluctuation and subsequent the loss of permanganate from the HPRB. This would shorten the longevity of the HPRB for oxidizing VOC vapours in the unsaturated zone. Therefore, the optimal location of the HPRB is as close to the water table as possible without risking saturation of the HPRB.

5.1. Introduction

Volatile organic compounds (VOCs) are soil and groundwater contaminants of widespread concern because of (1) the large volumes that are sometimes released into the environment, (2) their toxicity, and (3) the fact that some VOCs, once they have reached groundwater, tend to persist and migrate to drinking water wells or may diffuse upward through the unsaturated zone to indoor spaces (Berscheid et al., 2010). Extended exposure to some VOCs may affect the central nervous system and internal organs, and cause the Sick Building Syndrome with symptoms such as headache, respiratory tract irritation, dizziness and nausea (Yu and Lee, 2007). For our study, we selected three VOCs (to which we also refer as target compounds). These were trichloroethylene (TCE), toluene, and ethanol as representative of chlorinated hydrocarbons, petroleum hydrocarbons (PHCs) and biofuel, respectively, for reasons explained below.

TCE is one the most common chlorinated hydrocarbons found in the environment (Albergaria et al., 2012). TCE has been used widely as a dry cleaning solvent, degreasing agent, and chemical extraction agent (Sadeghi et al., 2014). As for health effects, TCE is classified as carcinogenic to humans (IARC, 1995; EuroChlor, 2008; Picone, 2012). Prolonged exposure to TCE may have adverse effects on kidney, liver, cervix, and the lymphatic system, including cancer (Yu and Lee, 2007; Rastkari al et., 2011; Picone, 2012; Sadeghi et al., 2014). Hence, TCE vapour movement from contaminated groundwater and soil into the indoor air of overlying buildings is a major concern (EPA, 2011).

As a PHC, toluene is the primary constituent of oil, gasoline, diesel, and a variety of solvents and penetrating oils (Yu and Lee, 2007). Toluene is listed as one of the six major classes of indoor VOCs (Yu and Lee, 2007). Although, toluene has a relatively low toxicity, it still may result in adverse health effects (Picone, 2012). Extended exposure to toluene can damage the central nervous system (ATSDR, 1994).

Ethanol is being used increasingly in (renewable) fuel alternatives and as replacement for methyl tertiary-butyl ether (MTBE). The increased use of ethanol

as a gasoline additive has raised concerns over its potential impact on groundwater (Johnson et al., 2000; Capiro et al., 2007; Freitas et al., 2010). Ethanol is thought to increase the mobility of NAPLs, create higher hydrocarbon concentrations in groundwater due to cosolvency, and decrease the rate of gasoline hydrocarbon biodegradation, with subsequent increases in the length of dissolved contaminant plumes (Mackay et al., 2007; Freitas et al., 2010).

Vapour intrusion refers to the upward migration of volatile contaminants through the unsaturated zone into overlying buildings (Picone, 2012; Yao et al., 2013). Vapour intrusion provides a pathway of potential exposure to VOC vapours that migrate upward from the subsurface to indoor spaces, mostly through the gas phase. VOC transport in the unsaturated zone commonly occurs between the upper part of the contaminated saturated zone and the soil surface. In this zone, depending upon soil type and the length of unsaturated zone, fluid saturation varies from complete saturation in the capillary fringe to generally very low water contents near the soil surface (Silliman et al., 2002; Sara, 2003; Picone, 2012). Volatilization occurs at the interface between the water saturated and first air-filled pores, with VOC partitioning between the fluid and gas phases and with mass transport process subsequently being driven by diffusion and possibly advection (Picone, 2012; Costanza-Robinson, 2013; You and Zhan, 2013). Simultaneously, sorption may occur on soil solid surfaces (Breus and Mishchenko, 2006). Sorption of gaseous organic compounds can be due to two mechanisms: (1) Adsorption on mineral surfaces (e.g. iron oxides) when soils are very dry (e.g., water content < 2%), and (2) Partitioning into water present the unsaturated zone. Additionally, VOC partitioning onto soil organic matter commonly occurs in wetter soil (water content > 4%) (Farrell and Reinhard, 1994; Batterman et al., 1995; Picone, 2012). This mechanism can indirectly affect VOC concentrations. Biodegradation of VOC vapours in the unsaturated zone can affect further the concentration of VOCs reaching the ground surface. However, biodegradation typically takes place at very low rates. In order for biodegradation to occur, sufficient hydrocarbon, oxygen, nutrients, moisture, and microbial population must be present in the unsaturated zone.

Diffusion is generally by far the dominant transport mechanism of VOCs in unsaturated soils. VOC diffusion occurs mostly in the gas phase since gas phase diffusion coefficients can be up to about 3 to 4 orders of magnitude larger than aqueous phase diffusion coefficients (Wiedemeier et al., 1999; Dane and Topp, 2002; Pasteris et al., 2002; Tillman and Weaver, 2005). Diffusion acts as a resistance to the volatilization flux (Brusseau, 1991; Sanders and Talimcioglu, 1997; Murphy and Chan, 2011). As such, diffusion in the unsaturated zone is influenced very much by soil texture and especially the water content. Soil moisture is hence one of the most crucial parameters regulating the transport of volatile compounds in the subsurface (Johnson et al., 1999).

A number of techniques exist for treating an unsaturated zone contaminated with VOCs. Despite their successful use, they all suffer from several shortcomings. For instance, soil vapour extraction requires long-term operation and does not transform the contaminants to less toxic compounds or environmentally acceptable forms (Cho et al., 2002). Bioventing is an in-situ bioremediation technology that degrades VOCs. However, its performance is affected by soil permeability and water content restrictions. Moreover, bioventing is not effective for aerobic biodegradation of many chlorinated hydrocarbons (Hinchee, 1993; USEPA, 1995). In-situ chemical oxidation (ISCO) of VOCs has been well developed as a remediation technology of dissolved VOCs in groundwater (Li and Schwartz, 2004; Heiderscheidt et al., 2008; Tsitonaki et al., 2010; Yuan et al., 2013). However, only a few studies have applied ISCO methods to the unsaturated zone using dissolved permanganate (Hesemann and Hildebrandt, 2009) or other oxidants (Cronk et al., 2010).

Permeable reactive barriers (PRBs) provide an in-situ remediation technique designed to treat contaminated plumes by transforming the contaminants into environmentally acceptable forms. Vertical permeable reactive barriers (VPRBs) are a well-established technique and common configuration for remediation of contaminants in saturated zone (Yeh et. al, 2010; Gibert et al., 2013). Horizontal permeable reactive barriers (HPRBs), on the other hand, can be employed in the unsaturated zone to prevent or limit the vertical leaching of

contaminants (Siegrist et al., 1998; Mackova et al., 2006; Leal et al., 2013) or the upward migration of contaminant vapours. In some studies, the oxidant was introduced mostly as an aqueous solution, thus effectively saturating all or parts of the unsaturated zone (Cronk, 2010). Siegrist et al. (1998) have focused on the delivery method of a solid oxidant into the unsaturated zone using soil fracturing techniques (e.g. hydraulic or pneumatic fluids) to evaluate the feasibility of creating HPRBs by emplacement of chemically reactive solids.

Current literature lacks data on the potential of using solid oxidants in HPRBs to oxidize VOC vapours in the unsaturated zone. Our recent studies (Mahmoodlu et al., 2013, 2014b) showed that dry solid potassium permanganate granules were able to oxidize vapours of TCE, toluene, and ethanol (the target compounds of this study) according to the following overall reaction equations:

$$C_2HCl_{3(g)} + 2KMnO_{4(s)} \rightarrow 2K^+ + 2MnO_{2(s)} + 3Cl^- + 2CO_{2(g)} + H^+ \quad (5.1)$$

$$C_6H_5CH_{3(g)} + 12KMnO_{4(s)} + 2H_2O \rightarrow 12K^+ + 12OH^- + 12MnO_{2(s)} + 7CO_{2(g)} \quad (5.2)$$

$$C_2H_5OH_{(g)} + 4KMnO_{4(s)} \rightarrow 4K^+ + 4OH^- + 4MnO_{2(s)} + 2CO_{2(g)} + H_2O \quad (5.3)$$

In an earlier study of VOC vapour diffusion through a partially saturated reactive permeable layer (Mahmoodlu et al., 2014b) we showed that water saturation has a major effect on the removal capacity of the HPRB. Lower pH values generated during the TCE experiment, and higher pH values during the toluene and ethanol experiments, as suggested by their stoichiometric reactions, were found to be responsible for reduction in the oxidation rates of the target compounds. While that study confirmed that water content and the prevailing chemical processes do affect the reactivity of a HPRB, it remained unclear how exactly the HPRB thickness, the location of the HPRB relative to the water table, and water availability would affect the oxidation process and hence reactivity of the HPRB in the unsaturated zone.

We hence performed a series of VOC column transport experiments under field-like conditions to (1) evaluate the ability of a HPRB to oxidize the vapour of

three VOCs in the unsaturated zone, (2) investigate the effect of a HPRB thickness on the oxidation process, (3) evaluate the impact of the HPRB location relative to the water table on the long-term reactivity of the barrier, and (4) numerically simulate the reactive transport of VOC vapours diffusing through the unsaturated zone and a HPRB.

5.2. Materials and Methods

5.2.1. Experimental setup

Fig. 5.1 shows a schematic of the experimental setup. A glass cylinder of 30 cm length and 5.0 cm internal diameter, capped by a steel stainless lid, was used to construct the experimental columns. Five inlet and outlet ports and three sampling ports were made along the column. A peristaltic pump (Ismatec, Switzerland) was employed to transfer DI water and dissolved VOC from stock solutions into the lower part of the column. A 10-liter aluminum balloon (from Tesseraux Company, Germany), which did not adsorb our target compound vapours, was attached to the stock solution container to prevent changes in air pressure as liquid pumped into the column.

Fig. 5.2 provides a close-up of the column. It contained four domains. The lower part was the saturated zone contaminated with a dissolved VOC. The second domain comprised the unsaturated zone between the water table and the top of the sand column. The third domain was the HPRB within the unsaturated zone consisting of a mixture of potassium permanganate and sand. The unsaturated zone and HPRB contained water due to capillary rise. The fourth domain was the headspace above the unsaturated zone. For control experiments we used the same columns, but without any potassium permanganate.

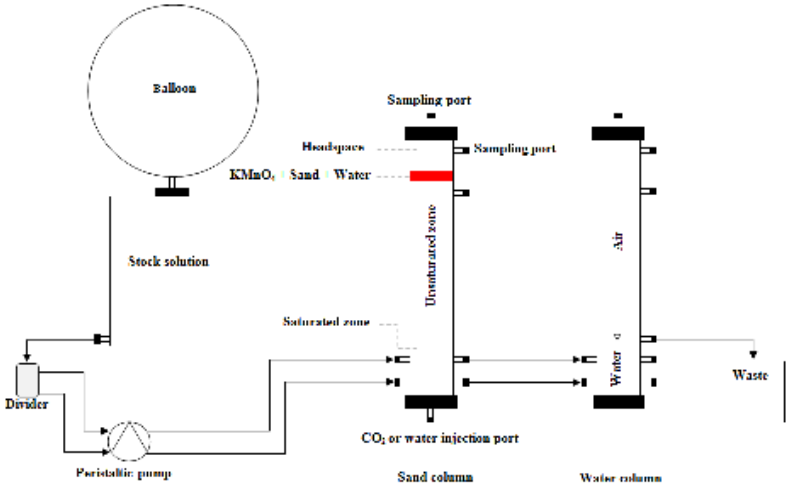

Fig. 5.1: Schematic view of experimental setup for the column experiment.

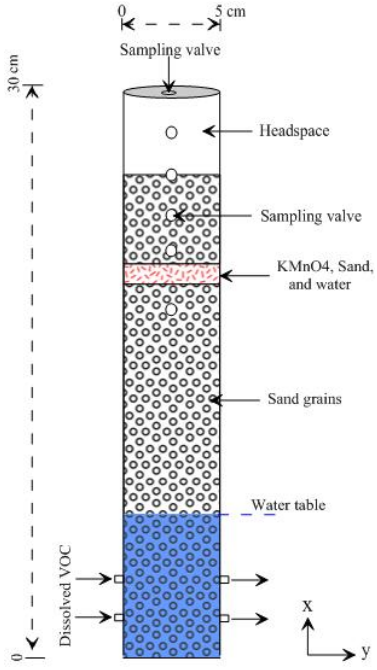

Fig. 5.2: Schematic of the sand columns used in the experiments.

5.2.2. Target compounds and porous medium

The target contaminants used in this study were pure TCE, toluene, and ethanol (from Sigma-Aldrich, Merck, and ACROS, respectively). Stock solutions of aqueous-phase TCE, ethanol, and toluene were individually prepared in 10-liter glass vessels (Fisherbrand) by dissolving the chemicals in degassed deionized (DI) water. Degassing was accomplished overnight using argon gas. The vessels containing the stock solutions were continuously mixed using magnetic stirrers (IKA, Germany) to maintain homogeneous stock solutions. The vessels containing the stock solutions were connected to aluminum balloons filled with argon gas.

The sand used for the column experiments originated from a river bed in Papendrecht (Filcom Company, The Netherlands) and was sieved to retain sizes of 0.5-1 mm. The properties of the sand are given in Table 5.1. The porosity of sand was estimated to be approximately 0.35. Before its use, we first soaked the sand in pure hydrochloric acid (Sigma-Aldrich) overnight to remove iron oxide coatings and then rinsed the sands with DI water to increase the pH to the natural background value. The pH was measured using a paper pH meter. The acid-washed sand was subsequently heated to 800 ºC for four hours to remove soil organic matter. Mercury chloride ($HgCl_2$) of 99.5% purity (Sigma-Aldrich) was used for both the stock solution and the sand to inactivate microorganisms, thus eliminating possible biodegradation processes during the experiments.

Solid potassium permanganate of 99% purity (Sigma-Aldrich) was used as the oxidant in the HPRB. Since the mean size of potassium permanganate grains was almost equal to the sand mean grain size, we assumed the same porosity for the potassium permanganate-sand mixture.

5.2.3. Column preparation

The 30-cm sand columns were packed with acid-washed and baked-dry sand from the bottom up to a height of 26 cm. This created two parts, sand and a 4-cm thick headspace in the top of the column. We took precautions to prevent any

Table 5.1: Properties of the natural sand used in the experiments

Property	Value
Porosity (-)	0.35
Particle size (mm)	0.5-1.0
Bulk density (g cm^{-3})	1.34
Specific weight (g cm^{-3})	2.66
Total organic carbon in dry sample (%)	0.05

segregation and layering of the sand in the column during packing. Before packing the columns, fiberglass (glass wool) was inserted into the inlet and outlet ports along the columns to prevent any migration of sand from the columns into the tubes.

Next, the sand column was flushed using CO_2 gas for four hours to replace air in the soil pore spaces with CO_2 gas. Subsequent filling of the sand with water dissolved CO_2 and created a fully–saturated domain. Two ways were used to create the saturated and unsaturated zones in the sand column in two different set of experiments. In the first set (to which we refer as setup a), we saturated only 6.0 cm of the column via the bottom port using a syringe. To control and monitor the water table, the sand column was connected to a water column using two tubes (Fig. 5.1). The water column was only filled with DI water up to 6.0 cm. The water column was connected in turn to a waste container using a tube at a level which allows us to maintain a desired constant water table in the sand column. DI water was then injected into the sand column via two ports using a peristaltic pump to permit flow into the saturated and unsaturated zones. In the second set (called setup b), the sand column was first fully saturated (over the whole length) through the bottom port using a syringe. The saturated sand column was subsequently desaturated down to the height of 6.0 cm. We then waited for three days for the unsaturated zone to reach equilibrium. To mimic groundwater flow, we injected DI water continuously

into the lower part of the sand column at the rate of approximately 0.8 ml min^{-1}, using a peristaltic pump.

A mixture of dry potassium permanganate grains and dry sand (10 g of each) was made for use in the horizontal permeable reactive layer (HPRB). In one case, the mixture was emplaced dry and in another case, it was mixed with DI water to reach a saturation of close to 0.2. The mixture was placed first into a small plastic container and shaken for 10 minutes in order to obtain a homogeneous mixture. This mixture subsequently was wetted with DI water required to obtain the desired water saturation. In order to obtain homogeneity, the wetted mixture was shaken for 15 minutes, after which the mixture was placed at the desired elevation in the unsaturated zone. This created a HPRB of about 1.0 cm thick with a surface area of 19.6 cm^2. The mixture (S^w=0.2) was placed at two elevations, 7.0 cm and 12.0 cm above the water table. This was done to investigate the elevation effect of HPRB relative to the water table on the VOC concentrations in the headspace. Furthermore, one experiment was conducted for all VOCs using a dry HPRB placed at 12.0 cm above the water table.

After placing the HPRBs in the unsaturated zone, the sand column was immediately capped with a vapour-tight stainless steel lid. Flow of DI water was subsequently established in the lower part of the sand column for five hours. We expected water saturation below, above, and in the HPRB to follow the capillary pressure saturation curve of the sand.

Two additional experiments were conducted for TCE in order to test the effect of the HPRB thickness on the concentration of VOC in the headspace. In the first experiment, 40.0 g potassium permanganate and for the second experiment 80 g potassium permanganate were employed. These resulted in layers of about 4.0 cm and 8.0 cm thick, respectively, with the ratio of initial mass of potassium permanganate to initial mass of sand kept equal to 1.0.

Part of the columns containing the HPRBs was wrapped in aluminum foil to prevent any photodecomposition of potassium permanganate in a HPRB. A series of control experiments without potassium permanganate was carried out for all target compounds. All experiments were conducted in a fume cabinet at room

temperature (22 ± 1 ºC) in duplicate. We assumed that the temperature and pressure inside the columns remained constant and were equal to room temperature and atmospheric pressure, respectively.

5.2.4. VOC transport experiments

To start a VOC transport experiment, the column inflow was switched from DI water to a stock solution containing dissolved VOC. We measured the constant concentration of dissolved VOC in the stock solution and also at the inlet and outlet ports during the experiments. Aqueous samples of 1.5 ml were periodically taken using a 2.5-ml gas-tight syringe (SGE Analytical Science, Australia). The aqueous samples were also injected into 10-ml transparent glass vials (Grace, The Netherlands) and sealed with a magnetic cap and hard septum (Magnetic Bitemall; Red lacquered, 8 mm center whole; Pharma-Fix-Septa, Silicone blue/PTFE grey; Grace Alltech).

Gas samples of 1.5 ml were also periodically taken from the headspace of the reactive (those containing the HPRB) and control columns using a 2.5-ml gas-tight syringe. To eliminate the effect of a pressure drop due to sampling, the same volume of air (1.5 ml) was simultaneously injected into the headspace through a separate port. Based on the very high compressibility of air, the extraction of very small volumes of air, and the large diffusion fluxes in air, we believe that this procedure prevented any pressure drop due to sampling, and thus there was no induced advective flow. The gas samples were injected into a10-ml transparent glass vial, which was sealed with a magnetic cap and hard septum.

Glass vials were immediately placed into the tray of a gas chromatograph (GC). Gas samples of 2.0 ml were taken from each vial with an autosampler using the headspace syringe of the GC. Samples were next injected into the GC. The GC (Agilent 6850) was equipped with a flame ionization detector (FID). Separation was done on an Agilent HP-1 capillary column (stationary phase: 100% dimethylpolysiloxane, length: 30 m, ID: 0.32 mm, film thickness: 0.25 μm). A temperature programmed run was used to analyze the samples. VOC concentrations

were determined using a headspace method as employed in other studies (e.g., Przyjazny and Kokosa, 2002; Snow, 2002; Almeida and Boas, 2004; Sieg et al. 2008). The limits of quantification (LOQ) were calculated using a signal-to-noise ratio of 10:1 (Kubinec et al., 2005).

Preliminary experimental results showed that the concentrations of the VOCs in the saturated zone quickly reached their maximum values (equal to the concentration at the inlet port). In our simulations, we hence assumed that the composition of VOCs in the saturated zone did not change with time. Also, diffusion in the headspace was thought to be fast enough to consider this domain to be well mixed (i.e., with no concentration gradients). However, to take into account the storage of VOCs within the headspace, and also to have well-defined boundary conditions, we chose to include the head space in the modelling.

5.3. Governing equations for VOC transport

Water flow can affect solute transport and rates of biological and chemical processes in soils (Pachepsky et al., 2003). The Richards equation is generally used for simulating water flow in the unsaturated zone. For one-dimensional vertical flow, the equation is given as (Richards, 1931):

$$\frac{\partial \theta^w}{\partial t} = \frac{\partial}{\partial x}\left[K(h)\left(\frac{\partial h}{\partial x} + 1\right)\right] \tag{5.4}$$

where θ^w denotes the volumetric water content, h is the water pressure head [L], K is the unsaturated hydraulic conductivity [LT^{-1}], x is the vertical coordinate, taken positive in the upward direction [L], and t is time [T]. Moreover, θ^w and K (h) are related to h using the equations of van Genuchten (1980) given by:

$$S_e^w = \frac{\theta^w - \theta_r^w}{\theta_s^w - \theta_r^w} = \left[1 + (\alpha|h|)^n\right]^{-m} \qquad (m = 1 - \frac{1}{n}) \tag{5.5}$$

$$K(h) = K_s S_e^{w\ 0.5}\left[1-(1-S_e^{1/m})^m\right]^2 \tag{5.6}$$

where S_e^w is effective saturation ($0 \leq S_e^w \leq 1$), θ_r^w and θ_s^w are the residual and saturated water contents [-], respectively, α [L^{-1}] and n [-] are shape factors, and K_s denotes the saturated hydraulic conductivity [LT^{-1}]. For the flow simulations, a zero flux boundary condition was assigned to the top of soil surface at the interface between the sand and the headspace, while a constant water pressure head (h=0 cm) was imposed at the water table 6.0 cm above the bottom of the column.

Since the VOC concentrations in the saturated zone quickly reached their maximum values and then did not change with time, we considered only transport processes in the unsaturated zone above the water table. In general, physical, chemical, and biological processes may all affect the fate and transport of a contaminant in the unsaturated zone. The main physical processes that may be active in both liquid and gas phases are (1) molecular diffusion, (2) advective transport, (3) dispersion, and (4) sorption to the solid phase. Since precautions were taken to prevent advection in the sealed columns, we assumed the flow velocity in the unsaturated zone to be negligible. Hydrodynamic dispersion hence could be neglected also. Before packing the columns, we rinsed the sand, first with acid and then DI water, and also heated the sand up to 800 ºC. This was expected to eliminate any significant adsorption. Biodegradation of VOC vapour in the unsaturated zone through biological reactions, such as those mediated by soil enzymes and microbial metabolisms, could possibly decrease in concentration of VOC during their upward migration. However, we used mercury chloride to eliminate biodegradation of VOC in the columns. Therefore, major chemical processes that needed to be considered in our study were the dissolution of VOCs into the water phase and chemical reactions such as the oxidation of VOCs by potassium permanganate and the consumption of potassium permanganate by the oxidizing VOCs. Therefore, the governing equation for VOC transport in the gas phase within the unsaturated zone, the HPRB, and the headspace is given by:

$$\theta^g \frac{\partial C_A^g}{\partial t} = \theta^g D_{e,A}^g \frac{\partial^2 C_A^g}{\partial x^2} - r_A^{diss} \qquad ; \text{A= TCE, ethanol, toluene} \qquad (5.7)$$

where θ^g denotes the air content, A denotes the target compound, C_A^g is the concentration in air [NL^{-3}], $D_{e,A}^g$ is the effective gas diffusion coefficient [L^2T^{-1}], and r_A^{diss} is the rate of dissolution into water [$NL^{-3}T^{-1}$]. In the headspace, the latter term is absent and θ^g is equal to 1.0. Here N denotes the number of moles.

Boundary conditions for Equation 5.7 are a constant concentration of the target compound at the water table boundary (i.e., C_A^g (t, x=0) = C_{A0}^g) and a no-flux condition at the top of the headspace. We further assumed continuity of fluxes at the interface between water and air. Since C_A^w was constant for all target compounds in the saturated zone during the experiment (equal to $C_{A,0}^w$), C_{A0}^g was taken to be equal to C_{A0}^w multiplied by the corresponding Henry's constant. Initial concentrations of the target compounds were zero throughout the modeling domain, i.e., C_A^g (t=0, x)=0.

VOC diffusion coefficients in the gas phase can be up to four orders of magnitude greater than those in the aqueous phase (Wiedemeier et al., 1999; Pasteris et al., 2002). The presence of air for this causes diffusive fluxes in the unsaturated zone to be significantly greater than those in the saturated zone. Particularly, for VOCs with high vapour pressures, the vapour diffusion dominates the migration of VOCs in unsaturated systems (USEPA, 1993; Berscheid et al., 2010; Shen et al., 2014). The rate of vapour diffusion is lower in soil than in free air because of pore space tortuosity and the presence of water (USEPA, 1993; Raoof and Hassanizadeh, 2013). The effective gas diffusion coefficient of VOC vapour in the unsaturated zone and HPRB is expressed as follows (Millington and Quirk, 1961; Pennell et al., 2009; Yao et al., 2013):

$$D^{g}_{e,A} = D^{g}_{A} \frac{\theta^{g\frac{10}{3}}}{\phi^{2}} \tag{5.8}$$

where D^{g}_{A} is the molecular diffusion coefficient of the target compound in free air [L^2T^{-1}] and ϕ denotes the porosity of porous medium.

The dissolution rate r^{diss}_{A} of the VOC compounds into water was modelled as a linear kinetic process (Yoshii et al., 2012):

$$r^{diss}_{A} = k^{diss}_{A} a_i \left(\frac{C^{g}_{A}}{H_{C,A}} - C^{w}_{A}\right) \tag{5.9}$$

In which k^{diss}_{A} is the dissolution rate constant [LT^{-1}], a_i is the specific air-water interfacial area [L^{-1}], $H_{C,A}$ denotes Henry's constant of the VOC [-], and C^{w}_{A} is the concentration of the target compound in soil water [NL^{-3}].

Many studies have shown that the dissolution rate depends on the specific air-water interfacial area (Costanza and Brusseau, 2000; Kim et al., 2001; Hoeg et al., 2004; Cho et al., 2005). The specific air-water interfacial area in turn is known to depend on the water content as well as on the capillary pressure (Hassanizadeh and Gray, 1993; Joekar-Niasar et al., 2010; Raoof et al., 2013). For the purpose of this study, we assumed that the specific surface area depends only on relative water saturation, S^w, according to (Zhang et al., 2012):

$$a_i = a_{i0} S^{w} (1 - S^{w})^{\sigma}$$

where a_{i0} is the specific interfacial area corresponding to residual saturation (Zhang et al., 2012) and σ is a fitting parameter.

The equations given above pertain to VOC transport in the gas phase. VOC transport within the water phase, both within the unsaturated zone and the HPRB, is assumed to be governed by:

$$\theta^{w}\frac{\partial C_A^w}{\partial t}=\frac{\partial}{\partial x}(\theta^{w}D_{e,A}^{w}\frac{\partial C_A^w}{\partial x})+r_A^{diss}-r_A^{oxid} \tag{5.11}$$

in which $D_{e,A}^{w}$ is the effective diffusion coefficient in the water phase [L^2T^{-1}] and r_A^{oxid} is oxidation rate [$NL^{-3}T^{-1}$].

Boundary conditions for Equation 5.11 are a constant concentration of the target compound at the water table boundary (i.e., $C_A^w(t, x=0)=C_{A,0}^w$) and no-flux at the top. We assumed that the target compounds initially were absent in the water phase in the unsaturated zone; i.e., $C_A^w(t=0, x)=0$.

The effective diffusion coefficient of the target compounds in water is assumed to be given by a similar equation as for the air (Pennell et al., 2009; Yao et al., 2013):

$$D_{eff,A}^{w}=D_A^w\frac{\theta^{w\frac{10}{3}}}{\phi^2} \tag{5.12}$$

where D_A^w denotes the molecular diffusion coefficient of the target compound in the water phase [L^2T^{-1}].

Several previous studies have shown that permanganate is able to oxidize a variety of VOCs in water (Waldemer and Tratnyek, 2006; Kao et al., 2008; Mahmoodlu et al., 2014a). Mahmoodlu et al. (2014a) proposed a second order equation for the oxidation rate of VOC in the water phase, given as a function of the VOC and potassium permanganate concentrations. For unsaturated soil, the oxidation rate can be written as:

$$r^{oxid} = k_A C_A^w C_B^w \theta^w \tag{5.13}$$

where k_A is the reaction rate coefficient in the water phase, B denotes potassium permanganate, and C_B^w is the concentration of dissolved permanganate in water [NL^{-3}]. Since potassium permanganate commonly dissolves quickly into soil water up to its solubility of 64 g l^{-1} at 20 °C (USEPA, 1999), and assuming a high dissolution rate compared to the oxidation of dissolved potassium permanganate, mass transfer across the water/solid was considered not be limiting. We hence assumed C_B^w to be equal to $C_{B,max}^w$.

A preliminary analysis of the experiments showed that the oxidation rate decreased with time and even became zero after a certain period of time. We considered two hypotheses for the decrease in reactivity of the HPRB: (1) depletion of potassium permanganate in the water phase and (2) a pH dependency of the oxidation rate. In our earlier study (Mahmoodlu et al., 2014b), we used an excess amount of potassium permanganate in the HPRB. But, we the current experiments involved only a limited amount of potassium permanganate, which could be depleted due to oxidation of VOCs. Our experimental data confirmed that the concentration of potassium permanganate were not a limiting factor during the experiments. We hence considered the second hypothesis, i.e., the pH dependency of the VOC oxidation rates. Our earlier study suggested that a decrease in the pH during the TCE experiment and an increase in the pH during the toluene and ethanol experiments, as expressed by their stoichiometric reaction equations (Equations 5.1 to 5.3), were responsible for the decrease in oxidation rate (Mahmoodlu et al., 2014a). This effect was modelled by allowing a dependency of k_A on pH according to

$$k_{TCE} = \kappa_{TCE}(pH - \omega_{TCE})^{\beta_{TCE}} \tag{5.14}$$

with pH variations given by:

$$\frac{\partial H^+}{\partial t} = \zeta_{TCE} r_{TCE}^{oxid} \tag{5.15}$$

in which κ_{TCE} is the reaction rate constant in water [$N^{-1}T^{-1}$] as determined through batch experiments (Mahmoodlu et al., 2014a), ω_{TCE} and β_{TCE} are fitting parameters obtained as part of the simulation results, and H^+ denotes the proton concentration [NL^{-3}]. The parameter ζ_{TCE} in Equation 8.15 is the number of moles of protons produced during oxidation of TCE. According to Equation 1, its value is equal to unity.

Similar relationships were employed for the reaction rate coefficients of toluene and ethanol as follows:

$$k_A = \kappa_A (\omega_A - pH)^{\beta_A} \qquad ; A= \text{toluene, ethanol} \tag{5.16}$$

$$\frac{\partial OH^-}{\partial t} = \zeta_A r_A^{oxid} \tag{5.17}$$

where κ_A denotes the reaction rate constant in water [$N^{-1}T^{-1}$], ω_A and β_A are fitting parameters, OH^- denotes the molar concentration of hydroxide ions, and ζ_A is the number of moles of hydroxide ions involved in the stoichiometric reaction ($\zeta_{toluene} = 12$ and $\zeta_{ethanol} = 4$).

The above set of coupled equations (5.7 to 5.17) was solved using COMSOL Multiphysics (Rolle et al., 2012; Müller et al., 2013).

5.4. Experimental results

5.4.1. VOC Concentrations in the headspace

Fig. 5.3 depicts normalized concentrations (C/C_0) of the three target compounds in the control experiments as a function of time for the two different sets of experiments (related to the saturating methods of the sand column, as explained in Section 5.2.3). Here, C denotes the observed concentration of VOC vapour in the headspace and C_0 is the maximum concentration of VOC vapour above the water table, being the interface between water/gas phases. The latter was calculated based on the concentration of VOCs in the water phase, which was constant during the experiments. The results in Fig. 5.3 indicate that the VOC concentration in the headspace increased gradually with time up to the maximum measured concentration. Results revealed that using different methods of saturating the sand in the columns did not have a significant effect on vapour migration. This is because the retention capacity of the sand is very small and water saturation in the unsaturated zone following the capillary pressure saturation curve.

Fig. 5.4 shows the transport of all target compounds through the unsaturated sand, including the partially saturated sand layer (S^w=0.2) of 1.0 cm thickness placed 12.0 cm above the water table in the control experiments. Results revealed that the upward migration of VOCs decreased from toluene towards ethanol. A likely explanation is the effect of VOC partitioning due to its dissolution in water. Ethanol moved slowest since it is fully miscible with water. Next is TCE with a solubility of 1.28 g/l, while toluene is the least retarded target compound, having a solubility of only 0.52 g/l. These results show that both chemical and physical processes affect the movement of vapour transport through the unsaturated zone and the sand layer.

A comparison of the control and reactive experiments showed that the HPRB was very effective in oxidizing VOC vapours. This can be clearly seen in Fig. 5.5, where the rise of VOC concentrations in the headspace is much slower

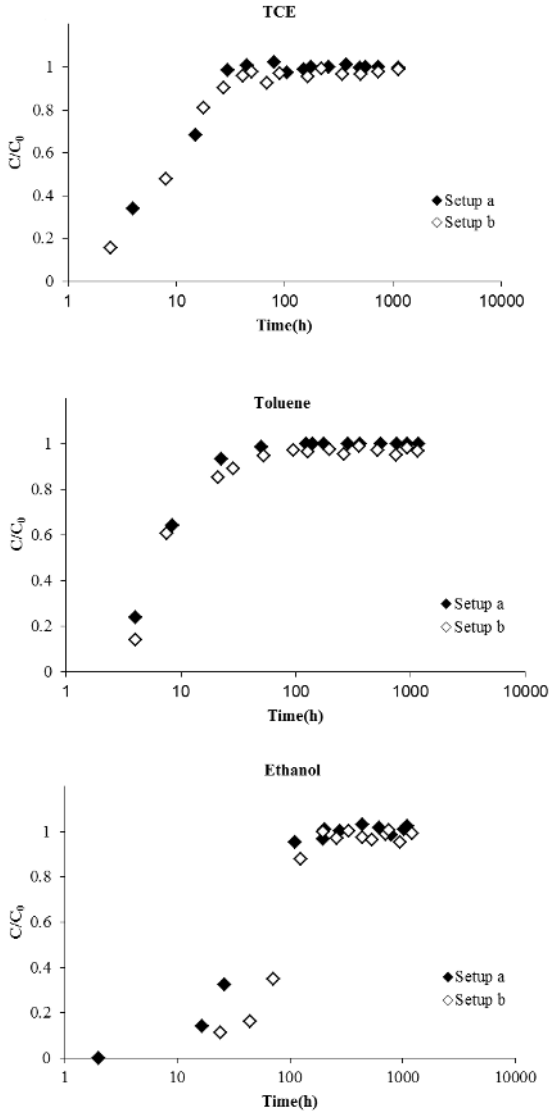

Fig .5.3: Effect of saturating method of the sands on VOC vapours diffusing through the unsaturated zone in the control experiments. Setup a: only 6.0 cm of the lower part of the column was saturated through the bottom port using a syringe. Setup b: column was first fully saturated and then desaturated to 6.0 cm level.

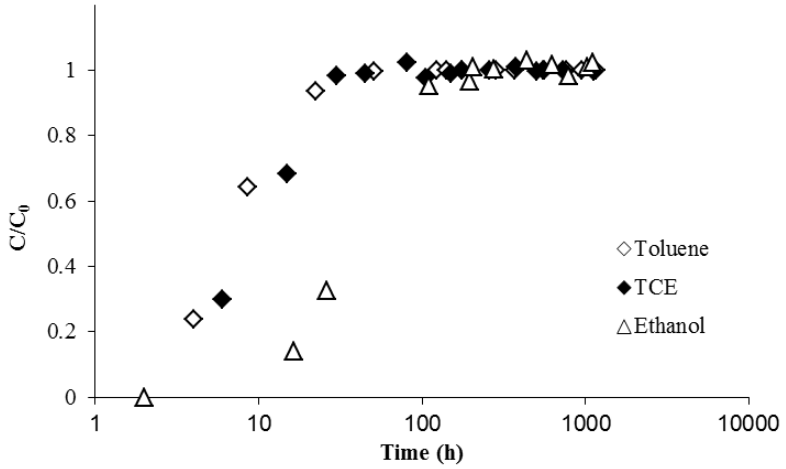

Fig. 5.4: Comparison of concentrations of VOC vapours measured in the headspace for control experiment (no HPRB).

for the HPRB columns than the control columns. Experimental results also show that the HPRB in the sand column was far more effective than our earlier setup (Mahmoodlu et al., 2014b) which allowed the VOC vapours to diffuse only through the HPRB. This may be because VOC concentrations in the gas phase reaching a HPRB were much lower than in our earlier experiments. Another likely explanation is the presence of a continuous water vapour flux from the saturated zone. The latter could provide a high and constant air humidity in the column.

Results show that the HPRB is more effective for ethanol than for the other two compounds. We observed a slow increase in the ethanol concentrations of the headspace. The reactivity of the HPRB for ethanol lasted much longer than for TCE and toluene. We believe that production of water during the oxidation of ethanol (Equation 5.3) can temper the concentration rise of produced hydroxide ions, consequently causing a slower increase in pH of the HPRB. An increase in the residence time of ethanol in the water phase due to its dissolution and hydrophilic

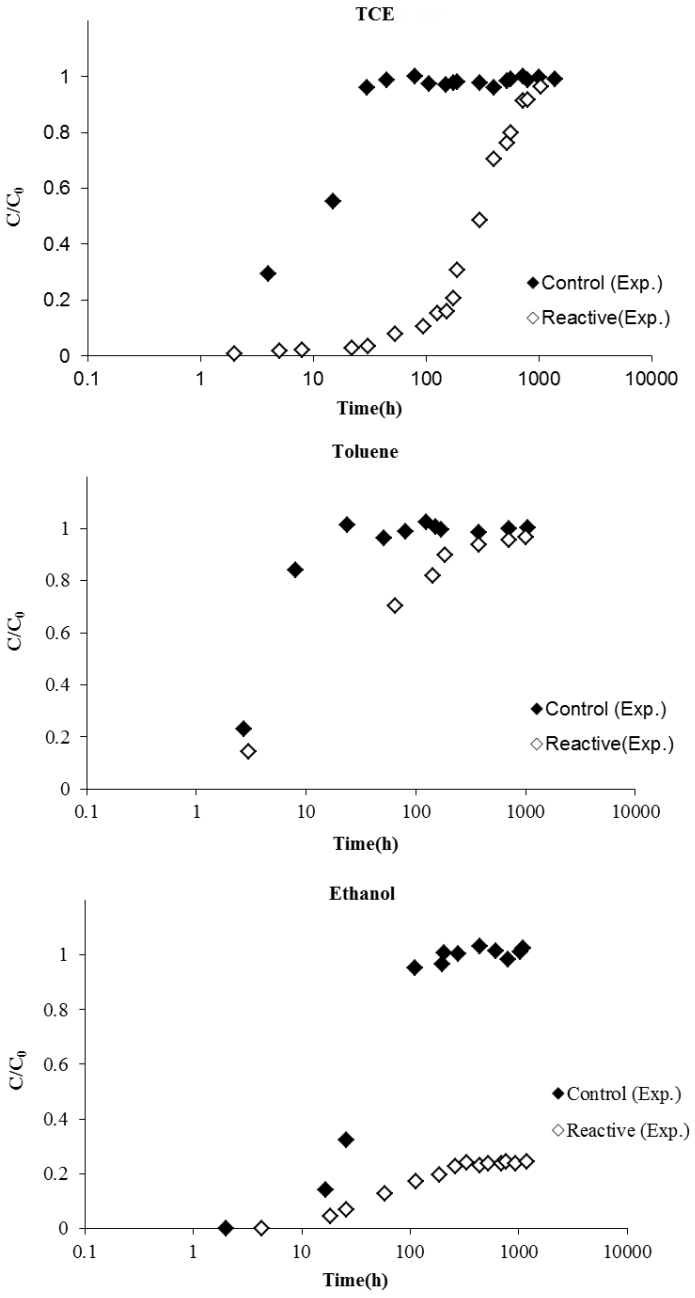

Fig. 5.5: Concentrations of VOC vapours in the headspace of control and reactive experiments. A HPRB of 0.2 water saturation was placed 12.0 cm above the water table. The experiment containing HPRB was reactive.

property may increase the exposure time to dissolved potassium permanganate and consequently a high removal of ethanol mass in the water phase.

5.4.2. Effect of initial water saturation of the HPRB on VOC concentrations in the headspace

To investigate the effect of initial water saturation on the reactivity of the HPRBs, two sets of complementary experiments were performed for the TCE experiments (Fig. 5.6). As explained earlier, in the first set of experiments, 1.0 cm of HPRB, containing dry potassium permanganate and sand, was placed 12.0 cm above the water table. In the second set of experiments, the sand and potassium permanganate mixture was first wetted to a saturation of 0.2 and then placed in the unsaturated zone. Results for both cases showed that the build-up of VOC concentrations in the headspace was much slower for the HPRB columns than for the control columns (Fig. 5.6).

Although the overall effect of the dry HPRB was still smaller than the partially saturated HPRB, it was more effective than our earlier setup involving diffusion of VOC vapours through a dry permeable reactive layer (Mahmoodlu et al., 2014b). A likely explanation was the initial concentration of VOC in the gas phase, which was lower than our previous setup having high initial concentration in the gas phase corresponding to its vapour pressure. Another reason may be the effect of the air humidity on the reactivity of HPRB which may increase the availability of water. We expected that technical grades of potassium permanganate as a salt would be able to absorb air moisture (Hazen and Sawyer, 1992). Therefore, in the presence of unlimited air moisture, reaction may occur relatively longer than for our previous setup that included limited amount of air moisture (Mahmoodlu et al., 2014b).

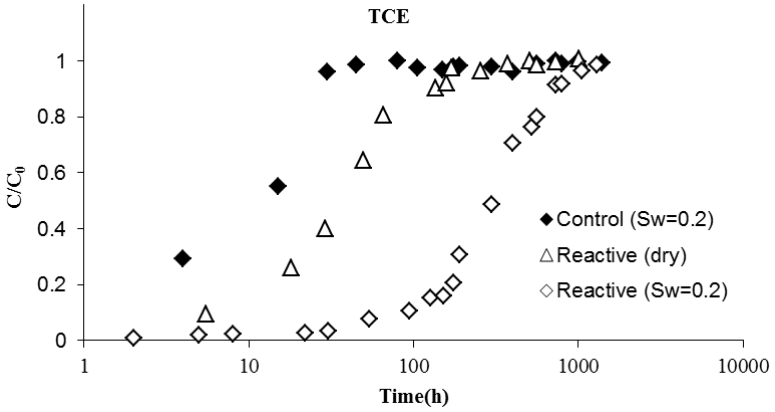

Fig. 5.6: Concentrations of TCE vapours in the headspace of the control and HPRB experiments at two different initial saturations. The HPRB was placed 12.0 cm above the water table using two different initial water saturations.

5.4.3. Effect of HPRB thickness on VOC concentrations in the headspace

Fig. 5.7 shows the effect of HPRB thickness on the VOC concentration in the headspace as a function of time. Three separate experiments were conducted for TCE using the same water saturation (S^w=0.2) but with a different initial mass of potassium permanganate in the HPRB. For one experiment, we used 10 g potassium permanganate and 10 g sand. Hence, the ratio of initial mass of potassium permanganate to initial mass of sand was equal to 1.0 and the thickness of HPRB was equal to about 1.0 cm. In the second experiment, we used 40.0 g potassium permanganate and for the third experiment 80 g. These cases resulted in layers of about 4.0 cm and 8.0 cm thick, respectively. The ratio of initial mass of potassium permanganate to initial mass of sand was kept at 1.0.

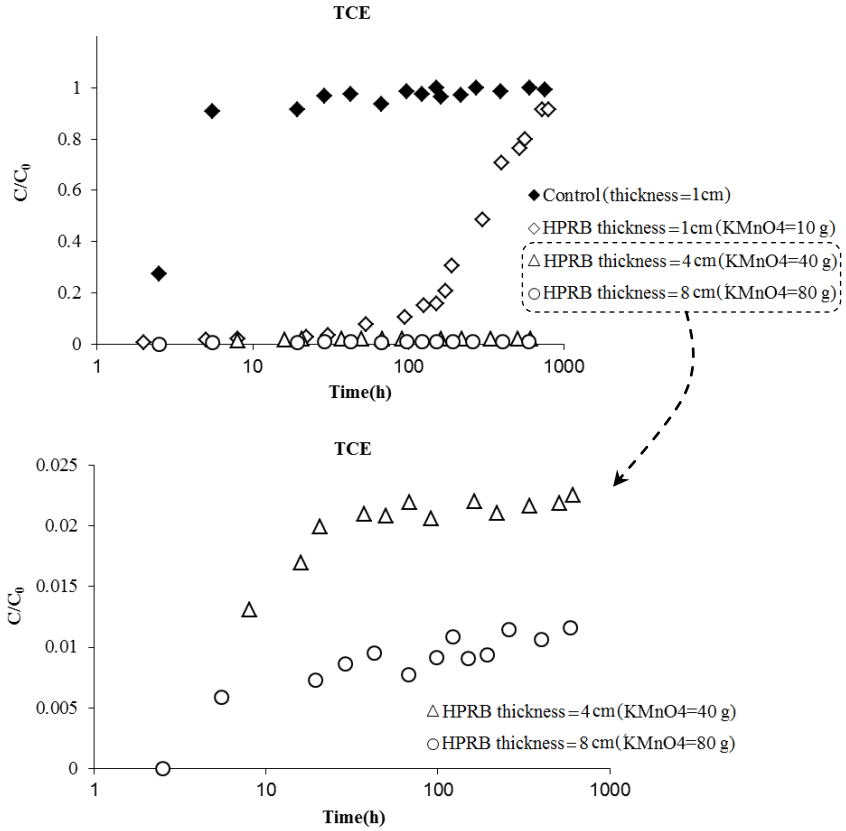

Fig. 5.7: Concentrations of TCE vapour in the headspace for three different HPRB thicknesses. The ratio of initial mass of $KMnO_4$ to initial mass of sand was equal to 1.0 for all experiments. The vertical axis of the lower plot was enlarged.

Results suggest that higher initial amount of potassium permanganate as well as a thicker HPRB leads to more effective oxidation of VOC vapours. This can be seen clearly in Fig. 5.7, where the build-up of VOC concentrations in the headspace is much slower for the columns with large amounts of potassium permanganate and consequent thicker HPRBs. The HPRB with a thicker layer remained effective for a much longer period under same water saturation degree. This is because travel time through the HPRB and consequent VOC dissolution in pore water increased. The presence of potassium permanganate in the water phase may have a resulted in large oxidation capacity for the thinker layer.

5.4.4. Effect of HPRB elevation on VOC concentrations in the headspace

In this experiment, the HPRB with a thickness of 1.0 cm and water saturation of 0.2 was placed 7.0 cm above the water table. The build-up of VOC concentrations in the headspace after diffusing through the unsaturated sand and the HPRB as a function of time is shown in Fig. 5.8. A comparison of Fig. 5.5 and Fig. 5.8 reveals that the HPRB in this experiment was far more effective than our earlier setup in which the same HPRB was located 12.0 cm above the water table. The observed VOC concentration in the headspace reached a maximum value far below the maximum possible concentration. This is because the high background water content and possible diffusion of proton or/and hydroxide (especially downwards to the higher water saturation area) neutralized the effect of pH on the oxidation rate, thus leading to a higher removal efficiency and reactivity of the HPRB for all VOCs.

As shown in Fig. 5.8, the increase in the concentration of toluene in the headspace was found to be much higher than for TCE and ethanol. This may be due to the reaction rate constant in the water phase, which is much smaller for toluene than for TCE and ethanol.

During this experiment we observed that the initially clean sand we used became gradually light purple on both sides of the HPRB. This was due to diffusion of dissolved potassium permanganate away from the HPRB. This also may have resulted in an increase in the thickness of the reaction zone containing potassium permanganate, and as such increased the exposure time of VOCs to potassium permanganate in the water phase.

5.4.5. Reactivity of the HPRBs

As shown in Fig. 5.5, the reactivity of the HPRB decreased during the course of the experiments. We found that water saturation had a strong effect on the reactivity of potassium permanganate in the HPRB. Results show that the reactivity

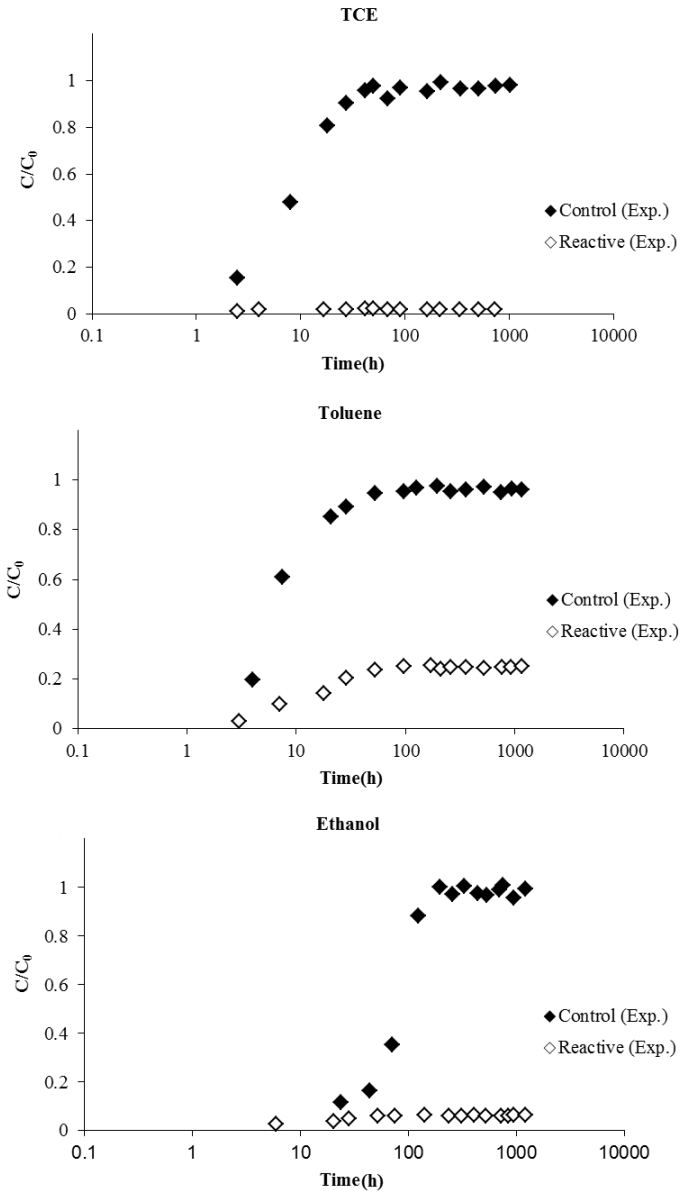

Fig. 5.8: Concentrations of VOC vapours in the headspace of the control and HPRB experiments. A HPRB of 0.2 water saturation was placed 7.0 cm above water table.

of the HPRB can be affected by both initial water saturation of the HPRB (Fig. 5.6) and also the water table (Fig. 5.8).

Mahmoodlu et al. (2013 and 2014b) showed that the accumulation of reaction products can cause a decrease in the reactivity of a permeable reactive layer. As seen in Equations 5.1 to 5.3, there are two main reaction products; manganese dioxide and protons or hydroxide ions. Manganese dioxide would precipitate on the potassium permanganate grains surfaces under normal conditions, thereby reducing the reactive surface. Furthermore, highly acidic or basic conditions would decrease the oxidation rate. Another explanation for the decrease in the reactivity of the HPRB may be the depletion of potassium permanganate mass and hence its concentration in the water phase due to oxidation. These possible causes of reduction of causes in HPRB are discussed in below.

For a partially saturated HPRB, our calculations for the TCE oxidation experiments showed that the pH could have decreased to highly acidic conditions (e.g., Huling and Pivetz, 2006; Kao et al., 2008). This has two effects: (1) an increase in the solubility of manganese dioxide and (2) a reduction in HPRB reactivity during the TCE oxidation experiments. For a dry HPRB, the precipitation of produced manganese dioxide on the reactive surface of potassium permanganate was the possible cause of reduction in HPRB reactivity during the TCE experiment (Fig. 5.6).

Similar to the TCE oxidation experiment, the reactivity of the HPRB for toluene decreased during the experiments. However, the pH decreased in toluene oxidation experiment, due to the production of hydroxide ion (Equation 5.2). The oxidation rate of aromatic rings has been shown to decrease with increasing basicity of the water phase (Forsey, 2004; Lobachev et al., 1997; Rudakov and Loachev, 1994).

In contrast to TCE and toluene, the HPRB reactivity in the ethanol experiment became constant and never reached zero (Fig. 5.5). This resulted in a concentration of about 20% of maximum concentration in the headspace for a partially saturated HPRB placed far above the water table. As shown by Equation

5.3, production of water should temper the rise of pH in the HPRB. In this case, the reactivity decreased slightly and did not change with time.

For the setup with the HPRB close to the water table (Fig. 5.8), the high background water content and the possible diffusion of protons or/and hydroxide, especially downwards to the higher water saturation area, could neutralize the effect of pH on the oxidation rate and lead to a higher removal efficiency and reactivity of the HPRB for all three contaminants. However, the higher water contents near the water table may accelerate the dissolution of potassium permanganate into water and its subsequent diffusion away from the HPRB.

5.5. Numerical modelling results

Equations 5.4 to 5.13 were solved numerically to determine the soil water distribution as well as the distribution of target compounds in the water and gas phases of the column. Since the VOC concentrations were considered to be constant in the saturated zone (equal to the input concentration), only the unsaturated zone and the headspace were modeled. All values of the various parameters used in the calculations are given in Table 5.2.

5.5.1. Soil water distribution

For determination of the soil water distribution, we used the capillary pressure-saturation curve. We used data of Fritz (2012), who had performed measurements for the same sand as used in our experiments. Our experimental procedure was such that equilibrium soil water distribution was reached in the column before starting the VOC transport experiment. This distribution was determine by solving Equations 5.4 to 5.6 for three different cases: (a) a dry HPRB placed 12.0 cm above the water table, (b) a partially saturated HPRB (S^w=0.2) placed 12.0 cm above water table, and (c) a partially saturated HPRB (S^w=0.2) placed at 7.0 cm above water table. The resulting soil water distributions are shown in Fig. 5.9.

Table 5.2: Experimental conditions and modeling parameters of the column experiments.

Parameter	VOC	Value	References
Porosity of the permeable reactive layer, ϕ, (-)	-	0.35	-
Residual water content, θ_r^W, (-)	-	0.02	-
Saturated water content, θ_s^W, (-)	-	0.4	-
van Genuchten parameter α, (-) in Equation 5.5	-	20	-
van Genuchten parameter n, (-) in Equation 5.5	-	4.5	USEPA (1999)
Specific interfacial area corresponding to residual saturation, a_{i0}, (m^{-1})	-	4.0	Zhang et al. (2012)
Saturated hydraulic conductivity (m s^{-1})	-	2.2×10^{-3}	
Fitting parameter σ in Equation 5.10 (-)	-	6.0	-
Henry's constant of VOCs, H_C, (-)	TCE	4.3×10^{-1}	Fan and Scow (1993)
	Toluene	2.8×10^{-1}	Fan and Scow (1993)
	Ethanol	2.4×10^{-4}	ITRC (2011)
Reaction rate constant of VOCs in water, κ_A, (M^{-1} s^{-1})	TCE	8.0×10^{-1}	
	Toluene	2.5×10^{-4}	Mahmoodlu et al. (2013b)
	Ethanol	6.5×10^{-4}	
Molecular diffusion coefficient of VOCs in air, D_A^g, (m^2 s^{-1})	TCE	7.9×10^{-6}	Estivill et al. (2007)
	Toluene	7.6×10^{-6}	Hers et al. (2000)
	Ethanol	1.1×10^{-5}	Green and Perry (2007)
Molecular diffusion coefficient of VOCs in water, D_A^W, (m^2 s^{-1})	TCE	9.1×10^{-10}	Fogler (2006) and Lewis et al. (2009)
	Toluene	9.4×10^{-10}	Hers et al. (2000)
	Ethanol	1.2×10^{-9}	Green and Perry (2007)
Dissolution rate coefficient of VOC vapours in water, k_A^{diss}, (m s^{-1})	TCE	8.0×10^{-5}	
	Toluene	1.3×10^{-5}	[a]Measured
	Ethanol	1.0×10^{-4}	
Fitting parameter β in Equations 5.14 and 5.16 (-)	TCE	2.0	-
	Toluene	3.0	-
Fitting parameter ω in Equations 5.14 and 5.16 (-)	TCE	1.25	-
	Toluene	14.0	-
Number of mole of [b]proton or [c]hydroxide in Equations 5.1 to 5.4, ζ, (-)	TCE	1.0	-
	Toluene	12.0	-

[a]Additional batch experiments were performed to estimate the dissolution rate coefficient of VOCs; [b]Produced during oxidation of TCE; c [b]Produced during oxidation of toluene.

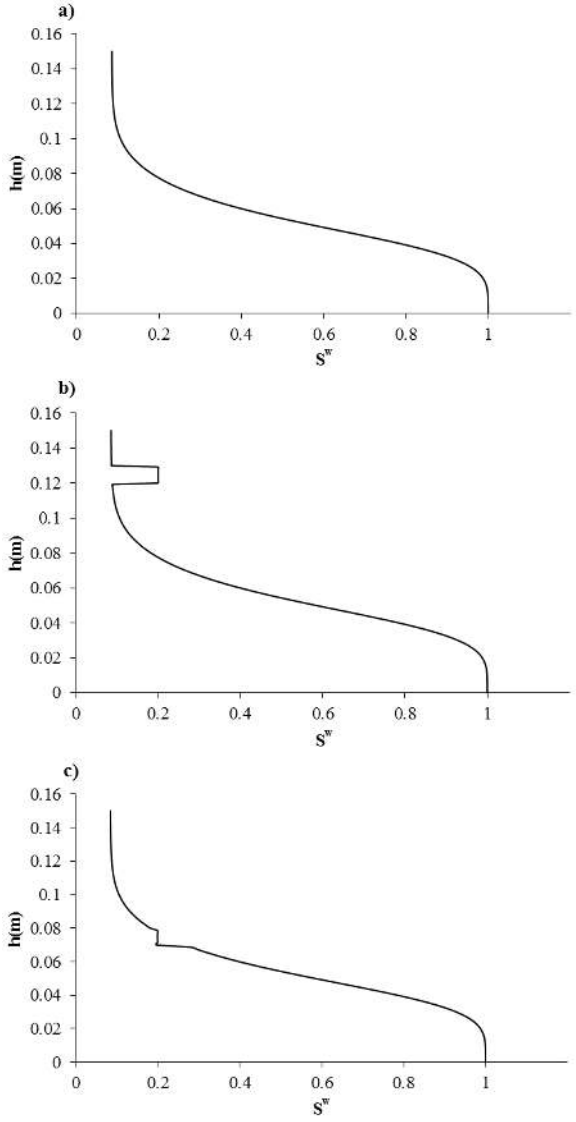

Fig. 5.9: Soil water distribution as a function of height above the water table for three cases: a) a dry HPRB placed 12.0 cm above the water table, b) a HPRB with S^w=0.2 placed 12.0 cm above the water table, and c) a HPRB with S^w=0.2 placed 7.0 cm above the water table.

5.5.2. VOC distribution for HPRB placed 12 cm above the water table

Simulation results and our experimental data for the partially saturated HPRB (S^w=0.2) as well as the control experiments are shown in Fig. 5.10. We obtained reasonably good agreement between the simulation results and the VOC data for all experiments. As explained in Section 5.4.4, we expected the change in pH to be the main reason for the decrease in the VOC oxidation rates during the experiments. However, preliminary simulations based on our two alternative hypotheses (e.g., assuming manganese dioxide and subsequent coating of the reactive surface of potassium permanganate, or depletion of potassium permanganate mass and consequently its concentration in the water phase) could not describe the experimental data. This is in line with our first hypothesis that pH exerted the main control on the oxidation rates. The model in this case accurately described the observed breakthrough curve of TCE and toluene vapours in the headspace of the sand column. Modelling results confirmed the controlling effect of pH on the oxidation rate of TCE and toluene by potassium permanganate (Fig. 5.10). While the oxidation rate became zero at relatively long times, with the concentrations of TCE and toluene in the headspace reaching the corresponding concentrations of the control experiments, the oxidation rate for the ethanol experiment decreased slightly and remained constant during the experiment due to the produced water (Fig. 5.10). This can temper the rise of pH within the HPRB. Hence, the experimental data for ethanol was model without accounting for the effect of pH on the oxidation rate.

5.5.3. VOC distribution for HPRB placed 7.0 cm above the water table

We used Equations 5.7 and 5.11 to simulate the soil water distribution of case c where the HPRB was placed 7.0 cm above the water table (Fig. 5.9). Two different sets of simulations were carried out. In one set, we included a dependence of the reaction rate on pH (Equations 5.14 or 5.16), while in another set we disregarded the pH effect on the reaction rate. As shown in Figs. 5.11a, b, c, good

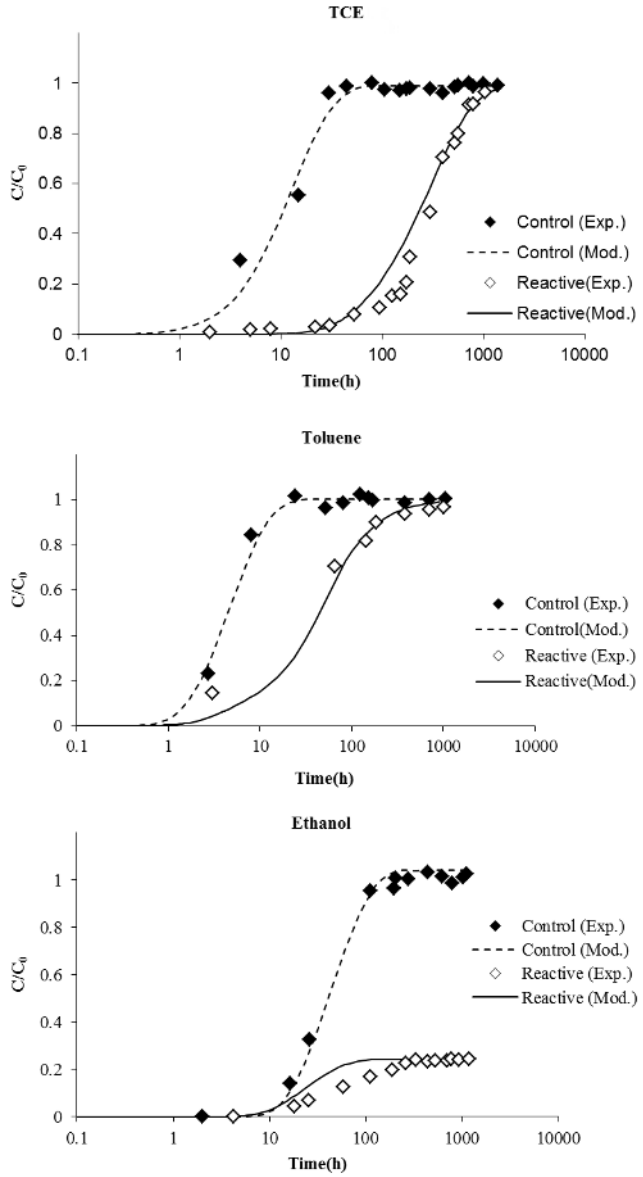

Fig. 5.10: Comparison of measured and simulated breakthrough curves for the vapour of three target compounds in the headspace. A partially saturated HPRB (S^w=0.2) was placed 12.0 cm above the water table.

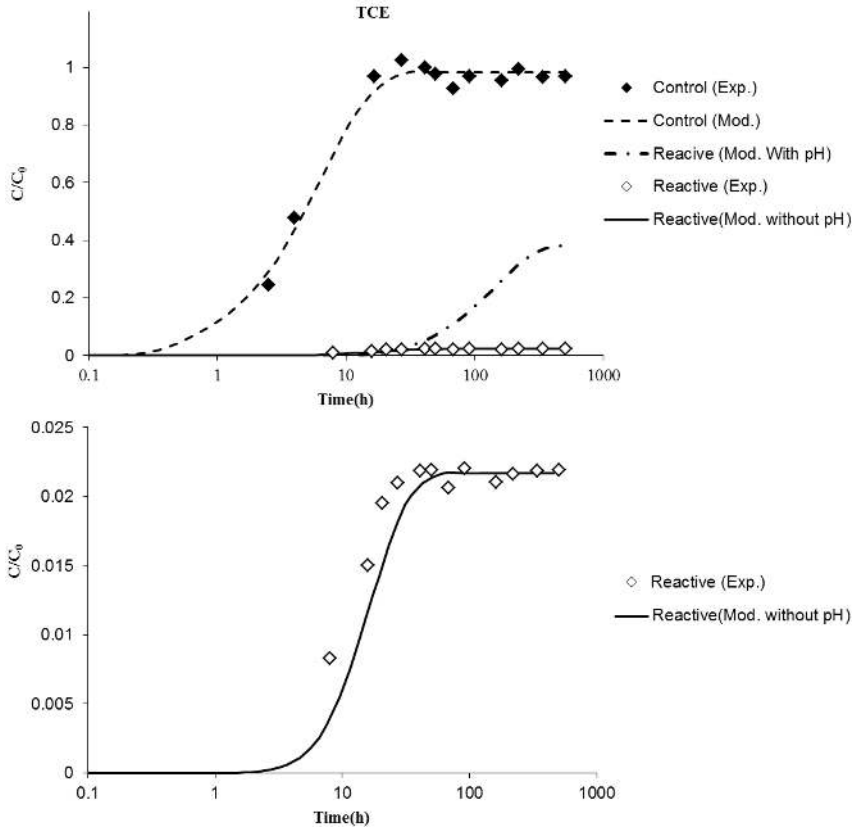

Fig. 5.11a: Comparison of measured and simulated breakthrough curves for the vapour of TCE in the headspace. A partially saturated (S^w=0.2) HPRB was placed 7.0 cm above the water table. The vertical axis of the lower graph was enlarged.

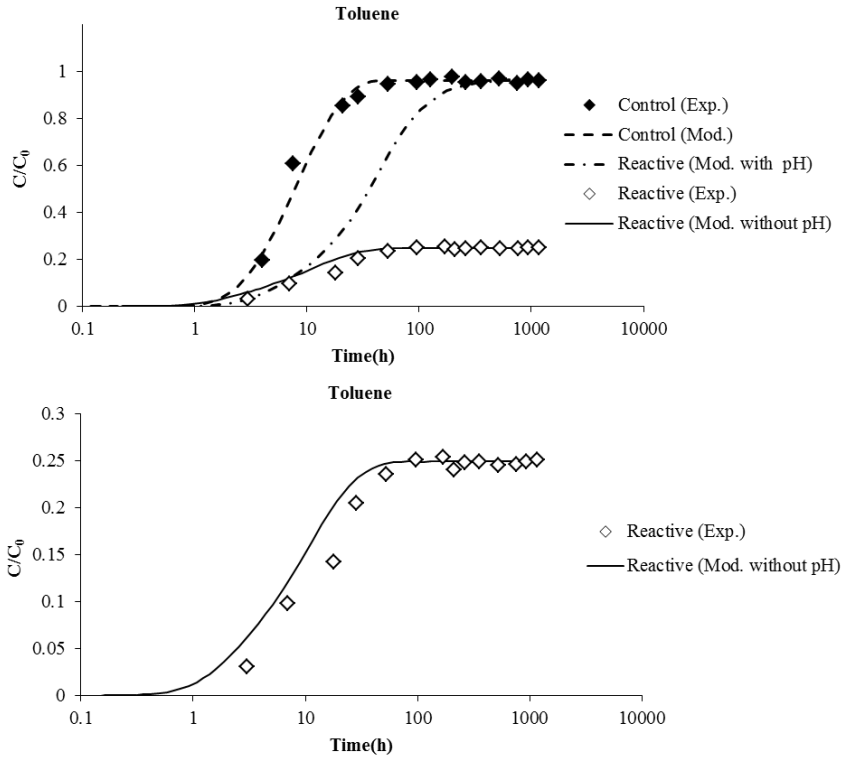

Fig. 5.11b: Comparison of measured and simulated breakthrough curves for toluene vapour in the headspace. A partially saturated (S^w=0.2) HPRB was placed 7.0 cm above the water table. The vertical axis of the lower graph was enlarged.

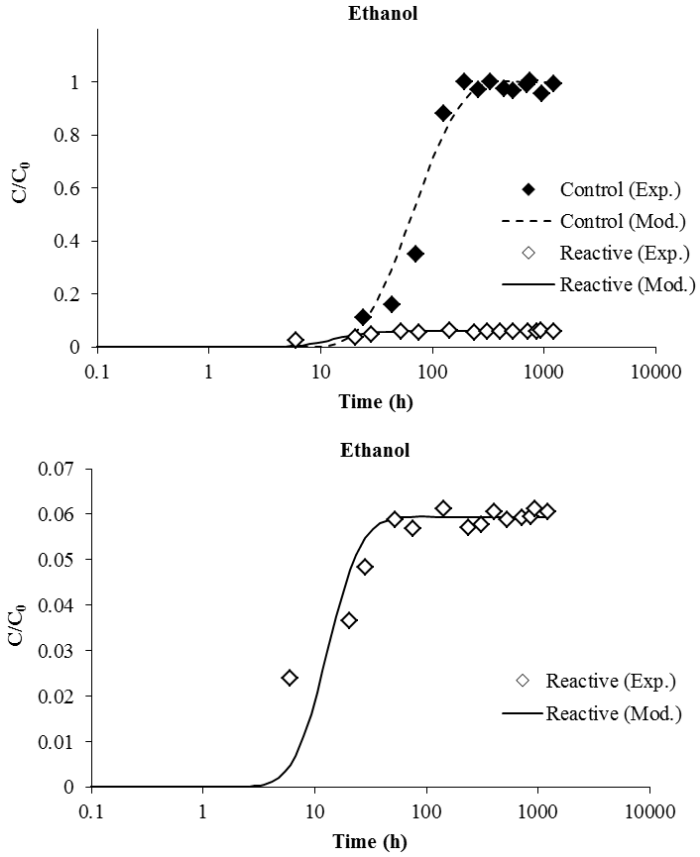

Fig. 5.11c: Comparison of measured and simulated breakthrough curves of ethanol vapour in the headspace. A partially saturated (S^w=0.2) HPRB was placed 7.0 cm above the water table. The vertical axis of the lower graph was enlarged.

agreement was obtained between the simulation results and the experimental data for all target compounds.

As explained in Sections 5.4.5, we did not expect the pH to be the main cause for the decrease in the oxidation rate of the target compounds for the HPRB placed 7.0 cm above the water table. This is because the high background water content and possible diffusion of proton or/and hydroxide neutralized the effect of pH on the oxidation rate. Modeling results confirmed our assumption of a negligible change in pH within the HPRB during the oxidation of all VOCs. Hence, the reactivity of HPRB remained high and constant over relatively long time periods.

5.6. Conclusions

This study involved a series of column experiments to evaluate the performance of a partially saturated HPRB consisting of solid potassium permanganate, sand, and water, for oxidizing TCE, toluene, and ethanol vapours under unsaturated conditions.

Result from control experiments showed that the migration time for ethanol vapour due to its partitioning effect into the water phase was much longer that for TCE and toluene vapours. A comparison of the control and reactive experiments revealed that the HPRB was very effective in oxidizing VOC vapours. Experimental results showed that the HPRB in the sand column experiment was far more effective than our earlier setup in which VOC vapours diffused through only a partially saturated HPRB (Mahmoodlu et al., 2014). This may be because the concentration of VOCs in the gas phase entering the HPRB was much lower than in our earlier experiments. We observed a slow rise of ethanol concentrations in the headspace.

The reactivity of HPRB for ethanol was much longer than for TCE and toluene. Production of water during the oxidation of ethanol can temper the concentration of produced hydroxide ions and consequently can lead to a high and constant reactivity of the HPRB. An increase in the residence time of ethanol within the water phase due to its dissolution and hydrophilic property may increase the

exposure time to dissolved potassium permanganate, thus causing a more transfer of ethanol into the water phase.

Results show that an increase in initial water saturation of the HPRB was more effective for oxidizing VOC vapours. Moreover, the build-up of VOC concentrations in the headspace was much slower for the columns with a thicker layer. This is because travel times through the HPRB and consequently dissolution of VOC in the pore water increased. In the presence of potassium permanganate in the water phase, the oxidation capacity for a thicker layer might be increased.

We further found that the location of the HPRB relative to the water table, and consequently its background water saturation, had a strong effect on the removal capacity of the HPRB. This is because the high background water content and possible diffusion of protons or/and hydroxide (especially downwards to higher water saturation area) neutralized the effect of pH on the oxidation rate and leading to a higher removal efficiency and reactivity of the HPRB for all VOCs. However, the higher water contents near the water table may increase the dissolution of potassium permanganate into water and its subsequent diffusion away from the HPRB. Furthermore, closeness to the water table may increase the risk of occasionally saturating the HPRB due to groundwater fluctuations and subsequent loss of permanganate from the HPRB. This would shorten the longevity of the HPRB for oxidizing VOC vapours in the unsaturated zone.

For the experimental setup with the HPRB placed 12.0 cm above the water table, we found a change in the pH within the HPRB, which could explain the reduction in the oxidation rate of TCE and toluene. A reactive vapour transport model that included the effect of pH on the oxidation rate could satisfactorily simulate the TCE and toluene experimental data. However, the simulations for ethanol vapour transport were conducted without the pH effect on the ethanol oxidation rate due to production of water and subsequent dilution of the hydroxide ion concentration during ethanol oxidation. For the setup with the HPRB at 7.0 cm above the water table, the experimental data of all target compounds could be modeled without accounting for the effects of pH on the oxidation rate.

As a result, the optimal location of the HPRB is as close to the water table as possible without risking saturation of the HPRB. However, we have shown in our earlier study (Mahmoodlu et al., 2014b) that the use of carbonate minerals in the HPRB can increase the reactivity of the HPRB in the TCE oxidation experiments. Hence, we believe that employing some acid minerals can temper the rise of hydroxide concentration during toluene and ethanol oxidation, thus increasing the reactivity of the HPRB. Therefore, the use of proper salts in the HPRB would increase the longevity of HPRBs far above the water table in the unsaturated zone. The performance of such a methodology is affected by various environmental factors.

5.7. References

[1] Albergaria, J.T., Alvim-Ferraz, M.dc.M., and Delerue-Matos, C., 2012. Remediation of sandy soils contaminated with hydrocarbons and halogenated hydrocarbons by soil vapour extraction. Environ. Manage. 104: 195-201.

[2] Almeida, C.M.M., and Boas, L.V., 2004. Analysis of BTEX and other substituted benzenes in water using headspace SPME-GC-FID: method validation. J. Environ. Monit. 6: 80-88.

[3] ATSDR (Agency for Toxic Substances and Disease Registry) 1994. Toxicological Profile for Toluene (Update). ATDSR, Atlanta, US.

[4] Berscheid, M., Burger, K., Hutchison, N., Muniz-Ghazi, H., Renzi, B., Ruttan, P., and Sterling, S., 2010. Proven Technologies and Remedies Guidance: Remediation of Chlorinated Volatile Organic Compounds in Vadose Zone Soil. California Department of Toxic Substances Control. http://www.dtsc.ca.gov/ sitecleanup/upload/cVOC_040110.pdf, 2010.

[5] Breus, I.P., and Mishchenko, A.A., 2006. Sorption of volatile organic contaminants by soils (a review). Eurasian Soil. Sci. 39: 1271-1283.

[6] Brooks, R.H., and Corey, A.T., 1964. Hydraulic properties of porous media. Hydrol. Papers 3. Colo. State Univ., Fort Collins, CO. 27.

[7] Brusseau, M.L., 1991. Transport of organic chemicals by gas advection in structured or heterogeneous porous media: development of a model and application to column experiments. Water Resour. Res. 27(12): 3189-3199.

[8] Capiro, N.L., Stafford, B.P., Rixey, W.G., Bedient, P.B., and Alvarez, P.J.J., 2007. Fuel-grade ethanol transport and impacts to groundwater in a pilot-scale aquifer tank. Water. Res. 41: 656-664.

[9] Cho, J., Annabel, M.D., and Rao, P.S.C., 2005. Measured mass transfer coefficients in porous media using specific interfacial area. Environ. Sci. Technol. 39: 7883-7888.

[10] Cho, H.J., Fiaco, R.J., and Daly, M.H., 2002. Soil vapour extraction and chemical oxidation to remediate chlorinated solvents in fractured crystalline bedrock: pilot study results and lessons learned, Remediation J. 12(2): 35-50.

[11] Costanza, M., and Brusseau, A., 2000. Contaminant vapor adsorption at the gas-water interface in soils. Environ. Sci. Technol. 34(1): 1-11.

[12] Costanza-Robinson, M.S., Carlson, T.D., and Brusseau, M.L., 2013. Vapor-phase transport of trichloroethene in an intermediate-scale vadose-zone system: Retention processes and tracer-based prediction. J. Contam. Hydrol. 145: 82-89.

[13] Cronk, G., Koenigsberg, S., Coughlin, B., Travers, M., and Schlott, D., 2010. Controlled vadose zone saturation and remediation (CVSR) using chemical oxidation, 7th International Conference on Remediation of Chlorinated and Recalcitrant Compounds. May 24-27, 2010. Battelle Press, Columbus, OH. 8.

[14] EPA (Environmental Protection Agency), 2011. Toxicological review of trichloroethylene. CAS No. 79-01-6.http://www.epa.gov/iris/toxreviews/0199tr/0199tr.pdf, 2011.

[15] EPA (Environmental Protection Agency), 2012. Petroleum hydrocarbons and chlorinated hydrocarbons differ in their potential for vapour intrusion. Office of Underground Storage Tanks, Washington, D.C. 20460. www.epa.gov/oust/cat/pvi/pvicvi.pdf.

[16] Estivill, I.S., Hargreaves, D.M., and Puma, G.L., 2007. Evaluation of the intrinsic photocatalytic oxidation kinetics of indoor air pollutants. Environ. Sci. Technol. 41(6): 2028-2035.

[17] EuroChlor (European Chloroalkali Industry), 2008. Chlorine Industry Review 2007-2008, Euro Chlor, Bruxelles, BE.

[18] Fan, S., and Scow, K.M., 1993. Biodegradation of trichloroethylene and toluene by indigenous microbial populations in soil. App. Environ. Microbiol. 59(6): 1911-1918.

[19] Farrell, J., and Reinhard, M., 1994. Desorption of halogenated organics from model solids, sediments, and soil under unsaturated conditions. 1. Isotherms. Environ. Sci. Technol. 28(1): 53-62.

[20] Fogler, H.S., 2006. Elements of Chemical Reaction Engineering, Fourth ed. Boston, MA: Prentice Hall.

[21] Forsey, S.P., 2004. In situ Chemical Oxidation of Creosote/Coal Tar Residuals: Experimental and Numerical Investigation. PhD thesis, University of Waterloo, Waterloo Ontario, Canada.

[22] Freitas, J.G., 2009. Impacts of ethanol in gasoline on subsurface contamination. PhD thesis. University of Waterloo, Waterloo Ontario, Canada.

[23] Freitas, J.G., Fletcher, B., Aravena, R., and Baker, J.F., 2010. Methane production and isotopic fingering in ethanol fuel contaminated sites. Groundwater 48: 844-857.

[24] Fritz, S., 2012. Experimental Investigations of Water Infiltration Into Unsaturated Soil-Analysis of Dynamic Capillarity Effects. Master's thesis. University of Stuttgart. Germany.

[25] Gardner, W.R. 1958. Some steady state solutions of unsaturated moisture flow equations with application to evaporation from a water table. Soil Sci. 85(4): 228-232.

[26] Gibert, O., Cortina, J.L., de Pablo, J., and Ayora, C., 2013. Performance of a field-scale permeable reactive barrier based on organic substrate and zero-valent iron for in situ remediation of acid mine drainage. Environ. Sci. Pollut. Res. 20: 7854-7862.

[27] Green, D.W., and Perry, R.H., 2007. Perry's Chemical Engineers' Handbook, eighth ed. McGraw-Hill. ISBN:0-07-142294-3.

[28] Hassanizadeh, S.M., and Gray, W.G., 1993. Thermodynamic basis of capillary pressure in porous media. Water. Resour. Res. 29: 3389-3405.

[29] Haverkamp, R., Vaclin, M., Touma, J., Wierenga, P.J., and Vachaud., G., 1977. A comparison of numerical simulation models for one-dimensional infiltration. Soil Sci. Soc. Am. J. 41: 285-294.

[30] Hazen and Sawyer. 1992. Disinfection Alternatives for Safe Drinking Water. Van Nostrand Reinhold, New York, NY.

[31] Heiderscheidt, J.L., Crimi, M., Siegrist, R.L., and Singletary, M.A., 2008. Optimization of full-scale permanganate ISCO system operation: laboratory and numerical studies. Groundwater Monitoring & Remediation. 28(4): 72-84.

[32] Hers, I., Atwater, J., Li, L., Gilje, R. Z., 2000. Evaluation of vadose zone biodegradation of BTX vapours. J. Contam. Hydro. 46: 233-264.

[33] Hesemann, J.R. and Hildebrandt, M., 2009. Successful unsaturated zone treatment of PCE with sodium permanganate. Remediation J. 19(2): 37-48.

[34] Hinchee, R.E., 1993. Bioventing of Petroleum Hydrocarbons, in Handbook of Bioremediation, CRC Press Inc.

[35] Hoeg, S., Scholer, H.F., and Warnatz, J., 2004. Assessment of interfacial mass transfer in water-unsaturated soils during vapor extraction. J. Contam. Hydrol. 74: 163-195.

[36] Huling, S.G., and B., Pivetz, 2006. In situ chemical oxidation-engineering issue. EPA/600/R-06/072.www.epa.gov/ada/gw/.../insituchemicaloxidation_engine-ering_issue.pdf

[37] IARC (International Agency for Research on Cancer), 1995. Dry cleaning, some chlorinated solvents and other industrial chemicals. Summary of Data Reported and Evaluation. Report n.63.

[38] ITRC (Interstate Technology & Regulatory Council), 2011. Biofuels: Release Prevention, Environmental Behavior, and Remediation. BIOFUELS-1. Washington, D.C.: Interstate Technology & Regulatory Council, Biofuels Team. www.itrcw eb.org.

[39] Joekar-Niasar, V., Hassanizadeh, S.M., and H.K., Dahle., 2010. Non-equilibrium effects in capillarity and interfacial area in two-phase flow: Dynamic and pore-network modeling. J. Fluid Mech. 655: 38-71.

[40] Johnson, P.C., Kemblowski, M.W., and Johnson, R.L., 1999. Assessing the significance of subsurface contaminant vapor migration to enclosed spaces: site-specific alternatives to generic estimates. Soil and Sediment Contam. 8(3): 389-421.

[41] Johnson, R., Pankow, D., Bender, C.P., Price, C.V., and Zogorski, J., 2000. MTBE: to what extent will past releases contaminate community water supply wells?. Environ Sci Technol. 34: 210-217.

[42] Kao, C.M., Huang, K.D., Wang, J.Y., Chen, T.Y., and Chien, H.Y., 2008. Application of potassium permanganate as an oxidant for in-situ oxidation of trichloroethylene-contaminated groundwater: A laboratory and kinetics study. J. Hazard Mater. 153: 919-927.

[43] Kim, H., Annable, M.D., and Rao, P.S.C., 2001. Gaseous transport of volatile organic chemicals in unsaturated porous media: effect of water-partitioning and Air-Water Interfacial Adsorption. Environ. Sci. Technol. 35: 4457-4462.

[44] Kubinec, R., Adamuscin J., Jurdakova, H., Foltin, M., Ostrovsky, I., Kraus, A., and Sojak, L., 2005. Gas chromatographic determination of benzene, toluene, ethylbenzene and xylenes using flame ionization detector in water samples with direct aqueous injection up to 250 µl. J. Chromatogr A 1084: 90-94.

[45] Leal, M., Martínez-Hernández, V., Lillo, J., Meffe, R., and de Bustamante, I., 2013. Zeolite in horizontal permeable reactive barriers for artificial groundwater recharge. Geophysical Research Abstracts, Vol. 15, EGU2013-924: http://meeting organizer.copernicus.org/EGU2013/EGU2013-924.pdf.

[46] Lewis, S., Lynch, A., Bachas, L., Hampson, S., Ormsbee, L., and Bhattacharyya, D., 2009. Chelate-modified fenton reaction for the degradation of trichloroethylene in aqueous and two-phase systems. Environ. Eng. Sci. 26(4): 849-59.

[47] Li, X.D., and Schwartz, F.W., 2004. DNAPL remediation with in situ chemical oxidation using potassium permanganate.II. Increasing removal efficiency by dissolving Mn oxide precipitates. J. Contam. Hydro. 68: 269-287.

[48] Lobachev, V.L., Radakov E.S., and Zaichuk E.V., 1997. Kinetics, kinetic isotope effects, and substrate selectivity of alkybenzene oxidation in aqueous permanganate solutions: VI. Reaction with MnO_3^+ . Kinet. Catal. 38(6): 745-761.

[49] Mackay, D., De Sieyes, N., Einarson, M., Feris, K., Pappas, A., Wood, I., Jacobson, L., Justice, L., Noske, M., Wilson, J., Adair, C., and Scow, K., 2007. Impact of ethanol on the natural attenuation of MTBE in a normally sulfate-reducing aquifer. Environ. Sci. Technol. 4: 2015-2021.

[50] Mackova, M., Dowling, D., and Macek, T., 2006. Focus on biotechnology; Phytoremediation and Rhizoremediation, Published by Springer.

[51] Mahmoodlu, M.G., Hartog, N., Hassanizadeh, S.M., and Raoof, A., 2013. Oxidation of volatile organic vapours in air by solid potassium permanganate. Chemosphere 91 (11): 1534-1538.

[52] Mahmoodlu, M.G., Hassanizadeh, S.M., and Hartog, N., 2014a. Evaluation of the kinetic oxidation of aqueous volatile organic compounds by permanganate. Sci. Total Environ. 485-86: 755-63.

[53] Mahmoodlu, M.G., Hartog, N., Hassanizadeh, S.M., and Raoof, A., 2014b. Oxidation of trichloroethylene, toluene, and ethanol vapours by a partially saturated permeable reactive barrier. J. Contam. Hydrol. 164:193-208.

[54] Millington, R.J., Quirk, J.P., 1961. Permeability of porous solids. Trans. Faraday Soc. 57: 1200-1207.

[55] Müller, D., Francke, H., Blöcher, G., and Shao, H.B., 2013. Simulation of reactive transport in porous media: A benchmark for a COMSOL-PHREEQC-Interface. Conference Proceedings of COMSOL Conference. Rotterdam, The Netherlands. www.comsol.com/paper/download/182397/maaller_abstract.pdf.

[56] Murphy, B.L. and Chan, W.R., 2011. A multi-compartment mass transfer model applied to building vapor intrusion. Atmos. Environ. 45 (37): 6650-6657.

[57] Pachepsky., Y., Timlin, D., and Rawls, W., 2003. Generalized Richards' equation to simulate water transport in unsaturated soils, J. Hydrol. 272: 3-13.

[58] Pasteris, G., Werner, D., Kaufmann, K., and Hohener, P., 2002. Vapor phase transport and biodegradation of volatile fuel compounds in the unsaturated zone: a large scale lysimeter study. Environ. Sci. Technol. 36: 30-39.

[59] Pennell, K.G., Bozkurt, O. and Suuberg, E., 2009. Development and application of a three-dimensional finite element vapor intrusion model. J. Air & Waste Manage. Assoc. 59: 447-460.

[60] Picone, S., 2012. Transport and biodegradation of volatile organic compounds: influence on vapor intrusion into buildings. PhD thesis. Wageningen University, The Netherlands.

[61] Przyjazny A., and Kokosa J.M., 2002. Analytical characteristics of the determination of benzene, toluene, ethylbenzene and xylenes in water by headspace solvent microextraction. J. Chromatogr A 977(2): 143-153.

[62] Raoof, A., and Hassanizadeh, S.M., 2013. Saturation-dependent solute dispersivity in porous media: Pore-scale processes. Water Resour. Res. 49(4): 1943-1951.

[63] Raoof, A., Nick, H.M., Hassanizadeh, S.M., and Spiers, C.J., 2013. PoreFlow: A complex pore-network model for simulation of reactive transport in variably saturated porous media. Comput. Geosci. 61: 160-174.

[64] Rastkari, N., Yunesian, M., and Ahmadkhaniha, R., 2011. Exposure assessment to trichloroethylene and perchloroethylene for workers in the dry cleaning industry. Bull Environ. Contam. Toxicol. 86:363-367.

[65] Richards, L. A., 1931: Capillary conduction of liquids through porous mediums. Physics, 1, 318-33.

[66] Rolle, M., Hochstetler, D., Chiogna, G., Kitanidis, P.K., and Grathwohl, P., 2012. Experimental investigation and pore-scale modeling interpretation of compound-specific transverse dispersion in porous media. Transp. Porous Med. 93: 347-362.

[67] Rudakov, E.S., and Loachev, V.L., 1994. Kinetics, kinetic isotope effects, and substrate selectivity of alkylbenzene oxidation in aqueous permanganate solutions: I Reactions with MnO_4^-G anion. Kinet. Catal. 35 (2): 175-79.

[68] Russo, D., 1988. Determining soil hydraulic properties by parameter estimation: On the selection of a model for the hydraulic properties. Water Resour. Res. 24: 453-459.

[69] Sadeghi, M., Nadfi, K., Nabizadeh, R., Nasseri, S., Mesdaghinia, Hosseini Mahvi, A., Ali Mohammadi, M., Nazmara, S., and Rastkari, N., 2014. Perchloroethylene and trichloroethylene in the air and effluent of dry cleaning shops. I.J.O.H. 6: 11-15.

[70] Sanders, P.F., and Talimcioglu, N.M., 1997. Soil-to-indoor air exposure models for volatile organic compounds: the effect of soil moisture. Environ. Toxicol. Chem. 16(12): 2597-604.

[71] Sara, M.N., 2003. Site Assessment and Remediation Handbook, 2nd edition. CRC Press LLC.

[72] Sen Gupta, K.K., Adhikari, M., and Sen Gupta, S., 1989. Kinetics of oxidation of ethanol by potassium permanganate in perchloric acid medium. React. Kinet. Catal. Lett. 38 (2): 313-318.

[73] Shen, R., Pennell, K.G., and Suuberg, E.M., 2014. Analytical modeling of the subsurface volatile organic vapor concentration in vapor intrusion. Chemosphere 95: 140-149.

[74] Sieg, K., Fries, E., and Püttmann, W., 2008. Analysis of benzene, toluene, ethylbenzene, xylenes and *n*-aldehydes in melted snow water via solid-phase dynamic extraction combined with gas chromatography/mass spectrometry. J. Chromatogr A 1178 (1-2): 178-186.

[75] Siegrist, R.L., Lowe, K.S., Murdoch, L.W., Case, T.L., Pickering, D.A., and Houk., T.C., 1998. horizontal treatment barriers of fracture-emplaced iron and permanganate particles. In North Atlantic Treaty Organization (NATO)/Committee on the Challenges of Modern Society (CCMS). Pilot Study: Special Session on Treatment Walls and Permeable Reactive Barrier. EPA report: EPA 542-R-98-003: 77-82.

[76] Silliman, S.E., Berkowitz, B., Simunek, J., and Van Genuchten, M.T., 2002. Fluid flow and solute migration within the capillary fringe. Ground Water 40(1): 76-84.

[77] Snow, N.H., 2002. Head-space analysis in modern gas chromatography. Trace-Trend Anal. Chem. 21: 608-617.

[78] Tillman, F.D., and Weaver, J.W., 2005. Review of Recent Research on Vapor Intrusion. United States Environmental Protection Agency, EPA/600/R-05/106,Washington,DC.http://209.190.206.131/download/contaminantfocus/vi/Review%20of%20Recent%20Research.pdf.

[79] Tsitonaki, A., Petri, B., Crimi, M., Mosbæk, H., Siegrist, R.L. and Bjerg, P.L., 2010. In situ chemical oxidation of contaminated soil and groundwater using persulfate: a review. Crit. Rev. Environ. Sci. Technol. 40: 55-91.

[80] USEPA (United States Environmental Protection Agency), 1993. Behavior and Determination of Volatile Organic Compounds in Soil: A Literature Review. EPA/600/R-93/140. http://www.epa.gov/esd/cmb/pdf/voclr.pdf.

[81] USEPA (United States Environmental Protection Agency) 1995. Principles and Practices of Bioventing. EPA/540/R-95/534.

[82] USEPA (United States Environmental Protection Agency), 1999. Alternative Disinfectants and Oxidants Guidance Manual. EPA 815-R-99-014. http://www.epa.gov/ogwdw/mdbp/alternative_disinfectants_guidance.pdf.

[83] van Genuchten, M.Th., 1980. A closed form equation for predicting the hydraulic conductivity of unsaturated soils. Soil Sci. Soc. Am. J. 44: 892-898.

[84] Waldemer R.H., Tratnyek P.G., 2006. Kinetics of contaminant degradation by permanganate. Environ. Sci. Technol. 40: 1055-1061.

[85] Wiedemeier, T.H., Rifai, H.S., Newell, C.J., and Wilson, J.T., 1999. Natural attenuation of fuels and chlorinated solvents in the subsurface. John Wiley & Sons, New York, US.

[86] Yao, Y., Shen, R., Pennell, K.G., and Suuberg, E.M., 2013. A review of vapor intrusion models. Environ. Sci. Technol. 47: 2457-2470.

[87] Yeh, C.H., Lin, C.W., and Wu., C.H., 2010. A permeable reactive barrier for the bioremediation of BTEX-contaminated groundwater: Microbial community distribution and removal efficiencies. J. Hazard. Mater.178: 74-80.

[88] Yoshii, T., Niibori, Y., Mimura, H., 2012. Some fundamental experiments on apparent dissolution rate of gas phase in the groundwater recovery processes of the geological disposal system. WM2012 Conference, February 26 - March 1, Phoenix, Arizona, USA.

[89] You, K., and Zhan, H., 2013. Comparisons of diffusive and advective fluxes of gas phase volatile organic compounds (VOCs) in unsaturated zones under natural conditions. Adv. Water Resour. 52: 221-231.

[90] Yuan, B., Li, F., Chen, Y., Fu, M.L., 2013. Laboratory-scale column study for remediation of TCE-contaminated aquifers using three-section controlled-release potassium permanganate barriers. J. Environ. Sci. 25(5): 971-977.

[91] Yu, K.P., Lee, G.W.M., 2007. Decomposition of gas-phase toluene by the combination of ozone and photocatalytic oxidation process (TiO_2/UV, TiO_2/UV/O_3, and UV/O_3). Appl. Catal. B: Environ. 75: 29-38.

[92] Zhang, Q., Hassanizadeh, S.M., Raoof, A., van Genuchten, M.Th., and Roels, S.M., 2012. Modeling virus transport and remobilization on during transient partially saturated flow. Vadose Zone J.11(2).

Chapter 6

Summary, conclusions, and suggestions for future work

6.1. Summary and conclusions

The focus of this research was to evaluate the potential of a solid oxidant for oxidizing VOC vapours under partiality saturated conditions. The main goal has been to investigate the feasibility of using a horizontal permeable reactive barrier (HPRB) containing a solid oxidant as a new option to control the upward migration of VOC vapours arising from contaminated soil and groundwater in the unsaturated zone.

In this study, we selected TCE, toluene, and ethanol as the model VOCs (target compounds) for chlorinated solvents, mineral oil, and biofuel, respectively. Potassium permanganate was selected as the oxidant for the following five reasons: (1) its relatively high oxidation potential (E_0 = 0.5-1.7 V), (2) its ability to oxidize a variety of organic chemicals (Powers et al., 2001; Siegrist et al., 2001; Struse et al., 2002; Hønning et al., 2004; Mumford et al., 2004; Mumford et al., 2005; Urynowicz, 2008), (3) its relatively low cost, (4) its significantly higher stability in the subsurface as compared to other chemical oxidants (Huang et al., 1999; Bryant et al., 2001), and (5) predictable chemistry and nontoxic by-products (Siegrist et al., 2011).

We next investigated the ability of solid potassium permanganate to fully oxidize target compound vapours. For this purpose, we designed and performed a series of batch experiments consisting of solid potassium permanganate and VOC vapours at room temperature (~20 $^{\circ}$C) and air humidity of 37 ± 2%, which was also the initial humidity inside the vials. Results showed that potassium permanganate is able to oxidize the vapour of TCE, ethanol, and toluene. We also found that TCE and ethanol in vapour phase could be rapidly oxidized by solid potassium permanganate. However, toluene was degraded slower.

Kinetic parameters are needed for modeling the design and performance assessment of an ISCO application. Hence, another goal of our study was to determine kinetic parameters for the oxidation of VOC vapours by solid potassium permanganate. A linear kinetic oxidation model (Equation 2.4), based on the concentration of VOC in gas and a constant relative surface area (surface area of

potassium permanganate divided by the gas volume), was employed to predict the oxidation rate of VOC vapours. The model could effectively predict the rate of TCE, ethanol, and toluene oxidation. The reaction rate constants for TCE, ethanol, and toluene were found to be 2.0×10^{-6} cm s^{-1}, 1.7×10^{-7} cm s^{-1}, and 7.0×10^{-8} cm s^{-1}, respectively. During oxidation, the reactivity of potassium permanganate can decrease due to the accumulation of reaction products, such as manganese dioxide and pH changes. In the case of limited air humidity, surface coating of potassium permanganate grains due to the produced manganese dioxide can be a main reason for diminishing permanganate reactivity. In this study, we used an excess amount of solid potassium permanganate. Hence, produced manganese dioxide was not a limiting factor. However, account for the effect of surface coating, we proposed an equation relating relative surface area to manganese dioxide concentration.

The oxidation reactions between an oxidant and contaminant typically occur in the water phase of the unsaturated zone. We hence investigated the kinetics of the oxidation of TCE, ethanol, and toluene by permanganate in the aqueous phase. For this purpose, we performed a series of batch experiments consisting of dissolved potassium permanganate and VOCs at room temperature (21 ± 1 $^{\circ}$C).

Results show that the oxidation rate decreased in the order TCE> ethanol>toluene. A comparison of VOC oxidation rates in the aqueous phase and gas phase revealed that the oxidation process in both phases follows a second-order model. This comparison also revealed that the oxidation rates for VOCs in the vapour phase are much smaller than those in aqueous phase. However, in both phases, the reaction rate for TCE was higher than for ethanol and toluene.

A more accurate second-order formulation was used for the oxidation of target compounds by permanganate rather than employing the common pseudo-first-order kinetic analysis. The reaction rate constants (k) based on the second-order model for TCE, toluene, and ethanol were found to be 8.0×10^{-1} (M^{-1} s^{-1}), 2.5×10^{-4} (M^{-1} s^{-1}), and 6.5×10^{-4} (M^{-1} s^{-1}), respectively. Results show that the inappropriate use of the pseudo-first-order approach in several previous studies produced biased estimates of the second-order rate constants. In our study this error was expressed as a function of the extent (P/N) in which the reactant concentrations

deviated from the stoichiometric ratio of each oxidation reaction. The error associated with the inappropriate use of the pseudo-first-order approach is negatively correlated with the P/N ratio and reached up to 25% of the estimated second-order rate constant in some previous studies of TCE oxidation. Neglecting these errors may have a significant effect on the design, modeling, and performance of ISCO remediation plans. Errors in k can also affect the desired injection rate of potassium permanganate solution to the contaminated site and the desirable concentration of potassium permanganate in the injected solution.

The batch experiment showed that dry solid potassium permanganate granules were able to oxidize TCE, toluene, and ethanol vapours. VOC vapour oxidation in this study occurred through the exposure of VOC vapour to excess amounts of solid potassium permanganate. As a result, any potential long-term effects on the reactivity of potassium permanganate through the accumulation of reaction products, such as manganese dioxide and pH changes, could not be assessed. The above experiments were performed at low moisture conditions with only ambient air providing initial humidity. Although the study confirmed the potential of using solid potassium permanganate in permeable reactive barriers (PRBs) in the unsaturated zone, it remained initially unclear how water content and chemical evolution would affect the reactivity of a PRB. A series of short column experiments was performed to (1) evaluate the ability of solid potassium permanganate as a horizontal permeable reactive barrier (HPRB) to oxidize the vapour of target compounds under various degrees of water saturation, (2) investigate the impact of the accumulations of reaction products on the long-term reactivity of potassium permanganate, and (3) numerically simulate the migration and oxidation process of each target compound diffusing through the permeable reactive barrier (PRB).

The short column experiments were carried out using a glass cylinder of 5.0 cm length and 4.0 cm internal diameter, capped by a steel stainless lid (Fig. 4.1). The columns contained four domains. The first domain consists of a pool of VOC liquid. The second domain comprised the air space above the liquid pool and below the PRB. The third domain was the PRB consisting of potassium permanganate and

sand with its water and air phases. The fourth domain was the headspace above the PRB. For the control experiments, we used the same column, but without potassium permanganate. Hence, only used a sand layer was used.

Results of the reactive experiments showed that water saturation had a strong effect on the removal capacity of the PRB. A high removal efficiency and reactivity of the PRB for all target compounds at the highest water saturation (S_w = 0.6) was observed.

The change in pH of the water phase during the oxidation of VOCs was found to be the main reason for a reduction in the oxidation rate of the PRB. Results showed that adding carbonate minerals such as sodium bicarbonate and calcium carbonate into the initial PRB increased the reactivity of potassium permanganate during oxidation of TCE vapour by buffering the pH. Furthermore, we found that the effect of the accumulated reaction products on the reactivity of the PRB should be reduced by adding water during the TCE experiment. The increase in the reactivity of the PRB due to added water is attributed to a reduction in the proton concentration. This allows the reaction to continue until protons accumulated again to previous levels.

A model was developed for reactive vapour transport, which included pH-dependent oxidation rates. The model was able to satisfactorily predict the experimental data for toluene and TCE. For ethanol was found increasing discrepancy between the simulation results and experimental data with increasing water contents. This was attributed to the fact that, due to the high solubility of ethanol in water, the vapour concentration of the air apace between the ethanol pool and the PRB (second domain) varied with time. We did not account for these variations. Instead, we assumed a constant ethanol vapour concentration to correspond to 80% of the saturated vapour based on the calculated mole faction of ethanol in the non-ideal mixture (Kuhn et al., 2009). To improve the simulations for ethanol, variations in the ethanol vapour concentration with time at the inlet boundary should be accounted for.

The total oxidized mass of ethanol vapour was found to be higher than TCE and toluene for identical water saturations, despite a larger oxidation rate

constant for TCE than for ethanol and toluene (Waldemer and Tratnyek, 2006). This is due to the fact that TCE and toluene oxidation is highly affected by a change in the pH of the water phase during their oxidation, as compared to ethanol.

In order to obtain a rough estimate of the longevity of a HPRB consisting of potassium permanganate and sand under field conditions, we considered a hypothetical field situation (typical water saturation of 0.4) with a building located above VOC-contaminated groundwater (Fig. 4.12). We considered a HPRB of 1.0 m thickness, which is constructed 2.0 m above the groundwater table, and mass ratio of potassium permanganate to sand equal to 2.0. We assumed the initial concentrations of TCE and toluene in groundwater to be 1% of their solubilities in water. However, for ethanol we considered groundwater with a volumetric ratio of 10% ethanol (e.g., as reported by Freitas (2009) for North America). Assuming that VOC vapours are transported to the HPRB only by diffusion, the continuous mass fluxes reaching the permeable reactive layer could be calculated. Then, using total oxidized mass of VOC (As shown in Fig 4.12), the life time of the HPRB will be around of 247, 227 and 785 days. However, the longevity of a HPRB is affected by many environmental factors. In fact, these estimates are based on experimental results that suffered from water limitations in a sealed column. This caused the built-up of reaction products in the water phase that negatively affected the reactivity of the HPRB. We expect that the absence or prevention of limitations in water availability during field applications could further enhance the effectiveness of a HPRB to mitigate vapour intrusion risks. This could be a focus of future studies.

Next, we performed larger column experiments to test the effectiveness of the HPRB under situations similar to field conditions. For this, an experiment was designed to have a source of VOCs at the bottom of a 30-cm long sand-filled glass column having an internal diameter of 5.0 cm and containing several inlet and outlet valves, and headspace of 4.0 cm capped by stainless steel lids (Fig. 5.2). The system contained four domains. The first domain was a 6-cm thick saturated zone through which horizontal flow of water containing a dissolved VOC occurred. The second domain comprised the unsaturated zone between the water table and the top

of the sand column. The third domain was the HPRB within the unsaturated zone consisting of a mixture of potassium permanganate and sand, but also containing a certain amount of water depending upon its height above the water table. For the control experiments, we used the same columns, but without any potassium permanganate. The fourth domain is the headspace above the unsaturated zone.

A comparison of the control and reactive experiments showed that the HPRB was very effective in oxidizing VOC vapours. Experimental results also show that the HPRB in the sand column was far more effective than the short column setup (Chapter 4). This may be because the VOC concentrations in the gas phase reaching a HPRB were much lower than in our earlier experiments. An increase in the residence time of ethanol in the water phase due to its dissolution and hydrophilic property may increase the exposure time to dissolved potassium permanganate and consequent a high removal mass of ethanol in the water phase.

Two sets of complementary TCE experiments to investigate were performed the effect of initial water saturation on the reactivity of HPRB. The partially saturated HPRB was found to be more effective than dry HPRB. Although the overall efficiency of dry HPRB was smaller than the partially saturated HPRB, it was more effective than our short column. A reliable explanation was the initial concentration of VOC in gas phase which was more lower than our earlier setup (Chapter 4). Another likely reason is the effect of the air humidity content on the reactivity of HPRB which may relatively increase the availability of water.

Results suggest that the thickness of the HPRB had a major effect on the removal capacity of the HPRB. Thinker HPRB under the same water saturation was more effective for any given period of time. This is because travel time through the HPRB and consequent dissolution of VOC in the pore water increased. In the presence of potassium permanganate in the water phase, this may have resulted in large oxidation capacity for a thinker layer.

We further found that the location of the HPRB relative to the water table, and consequently its background water saturation, had a strong effect on the removal capacity of the HPRB. This is because the high background water content and possible diffusion of protons or/and hydroxide, mainly downwards to higher

water saturation area, neutralized the effect of pH on the oxidation rate and leading to a higher removal efficiency and reactivity of the HPRB for all VOCs. However, the higher water contents near the water table may also increase the dissolution of potassium permanganate into water and its subsequent diffusion away from the HPRB.

A reactive vapour transport model that included the effect of pH on the oxidation rate could satisfactorily predict the experimental data. However, the simulation for ethanol vapour transport was conducted without the pH effect on the ethanol oxidation rate due to possible production of water and subsequent dilution of hydroxide ion concentration during ethanol oxidation. For the case of HPRB at 7 cm above the water table, the experimental data for all target compounds could be modeled without accounting for the effect of pH on the oxidation rate.

An estimate of the total oxidized mass capacity and longevity of a partially saturated HPRB suggested that HPRBs can provide a viable option for preventing VOC vapours to reach the land surface. However, the performance of such a methodology is affected by various environmental factors.

We believe that the HPRB concept can be applicable to the following situations.

(1) Treating VOC vapours emitting from waste-buried land or a contaminated site located in open spaces, such as a park, stadium, or other public places. In these cases, topsoil should be removed first. The reactive materials including potassium permanganate, sand, and water should be spread out laterally for creating a HPRB like a blanket. Eventually, the HPRB should be covered by extracted soil.

(2) For waste-buried land or a contaminated site to be used for construction purposes. The HPRB can be created before construction of a building.

6.2. Suggestions for future work

The results of this research give considerable insight into treatment methods for the remediation of VOC vapours in the unsaturated zone. Although we investigated many scenarios about the efficiency of HPRB in the unsaturated zone, the performance of a particular methodology may be affected by the scale as well as various environmental factors.

The results of this research were obtained based on a series of batch and column experiments. It is important to perform larger-scale experiments, such as tank and pilot studies under different conditions. Results would then be expected to be more appropriate for field application of the HPRB methods.

Diffusion in the various experiments was the dominant transport process for driving VOC vapours to the headspace. In actuality, the transport of VOC vapours may be affected by other transport processes, particularly air advection and water movement in the unsaturated zone (You and Zhan, 2012; Wang et al., 2013). Hence, additional experimental setups that consider also advection process should be conducted.

The experiments were performed with water and potassium permanganate distributed almost homogenous in the HPRB. This may not be the case for field applications. To determine any heterogeneity effect on HPRB performance, experiments should be performed under different degrees of heterogeneity in the HPRB.

The VOC studies were carried out at almost constant temperature. Although the effects of temperature on chemical reactions are generally known, performing experiments at different temperatures, especially closed to field temperatures would be informative.

Various studies were carried out using grain diameters varying between of 0.5-1 mm and a porosity of 0.35 to create the HPRB. The water-retention capacity and the tortuosity of soil within the HPRB can be changed by using different soil type. For instance, the use of fine-texture medium instead of sand would have increased the water-retention capacity and tortuosity of the HPRB. This could then

increase the residence time of the VOC and consequently decrease the diffusion flux. This would improve the removal efficiency due to longer contact time of the VOC with potassium permanganate in the water phase. We therefore suggest new experimental setups using different soils in the HPRB to better assess the effect of the soil type on the removal efficiency of the HPRB.

We found that accurate simulation of ethanol vapour transport is not easy, because of hydrophilic property and partitioning into the water phase during migration in the unsaturated zone. Furthermore, water-ethanol solutions normally do not behave as an ideal solution. Hence, more experiments should be conducted to have a better understanding of ethanol vapour transport within a partially saturated porous medium. In addition, the effect of accumulated reaction products on the oxidation rate of VOCs (particularly ethanol) within the HPRB should be considered.

In the literature, a few methods such as hydraulic or pneumatic fracturing are suggested to create horizontal wells in low permeable formations. Although these methods can be employed for creating a HPRB in the unsaturated zone, further experiments should be conducted for constructing a HPRB in medium to high permeable formations. Moreover, as explained in Chapter 1, several methods have already been developed for delivering solid oxidants or slurry for treating contaminated-aqueous phase. Research is needed on how a mixture of solid potassium permanganate and soil under various degree of water saturations can be placed optimally in the unsaturated zone.

6.3. References

[1] Bryant, D., Battey, T., Coleman, K., Mullen, D., Oyelowo, L., 2001. Permanganate in-situ chemical oxidation of TCE in a fractured bedrock aquifer. Proceeding of the First International Conference on Oxidation and Reduction Technologies for In-Situ Treatment of Soil and Groundwater; 2001 June 25-29; Niagara Falls, Ontario, Canada.

[2] Freitas, J.G., 2009. Impacts of Ethanol in Gasoline on Subsurface Contamination. PhD thesis. University of Waterloo, Waterloo Ontario, Canada.

[3] Hønning, J., Broholm, M.M., and Larsen, T.H., 2005. Oxidation kinetics and consumption of potassium permanganate in moraine clay, Third International Conferences on Oxidation and Reduction Technologies for In-Situ Treatment of Soil and Groundwater (ORT-3); 2004 October 24-28; San Diego, US. Ontario: Redox Technologies, Inc.

[4] Huang, K.C., Hoag, G.E., Chheda, P., and Woody, B.A., 1999. Dobbs GM. Kinetic study of oxidation of trichloroethylene by potassium permanganate. Environ. Eng. Sci. 16: 265-74.

[5] Kuhn, H., Försterling, H.D., and Waldeck, D.H., 2009. Principles of Physical Chemistry, Second ed. John Wiley & Sons, Inc.

[6] Mumford, K.G., Lamarche, C.S, and Thomson, N.R., 2004. Natural oxidant demand of aquifer materials using the push-pull technique. Environ. Eng. 130: 1139-46.

[7] Mumford, K.G., Thomson, N.R., and Allen-King, R.M., 2005. Bench-scale investigation of permanganate national oxidant demand kinetics. Environ. Sci. Technol. 39: 2835-40.

[8] Powers, S.E., Rice, D., and Dooher, B., Alvarez P.J.J., 2001. Will ethanol-blended gasoline affect groundwater quality?. Environ. Sci. Technol. 35: 26A-30A.

[9] Siegrist, R.L., Crimi, M., and Simkin, T.J., 2011. Chemical Oxidation for Groundwater Remediation. Springer Science+Business Media, LLC, New York.

[10] Siegrist, R.L., Urynowicz, M.A., West, O.R., Crimi, M.L., and Lowe, K.S., 2001. Principles and practices of in-situ chemical oxidation using permanganate. Columbus, OH: Battelle Press.

[11] Struse, A.M., Siegrist, R.L., Dawson, H.E., and Urynowicz, M.A., 2002. Diffusive transport of permanganate during in-situ oxidation. Environ. Eng. 128: 327-34.

[12] Urynowicz, M.A., 2008. In-situ chemical oxidation with permanganate: assessing the competitive interactions between target and nontarget compounds. Soil & Sediment Contam. 17: 53-62.

[13] Waldemer R.H., Tratnyek P.G., 2006. Kinetics of contaminant degradation by permanganate. Environ. Sci. Technol. 40: 1055-1061.

[14] Wang, S., Huang, G.H., Wei, J., and He, L., 2013. Simulation-based variance components analysis for characterization of interaction effects of random factors on trichloroethylene vapor transport in unsaturated porous media. Ind. Eng. Chem. Res. 52: 8602-8611.

[15] You, K., and Zhan, H., 2012. Can atmospheric pressure and water table fluctuation be neglected in soil vapor extraction? Adv. Water Resour.35: 41-54.

Samenvatting

In dit onderzoek is de potentie van vaste kaliumpermanganaat onderzocht voor het oxideren van dampen van vluchtige organische stoffen (VOCs) in zogenaamde horizontale doorlatende barrières (HPRB) in onverzadigde zones. We hebben batch-experimenten gedaan in korte en lange kolommen, waarvan we de data volledig hebben geanalyseerd.

In deze experimenten bestuderen we het vermogen van kaliumpermanganaat om drie geselecteerde VOCs volledig te oxideren: trichloroethyleen (TCE), tolueen en ethanol. Daarnaast hebben we ook de bijbehorende oxidatiesnelheden bepaald zowel voor VOCs opgelost in water als VOCs in de gasfase. Een serie batch-experimenten zijn uitgevoerd waarin VOC dampen en kaliumpermanganaat reageren bij kamertemperatuur (~20 $^{\circ}$C) en een luchtvochtigheid van 37 ± 2 %. Daarnaast hebben we batch-experimenten gedaan waarin opgeloste kaliumpermanganaat en VOCs reageren bij kamertemperatuur (21 ± 1 $^{\circ}$C). De resultaten voor VOC dampen en opgelost VOC geven aan dat de reactiesnelheid afneemt van TCE>ethanol>tolueen. Een vergelijking tussen de verschillende oxidatiesnelheden van de drie geselecteerde VOCs voor de gasfase en opgelost in water geeft aan dat de kinetiek beschreven kan worden met een tweede-orde model. Ook zijn de oxidatiesnelheden voor the gasfase vele malen kleiner dan voor de opgeloste-fase.

Een horizontale doorlatende reactieve barrière, bestaande uit zand en vaste kaliumpermanganaat was ingebracht in een ander korte kolom experiment waarin VOC dampen vanuit de onderkant via diffusie door de HPRB konden migreren en konden accumuleren boven in de kolom. Dit experiment was meerdere keren uitgevoerd bij verschillende waterverzadigingen. Door het analyseren van de luchtverzadiging in de kop van de kolom was de oxidatie-efficiëntie van de HPRB voor VOCs berekend. De waterverzadiging had een groot effect op de oxidatiecapaciteit van de HPRB. Bij een hoge water verzadiging (S^w=0.6) was de effectiviteit en de reactiviteit van de HPRB het hoogst voor al de drie geselecteerde organische stoffen. Limiterend was de verandering in de pH van het water

gedurende de oxidatie van VOCs: het verlaagde de reactie snelheid die uiteindelijk naar nul ging. De reactieduur kan worden verlengd door het toevoegen van carbonaat mineralen in de HPRB, dit vanwege de buffercapaciteit van het carbonaat. Daarnaast kunnen de negatieve effecten van een lage pH op de reactiviteit worden gemitigeerd door het toevoegen van water tijdens het oxideren van TCE. Een model voor reactief dampen transport, waarin de oxidatiesnelheid afhankelijk is van de pH, kon de experimentele data voor tolueen en TCE goed nabootsen. Het verschil tussen simulaties en experimentele data voor ethanol werd groter naarmate de waterverzadiging omhoog ging. Dit komt door de mixbaarheid van ethanol in water waardoor de dampconcentratie dat de HPRB van de onderkant infiltreert een functie is van de tijd. Dit is niet meegenomen in het model. We hebben in plaats daarvan een constante ethanol dampconcentratie aangenomen die correspondeert met de dampdruk die weer gebaseerd is op de berekende molaire fractie van ethanol in een niet-ideaal mengsel. De totale geoxideerde massa van ethanol damp was groter dan dat van TCE en tolueen, bij constante waterverzadigingen, ondanks een grotere oxidatiesnelheid van TCE in vergelijking tot ethanol en tolueen. Dit omdat de oxidatiesnelheid van TCE en tolueen sterk wordt beïnvloed door een verandering van pH tijdens het oxidatieproces.

De effectiviteit van de HPRB in het veld was bepaald in lange kolom experimenten, waarin een VOC vervuiling aanwezig was op de bodem. Hiervoor was een 30-cm lange glazen kolom gebruikt gevuld met zand, met een binnen diameter van 5,0 cm met verschillende in- en uitgangen en een ruimte aan de bovenkant van 4,0 cm afgesloten met een roestvrijstalen deksel. In een serie van experimenten hebben we verschillende factoren die het oxidatieproces kunnen beïnvloeden onderzocht, bijvoorbeeld de dikte van de HPRB, de locatie van HPRB ten opzichte van de grondwaterspiegel. Uit de resultaten bleek dat de HPRB in een zand kolom vele malen effectiever is dan in de voorgaande opzet (korte kolom experimenten). De dikte van de HPRB is een belangrijke component in de oxidatie van VOC dampen. Dit vanwege de reistijd door de HPRB, waardoor de VOC meer oplost in het porie water. Door de aanwezigheid van kaliumpermanganaat in het water, is de oxidatiecapaciteit van een dikkere laag groter dan voor een minder

dikke laag.

Daarnaast heeft de locatie van de HPRB ten opzichte van de waterspiegel een groot effect op de oxidatiecapaciteit van de HPRB vanwege een hoge waterverzadiging in de HPRB laag. Dit komt door de diffusie van protonen en/of hydroxide ionen in de richting van hogere waterverzadigingen, waardoor de pH minder verandert en de oxidatiesnelheid op pijl blijft. Dit resulteert in een hogere efficiëntie en reactiviteit van de HPRB voor al de VOCs. Dus de optimale locatie van de HPRB is zo dicht bij de grondwaterspiegel als mogelijk, zonder dat de HPRB volledig verzadigd wordt. Een ruwe schatting van de levensduur laat zien dat de HPRB een serieuze optie is voor het voorkomen van VOC migratie naar ruimtes binnenshuis. De duurzaamheid van een HPRB wordt ook beïnvloedt door andere omgevingsfactoren die in kaart moeten worden gebracht tijdens vervolg onderzoek.